UNIVERSITÀ DEGLI STUDI DI PALERMO

DOTTORATO DI RICERCA IN SCIENZE DELLA TERRA E DEL MARE
XXIX CICLO

Dipartimento di Scienze della Terra e del Mare
Settore Scientifico Disciplinare Geografia Fisica e Geomorfologia

LANDSLIDE SUSCEPTIBILITY MODELS FOR STORM-TRIGGERED MULTIPLE OCCURRING DEBRIS FLOWS IN EL SALVADOR

IL DOTTORE
ING. MIGUEL ÁNGEL HERNÁNDEZ MARTÍNEZ

IL COORDINATORE
PROF. ALESSANDRO AIUPPA

IL TUTOR
PROF. EDOARDO ROTIGLIANO

CO-TUTOR
PROF. CHRISTIAN CONOSCENTI

ACKNOWLEDGEMENTS

To the Italian Agency for International Cooperation, this work is derived from the projects supported with their resources in El Salvador, specifically the Peligrosidades Naturales Project 2009-2015, and RIESCA 2016, where the enthusiasm of studying the doctorate is born.

To the University of Palermo Italia

My eternal thanks to my Tutor Prof. Dr. Edoardo Rotigliano, as well as to my Co-Tutor Prof. Dr. Christian Conoscenti, of the Department of Earth and Sea Sciences, for all the time dedicated in support of this work, with their experience, knowledge and invaluable contribution, knew how to direct this thesis, all your sleepless nights and early mornings, I thank them very much.

Chiara Martinello thank you very much also for all your help.

To the Professors of the University of Palermo who came to El Salvador in the Peligrosidades Naturales Project lead by Prof. Giuseppe Giunta, whose teachings and helpful tips served to advance this effort, Attilio Sulli, Chiara Cappadonia, Silvio Rotolo, Valerio Agnessi and Benedetto Abate, to all of you, thank you very much.

To the Secretariat of International Relations of UNIPA, in particular the General Secretary Pascuale Assenato, Antonio Serafinni, Paola Turchetta, Francesco D'Giovanni and Vincenzo Fumetta.

To the Researchers of the National Research Council CNR of Italy: Antonio Caprai, Eliana Esposito and Sabina Porfido.

To the University of El Salvador

Sincere thanks to the authorities of the Faculty of Agronomic Sciences of the University of El Salvador, the Decano Juan Rosa Quintanilla, the Vice Decano Francisco Lara Ascencio, the Directors of the Postgraduate School Mario Antonio Orellana and the ex Director Efrain Antonio Rodríguez Urrutia, Fernando Castaneda, Rigoberto Quintanilla, Maria Julia de Sosa, many thanks for all your support.

To my colleagues: Reynaldo Landaverde, José Miguel Sermeño, Agustín Hernández De la Cruz, Abel Alexei Argueta, Luis Alonso Alas Romero, Carlos Aguirre, all colleagues of the Agricultural Chemistry Department, Mrs. Milagro Figueroa, Mrs. Lissette Ponce and Mrs. Lily Solís, Ovidio Marquez.

To the colleagues of the Volcanology Research Group of the University of El Salvador: Rodolfo Olmos, José Benítez, Francisco Barahona, Benancio Henríquez, Edgar Orantes, Renan Funes and Rafael Cartagena.

To the Ministry of Education of El Salvador "Strengthening Teachers 'Competence Project", for the economic support offered to culminate the Doctorate, in particular thanks to Dra. Erlinda Handal Vice Minister of Science and Technology, Eng. Jose Francisco Marroquin, National Director of Higher Education and Lic. Marta Hortensia Flores.

To the Ministry of Environment and Natural Resources for providing the meteorological and thematic information: special thanks to Celina Kattan, Manuel Díaz, Douglas Hernández, Eduardo

Gutiérrez, Demetrio Escobar, Griselda Marroquín, Walter Hernández, Luis Menjívar, Giovanni Molina, Thelma Chávez, Luis Mixco, Rodolfo Torres and Rosa María Araujo.

The main thing

God Almighty, "Todo lo puedo en Cristo que me fortalece"

To my wife Dora Alicia, my sons Doris Michelle and Miguel Hernández Junior, for all the time I stole them, to dedicate myself to these studies, this triumph is also yours.

To my parents, Nuria and Miguel, the life and education they gave me made me get away, thank you very much.

Miguel Hernández

INDEX

SUMMARY

The susceptibility to landslides triggered by extreme rains with an emphasis on DT96E / hurricane IDA 2009, which caused landslides in the Ilopango caldera El Salvador in Central America, was evaluated. To analyze the statistical effect of the extreme event, it was compared with an inventory of landslides of the same area of year 2003 considered as normal year and a landslides inventory of Río La Joya Basin in the Coatepeque Caldera about DT12E in 2011. The research was developed in the Arenal de Cujuapa basin, Ilopango caldera, with predominance of Geological Formations San Salvador, Cuscatlán and Bálsamo, upper strata of Tierra Blanca Jo4ven. Multivariate Logistic Regression was used, the predictors were Lithology, land use, elevation, slope, orientation, curvature, topographic index of humidity and roughness. Were used Open Source tools: QGIS, ZAGAGIS, R-Studio, and MARS (Multivariate Adaptive Regression Spline), using "EARTH" of "R". Digital Globe satellite imagery was used in Google Earth 2003, 2009 and 2011 to obtain 1503 (2003), 2237 (2009) and 1904 (2011) slides respectively, constituting the calibration data set. The validation schemes were: Autovalidation, based on random partition; Chrono-validation, based on the temporal partition; Transfer model, based on spatial partition. The accuracy was evaluated using the values of the areas under the curve (Receiver Operating Characteristics) and Confusion Matrices. The 2003 and 2009 self-validation models yielded the highest performance values according to their AUC value> 0.8, the Cronovalid models presented good performance although with a decrease of its AUC value> 0.77, the 2009 inventory was able to detect 80% of the landslides in 2003 and a high number of instabilities that were stable zones in 2003. The influence of predictive power of the models according to the set of data and the detonating conditions. The inventory of slips 2003 allowed to calibrate a predictive model of high performance referred to 2009 with decrease of sensitivity to identify the instabilities happened in 2009.

1. INTRODUCTION

El Salvador has an approximate area of 20,700 km^2 with a total of 5,744,113 inhabitants (DYGESTYC 2007), 88.7% of the territory is considered a risk zone and 95% of the population lives exposed to multiple types of hazard: hurricanes, destructive landslides, flood, earthquakes, volcanic eruptions, droughts and El Niño Southern Oscillation (Baum et al., 2001a, 2001b, Major et al., 2004, CEPAL 2011a, Chavez et al 2010).

The combination of tectonic activity, pyroclastic volcanic deposits scattered throughout the territory, fractured volcanic rocks, moderate frequency of earthquakes, tropical climate with heat, rainfall and geomorphology all contribute to an environment prone to landslides (Jibson et al. 2004).

The most populous cities of El Salvador, which house more than 40% of the population, are located a few kilometers from volcanic buildings, such as Santa Ana, San Salvador, San Vicente and San Miguel (Fig. 1.1). These towns are affected by very high hazard conditions not only due to volcanic eruptions but also to lahars type debris flows triggered by recurrent extreme weather events or earthquakes (Major et al., 2004). The capital city of San Salvador is located between two active volcanic centers (recent volcanic chain): volcano of San Salvador made up of products of ashes, scorias and andesitic lavas, its last eruption in 1917 preceded by an earthquake, with a part (the Picacho) of the ancestral VSS (paleovolcán), where a recent history of debris flows is known; the caldera of Ilopango which comprises a wide depression, about 11 kilometers long and 8 kilometers wide, which is occupied by a caldera lake (Ilopango lake), with an area of 75 km^2 (Sebesta 2006), whose steep slopes are formed by several layers of pyroclastic materials from ancient caldera explosions, predisposing to a high susceptibility to landslides.

According to Bommer et al. (2002a, 2002b), in El Salvador the frequency of landslides triggered by rain and earthquakes are the most important natural hazard.

Rain-induced landslides from surficial slope failures mainly in unconsolidated material and steep slopes such as the volcano of San Vicente and El Picacho of the San Salvador volcano can be converted into debris flows that travel hundreds of meters to several kilometers from its origin (Baum et al, 2001a); these sites have a fatal history, whose most recent records indicate significant earth movements for the years 1934, 2001 and 2009.

In the Central American Region including El Salvador, earthquakes also produce slope instabilities of various typologies mentioned by Tsige et al (2009) and represent a very important hazard factor for El Salvador and Central America (Hradecky 2001). Earthquakes are in fact responsible for the activation of large amounts of rock avalanches and landslides. The very high recurrence of seismic events in El Salvador is strictly related to its geological setting Jibson et al. (2004), as it spreads in a region associated to a triple conjunction of the Cocos-Northamerica-Caribe tectonic plates (DeMets 2001). Under these conditions, many landslides are normally preceded by earthquakes.

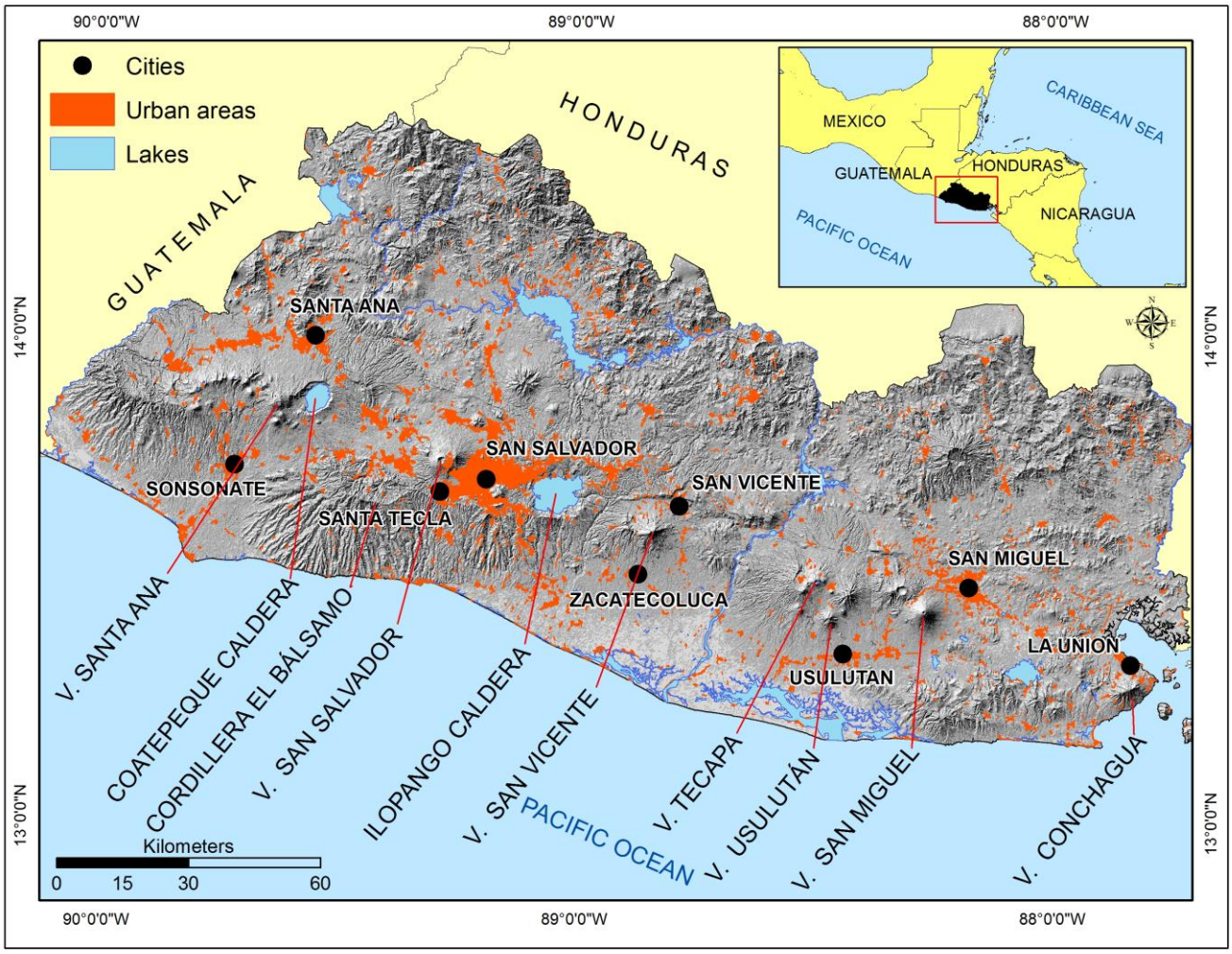

Fig. 1.1 - Urban areas across El Salvador in relation to location of volcanic buildings.

This research was focused on the analysis of extreme rainfall events (cyclones) driven landslides in volcanic tropical landscape and was aimed at assessing related landslide susceptibility stochastic models. El Salvador is in fact strongly exposed to this natural threat, in light of its geological setting and geographic position (just on the hurricane tracks!).

In El Salvador several landslide susceptibility studies have been developed at national level, including the use of statistical methodologies such as Logistic Regression for landslides triggered by earthquakes, but very rarely for landslides triggered by extreme storms, with very few validation protocol; a map of the whole country, produced by heuristic method is now officially used for general landslide

susceptibility assessment. However, in spite of the short time recurrence of debris flows, debris floods and lahars, no studies and validated models or maps have been produced for high scale storm triggered landslide scenario so far; in this sense, the final output of this research was to furnish a tool for Civil Protection and land use planning to the local authorities.

In landslide susceptibility assessment studies, the study area is partitioned into mapping units (typically cells) for each of which the probability of landslide occurrence (the outcome), conditioned to its physical environmental conditions (the conditioning factors), is to be estimated. In particular, by applying binary Logistic Regression the coefficients (b) of a set of i-covariates (x), which are typically derived from geo-thematic maps and digital elevation models, are regressed with respect to a known calibrating landslides inventories. The very simple structure of binary logistic regression models makes this techniques as one of the more largely adopted in scientific literature. MARS (Multivariate Adaptive Regression Spline) non-parametric regression techniques was here applied, which aims at fitting un-linear relationships between predictors and outcome, by fragmenting their range into an optimized number of linear branches. On the basis of the principle stating that the causes of landslides do not change in time and space, a model able to explain the spatial distribution of a calibration set of known landslides is also skilled in predicting the spatial distribution of potential unknown landslides.

Applying stochastic modeling for landslide susceptibility assessment in the case of storm triggered landslides requires the investigation of some methodological topics related to the specific relationships between the time recurrence of the triggering events, the very short duration on the field of the shapes which typically allow us to recognize the effect of past events, the linear/non-linear relationships between storm intensity and susceptibility conditions in resulting in a landslide scenario.

To this main topics, this PhD thesis aimed at giving some possible solutions for approaching susceptibility modeling.

A: THEORETICAL SECTION

2. LANDSLIDES AND DEBRIS FLOWS

The United Nations International Strategy for Disaster Reduction (UNISDR 2009) includes in its definition of geological hazard terrestrial processes such as mass movement, mudslides, rockslides, landslides on the surface and mud or debris streams, implying the hydro-meteorological events as triggers of these processes, as well as Guzzetti et al. (1999), in his definition of hazard by landslides incorporates the concept of dimension and intensity of the natural phenomena that trigger them and the probability of occurrence in a certain place, indicating that normally the studies of prediction of these phenomena are centered in the hillside unstable and potentially unstable and little where they impact.

According to Crozier et al. (2006) landslides hazard is represented as a potential physical damage due to the magnitude and frequency with which they occur, contrary to the risk of landslides, which is the anticipated impact, damages, losses and costs associated with that hazard.

Landslides are progressive, that is to say, the areas adjacent to the landslides could also be destabilized, which is why the identification of old landslides is important. They also indicate that the greatest landslide hazard is generally associated with areas where such phenomena have already occurred (Cruden and Varnes, 1994; Carrara et al., 1995; Aleotti and Chowdhury, 1999).

Varnes (1984) mentions that the alteration caused by a landslide weakens the adjacent areas in particular near the slip crown, creating faults through which water enters, causing block separation and other landslides, this condition helps to identify susceptible areas.

2.1. LANDSLIDE PHENOMENA

The term landslide has been commonly referred to all types and sizes of rock or soil movement on the slopes associated with various types, characteristics and mechanisms of rupture, and depending on the shape of the landslide movement of the material takes several names and is currently object study, aspects such as their occurrence, size, travel speed, triggers, direct and indirect effects, corrective measures and predictability (Highland, 2008). This term is often referred to almost all mass movements including rock falls, debris flows and avalanches (Varnes, 1984) and are associated with one or more of a triggering factor, usually linked to rainfall and earthquakes whose effect on the destabilization of slopes, generation of fractures and landslides; the material can be deposited a few meters away and depending on the size of the landslide deposit represents a hazard to the people, as happened in 2001 in the Quebrada El Muerto in San Vicente volcano, triggered by the earthquakes (Baum et al., 2001), or debris flows that can travel several kilometers causing loss of human life and material as in the same volcano of San Vicente in November 2009 that damaged the villages of Guadalupe, Verapaz and San Vicente (Bowman and Henquinet, 2015).

The identification of the factors that cause slope instability and of the potential failures surfaces is essential for predicting either the areas where landslides could be reactivated in the future or where new others may occur and it is a very important aspect of planning of land use (Chung et al., 1995; Aleotti and Chowdhury, 1999; García-Rodríguez et al., 2008). There are many factors that cause landslides, in recent years statistical methods have been applied that have the possibility to analyze more than one variable at a time, this has strengthened the evaluation of landslide susceptibility. Many of these multivariate methods require mapping of all the morphodynamic and geo-mechanical variables involved in slope instability, including an inventory of landslides that have occurred in the past, and are referred to as multivariate statistical methods used to assess the landslide susceptibility in terms of the probability of

occurrence of landslides. On this basis these methods incorporate model validation procedures and derive prediction models that can help predict where they can occur in the future (Rotigliano et al., 2011). Landslides are generally defined as instabilities of slopes driven primarily by the gravity force, and may manifest in different types of movements (Iverson and Denlinger, 1987). According to Cruden and Varnes (1994) and Varnes (1978), landslides are classified in 5 types depending on movement typology and the material mobilized: Falls, Topples, Slides (rotational and translational), Lateral spreads and Flows (Tab. 1 and Fig. 2).

Type of movement		Type of material		
		Bedrock	Engineering soils	
			Predominantly coarse	Predominantly fine
Fall		Rock fall	Debris fall	Earth fall
Topples		Rock topple	Debris topple	Earth topple
Slide	Rotational	Rock slide	Debris slide	Earth slide
	Translational			
Lateral spread		Rock spread	Debris spread	Earth spread
Flow		Rock flow	Debris flow	Earth flow
Complex		Combination of material or two or more principal types of movement		

Table 2.1 - Short version of the classification of landslides (Varnes 1978)

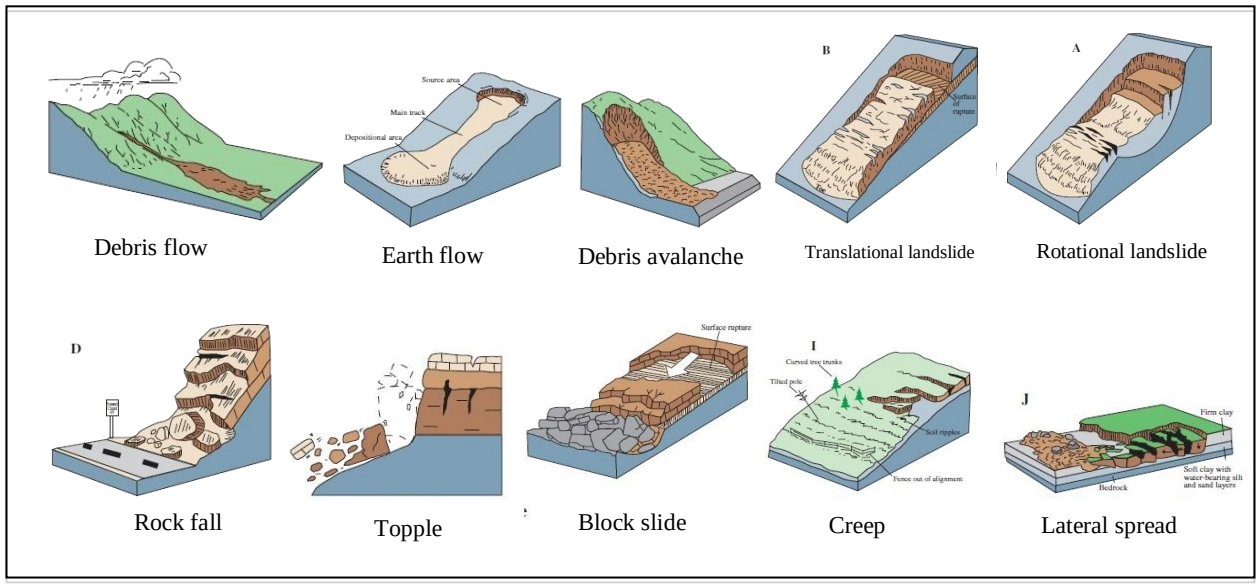

Fig. 2.1 - Major types of landslide movements (mod. from USGS, 2004).

Falls

Varnes (1978) corresponds to the extremely rapid fall of a mass of rocks, earth or debris, due to gravity, separated from a wall or cliff, usually do not travel large distances. Falls are abrupt movements of masses of geologic materials, such as rocks and boulders that become detached from steep slopes or cliffs. Separation occurs along discontinuities such as fractures, joints, and bedding planes, and movement occurs by free-fall, bouncing, and rolling. Falls are strongly influenced by gravity, mechanical weathering, and the presence of interstitial water. Hungr et al. (2014) mentions that the disassociated portions may be singular or clustered that may rupture during impact. Several rock falls were provoked by the earthquake of January of 2001 in Panamerican highway (Los Chorros) in El Salvador.

Topples

They consist of a forward rotation of one or more structural units with a pivot point, by the action of gravity and interaction of forces exerted by fluids in the fractures. Toppling failures are distinguished by the forward rotation of a unit or units about some pivotal point, below or low in the unit, under the actions of gravity and forces exerted by adjacent units or by fluids in cracks. According to Hungr et al. (2014) this movement is initiated by water pressure, by the acceleration produced by an earthquake and this movement can start slow and end extremely fast. Single or multiple blocks may also fall.

Slides

Varnes (1978) and Hungr et al. (2014) these are called landslides and are composed of rupture zone and a propagation zone along one or more surfaces. Although many types of mass movements are included in the general term “landslide,” the more restrictive use of the term refers only to mass movements, where there is a distinct zone of weakness that separates the slide material from more stable underlying material. The two major types of slides are rotational slides and translational slides.

- *Rotational slide*: This is a slide in which the surface of rupture is curved concavely upward and the slide movement is roughly rotational about an axis that is parallel to the ground surface and transverse across the slide).
- *Translational slide:* In this type of slide, the landslide mass moves along a roughly planar surface with little rotation or backward tilting. A block slide is a translational slide in which the moving mass consists of a single unit or a few closely related units that move downslope as a relatively coherent mass.

In tropical regions and volcanic ridges, organic soil layers on pyroclastic deposits are prone to translational landslides, often triggered by extreme rainfall, a correlation is commonly observed between rainfall intensity and soil slip density, as well as increased by the removal of vegetation due to forest fires (Hungr et al., 2014). Translational landslides may also occur in areas of debris accumulation that are subsequently reactivated by increased infiltration of water and seismic activity, to the debris flow by water effect until deposited in the natural drainage.

Rocchi and Vaciago (2013), typifies landslides according to potential characteristics with respect to geomorphology and hydrology, mainly referring to the slope of the terrain, the sequential stage of slippage before, during and after its occurrence and reactivation, and characteristics of the materials related to these movements.

Highland and Bobrowsky (2008) mention that many of the landslide studies apply to the characterization of the internal mechanisms of their displacement and the properties of the original ruptures, which are typically classified in rotational and translational landslides, or the combination of both, predefined the model of its potential behavior of velocity, volume, distance and possible affected areas, even in a single landslide can present several types of movements while the materials are stabilized and deposited. In terms of materials related to landslides and their fluidity, these are often linked to geotechnical

properties, particle size and are defined as the terms rock, soil or soil and debris, and their physical properties closely linked to the state of consolidation that determines the state of fluidity and its form of prosecution in the drainage, this related to the means of its displacement, potential of speed and distance to travel.

Lateral spreads

Lateral spreads are distinctive because they usually occur on very gentle slopes or flat terrain. The dominant mode of movement is lateral extension accompanied by shear or tensile fractures. The failure is caused by liquefaction, the process whereby saturated, loose, cohesionless sediments (usually sands and silts) are transformed from a solid into a liquefied state. Lateral spread were reported in the Ilopango caldera triggered by the earthquakes of 13 January and 13 February 2001 with potential debris and flood flows in the lower part of the caldera, endangering the local population (Baum et al. 2001).

Flows

Coussot and Meunier (1996) mentioned the different types of flows cites in the literature, mudfloods, hyperconcentrated flows, debris flows, lahars, laminar flows and avalanches, which are often complex phenomena whose progressive transition between a physical state of their materials to become a flow by the increase of the energy gained by the effect of the slope and by water, that depends on its speed and propagation (Fig. 2.2).

Pierson (2005) confirms that basins can discharge sediment flows in different proportions, their concentration plays a key role in the flow characteristics and thus the damage they can cause, can be classified into three basic forms: water flow (where the sediments occupy 5% of the volume and the properties of a newtonian flow are preserved), hyperconcentrated flows (the sediments occupy approximately the 40% of volume) and debris flows (where the sediments occupy more than 65% of the volume). The materials mobilized in a debris flow are not consolidated and consist of fragments of rocks, fine granular material, mixture of debris and water (Varnes, 1978). It is usually associated with rapid

movements of soil, rocks, organic matter and a large amount of fine material (Highland and Bobrowsky, 2008), involving complex mechanisms and is linked to volcanic buildings, slope geomorphology, different of elevation from where it originates the landslide until to its deposit (Davies and McSaveney, 2012).

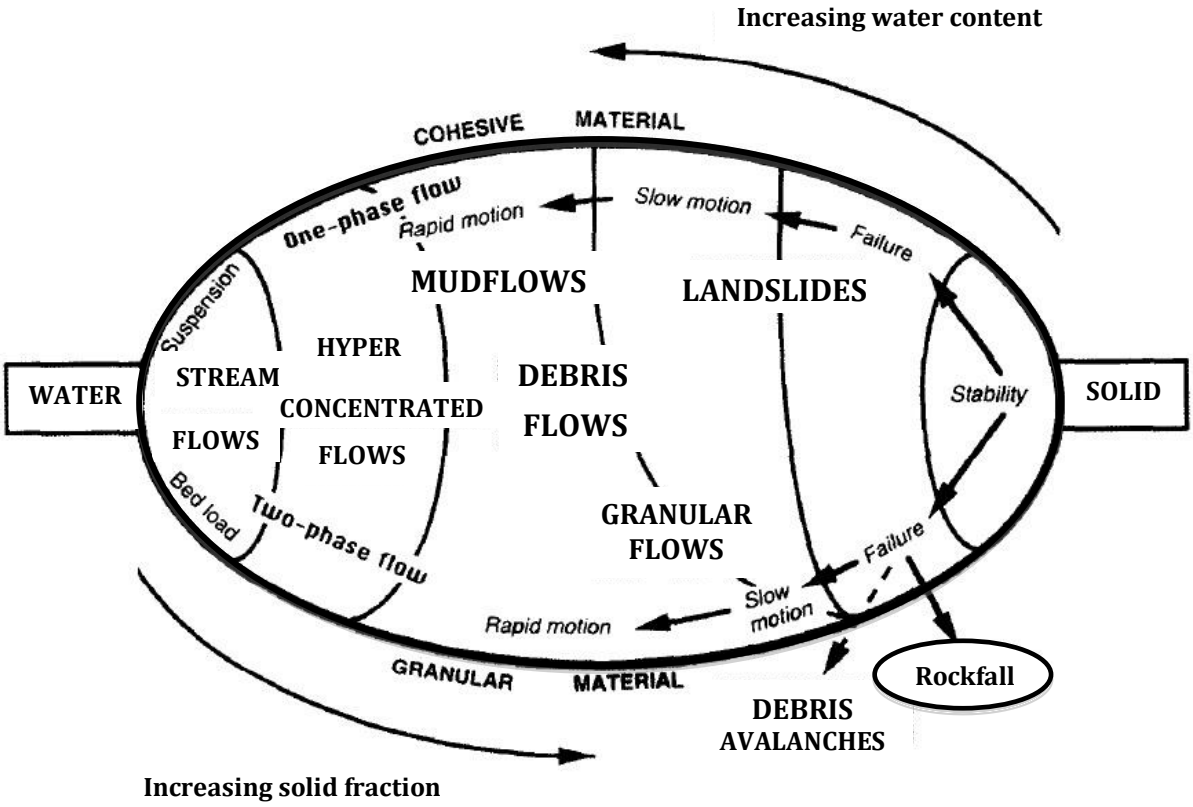

Fig. 2.2 - Classification of mass movements depending on water content (mod. from Coussot and Meunier, 1996).

Flow like landslides are the more complex category of landslide. Hungr et al. (2014) distinguished ten different types on the basis of the involved material:

- Rock/ice avalanche: Extremely rapid, massive, flow-like motion of fragmented rock from a large rock slide or rock fall.
- Dry (or non-liquefied) sand/silt/gravel/debris flow: Slow or rapid flow-like movement of loose dry, moist or subaqueous, sorted or unsorted granular material, without excess pore pressure.

- Sand/silt/debris flowslide: Very rapid to extremely rapid flow of sorted or unsorted saturated granular material on moderate slopes, involving excess pore-pressure or liquefaction of material originating from the landslide source. The material may range from loose sand to loose debris (fill or mine waste), loess and silt. Usually originates as a multiple retrogressive failure. May occur subaerially, or under water.
- Sensitive clay flowslide: Very rapid to extremely rapid flow of liquefied sensitive clay, due to remolding during a multiple retrogressive slide failure at, or close to the original water content.
- Debris flow: Very rapid to extremely rapid surging flow of saturated debris in a steep channel. Strong entrainment of material and water from the flow path.
- Mud flow: Very rapid to extremely rapid surging flow of saturated plastic soil in a steep channel, involving significantly greater water content relative to the source material. Strong entrainment of material and water from the flow path (Plasticity Index>5 %).
- Debris flood: Very rapid flow of water, heavily charged with debris, in a steep channel. Peak discharge comparable to that of a water flood.
- Debris avalanche: Very rapid to extremely rapid shallow flow of partially or fully saturated debris on a steep slope, without confinement in an established channel. Occurs at all scales.
- Earthflow: Rapid or slower, intermittent flow-like movement of plastic, clayey soil, facilitated by a combination of sliding along multiple discrete shear surfaces, and internal shear strains. Long periods of relative dormancy alternate with more rapid “surges”.
- Peat flow: Rapid flow of liquefied peat, caused by an undrained failure.

Complexes

Often in a landslide many kinds of landslides occur in their development and happen that are very difficult to typify them (Varnes 1978).

A recent revision of Varnes (1978) classification system has been proposed (Tabs 2.2), where a more deep insight into the failure-propagation stages and into the difference between landslide material and water content is proposed (Hungr et al., 2014).

On the basis of velocity, according to WP/WLI (1995), the landslides are classified in seven classes which are shown in the Table 2.3.

Type of movement	Rock	Soil
Fall	1. *Rock/ice* fall[a]	2. *Boulder/debris/silt* fall[a]
Topple	3. Rock block topple[a]	5. *Gravel/sand/silt* topple[a]
	4. Rock flexural topple	
Slide	6. Rock rotational slide	11. *Clay/silt* rotational slide
	7. Rock planar slide[a]	12. *Clay/silt* planar slide
	8. Rock wedge slide[a]	13. *Gravel/sand/debris* slide[a]
	9. Rock compound slide	14. *Clay/silt* compound slide
	10. Rock irregular slide[a]	
Spread	15. Rock slope spread	16. *Sand/silt* liquefaction spread[a]
		17. Sensitive clay spread[a]
Flow	18. *Rock/ice* avalanche[a]	19. *Sand/silt/debris* dry flow
		20. *Sand/silt/debris* flowslide[a]
		21. Sensitive clay flowslide[a]
		22. Debris flow[a]
		23. Mud flow[a]
		24. Debris flood
		25. Debris avalanche[a]
		26. Earthflow
		27. Peat flow
Slope deformation	28. Mountain slope deformation	30. Soil slope deformation
	29. Rock slope deformation	31. Soil creep
		32. Solifluction

For formal definitions of the landslide types, see text of the paper.

[a] Movement types that usually reach extremely rapid velocities as defined by Cruden and Varnes (1996). The other landslide types are most often (but not always) extremely slow to very rapid

Tab. 2.2- Summary of the Varnes classification system modified by Hungr et al (2014).

Velocity class	Description	Velocity (mm/s)	Typical velocity	Response[a]
7	Extremely rapid	5×10^{3}	5 m/s	Nil
6	Very rapid	5×10^{1}	3 m/min	Nil
5	Rapid	5×10^{-1}	1.8 m/h	Evacuation
4	Moderate	5×10^{-3}	13 m/month	Evacuation
3	Slow	5×10^{-5}	1.6 m/year	Maintenance
2	Very slow	5×10^{-7}	16 mm/year	Maintenance
1	Extremely Slow			Nil

[a] Based on Hungr (1981)

Tab. 2.3- Landslide velocity scale (WP/WLI 1995 and Cruden and Varnes 1996)

2.2. THE DEBRIS FLOWS

Debris Flow are triggered by heavy rains and can spread and travel channeled in a drainage for many kilometers from their point of origin causing great loss of lives and materials in the place where the materials are deposited.

"*Debris flow it's a flow of sediment and water mixture in a manner as if it was a flow of continuous fluid driven by gravity, and it attain large mobility from the enlarged void space saturated with water or slurry*" (Takahashi, 2014)**.**

Highland and Bobrowsky (2008) and Hungr et al. (2015) mention that a debris flow is sometimes preceded by other kinds of landslides, avalanches and rock fall, which cause the slopes to be detached and deposited in the channels, previous to the movement of the fluid.

The materials involved when combined with water are fluidized and channeled in a natural drainage, mobilizing in the form of leaves or lobes depending on the geotechnical and rheological properties of the material (Fookes et al., 2007), that is, the sediments are kept in suspension by effect of the fluid mechanics with respect to the properties of viscosity, concentration, density and fluid turbulence (Jakob et al. 2005). According to Bommer et al. (2002), debris flows are influenced by vegetation cover and land use, these factors also define the velocity of the flow and the distance to travel, not forgetting the

detonating factors of these movements, such as earthquakes and rain, which also define the failure mechanism.

Jakob et al. (2005) assumes that a debris flow is a complex phenomenon and must comprise the whole process from the place where landslides occur on the slope, their channeling to natural drainage, their mobilization by water effect and their Final deposition in the alluvial fan.

According to Takahashi (2014), the potential energy of the materials is converted to kinetic energy and is consumed by the frictional force that exists between the materials that move and the surface where they slide, this movement of materials is affected by the size of the particles in motion and their distribution, the concentration of the sediments in the flow, the properties of the interstitial fluid, the hydraulic conditions of the flow, the channel width and the elevation gradient.

Hungr et al (2014), stresses that debris flows in the propagation stage can entrain materials (from fine debris to even large boulders) of other landslides or fluvial processes, which are is kept in suspension by effect of the mechanics of the fluid deposits, increasing their kinetic energy and power of damage.

Unlike a debris avalanche where the materials interact through contact of the particles where collision, friction and cohesion phenomena occur, with air as an interstitial medium, in a debris flow there is a strong interaction between the particles and water as an interstitial medium behaving like a flow (Jakob et al., 2005).

2.3. LANDSLIDE CAUSES

Varnes (1984) mentioned that there are several factors that influence the stability of slopes and their typology, on the one hand intrinsic factors or those related to the conditions inherent in lithology (types of rocks and physical and chemical properties of soil, composition and their physical, geotechnical properties), structure (lithological discontinuities, degree of fracture of rocks), geomorphology (type,

degree and shape of slope), hydrological condition (water quantity and pressure) characteristics that do not change significantly in the time, and the vegetal cover.

On the other hand Chung et al. (1995) and Highland and Bobrowsky (2008) mention that the extrinsic factors known as triggers refer to the conditions prevailing in the area such as climatic conditions (temperature, extreme rains, precipitation pattern causing slope saturation and which correspond the first causes of landslides), earthquakes, anthropic factor (land use change, deforestation, forest fires, changes in drainage patterns, destabilizing slopes) and the effects of gravity force on materials. Many of these factors can act simultaneously and also separately, may act slowly, as is the case of moderate seismicity, or act suddenly as extreme rains and strong earthquakes that have the characteristic that affect large areas, also have an impact on the degree of fracture of the rocks, fall in the soil, increasing the infiltration of rainwater and the probability of landslides due to liquefaction.

Forest fires leave the soil uncovered and exposed to increased sun effects and consequent high temperatures, receiving the impact of water erosion and increased debris flows, increasing on strong slopes and slopes of volcanoes with pyroclastic deposits.

The slope stability depends on the combination of many factors which perturb the natural equilibrium. In particular, the causes of slope failure are following described:

- Increase of shear stress: It can be related with modifications of the slope geometry (erosion or anthropic actions, ecc.), seismicity and artificial vibrations.
- Decrease in shear strength: It depends on variations of pore pressure which can be related with increase of bulk density, slope angle and dynamic solicitation or decrease of cohesion and modification of resistance of soil.

The factors conditioning the slope stability can be distinguished in:

• Predisposing factors: they act constantly in time and are connected with lithology, geology, orography, morphometry, geomorphology, geotechnics, climate, hydrology, hydrogeology, tectonics, vegetation, land use and anthropic activity.

• Triggering factors: they are connected with external short time impulses which modify the natural equilibrium like extreme meteorological events, snow melting, accelerated erosion, earthquakes etc.

3. LANDSLIDE SUSCEPTIBILITY ASSESSMENT

3.1. LANDSLIDE SUSCEPTIBILITY

The term "landslide susceptibility" is a concept that expresses the spatial probability of occurrence of landslide given the specific characteristics of the area studied, using a model that relates past events and factors that cause landslides (Rotigliano et al., 2011).

Many are the methods for the evaluation of susceptibility to landslides, including deterministic, heuristic and stochastic (Pardeshi et al., 2013) approaches. According to the European Union, landslide susceptibility studies should be based on statistical methodologies, producing strategic tools for risk mitigation.

Many methods of evaluation have been applied for the landslide susceptibility models assessments, studies of rocks and lithologic characteristics, study of rocks alteration processes, soil analysis by quaternary events such as erosion, among others (Hradecky, 2011).

Landslide susceptibility is the likelihood of a landslide occurring in an area on the basis of local terrain conditions (Brabb, 1984). It estimates “where” landslides are likely to occur without considering the magnitude of the expected landslides and the temporal probability of failure (Committee on the Review of the National Landslide Hazards Mitigation Strategy, 2004). In mathematical language, landslide

susceptibility is the probability of spatial occurrence of slope failures, given a set of geo-environmental conditions. Landslide susceptibility zoning involves the spatial distribution and rating of the terrain units according to their propensity to produce landslides. The problem of whether the susceptibility zoning should include also potential travel and regression of landslide is still debated. Some experts think that it only should be considered in hazard zoning. However, being the frequency difficult to assess, information about travel and regression can be lost. For this reason, they should be considered, if possible, in susceptibility zonation (Fell et al., 2008).

Landslide hazard is the probability that a landslide of a given magnitude will occur in a given period and in a given area. It predicts "where", "when" or "how frequently" a slope failure will occur, and "how large" it will be (Guzzetti et al., 2005). Landslide hazard zoning should be done considering the conditions at the time of the study. The effect of urban development sometimes can increase the likelihood of landslides. In that case it should be done an a posteriori evaluation. Hazard zoning should be evaluated in quantitative terms. However, sometimes it is difficult to accurately estimate the frequency. In this case, a qualitative estimation can be adopted (Fell et al. 2008).

Landslide risk is the expected annual cost of landslide damages throughout an area. Risk maps combine the probability information from a landslide hazard map with an analysis of all possible consequences (property damage, casualties, and loss of service). Risk zoning should be updated on a regular basis.

Landslide susceptibility evaluation should satisfy the following widely accepted assumptions (Varnes et al., 1984; Carrara et al., 1991; Guzzetti et al., 1999):

- Slope failures leave discernible features that can be recognized, classified and mapped in the field or through remote sensing, chiefly stereoscopic aerial photographs.

- Landslides are controlled by mechanical laws that can be determined empirically, statistically or in deterministic fashion. Conditions that cause landslides (instability factors), or directly or indirectly linked to slope failures, can be collected and used to build predictive models of landslide occurrence.
- The past and present are keys to the future.
- Landslide occurrence, in space or time, can be inferred from heuristic investigations, computed through the analysis of environmental information or inferred from physical models. Therefore, a territory can be zoned into susceptibility (or hazard) classes ranked according to different probabilities.

Ideally, the evaluation of landslide susceptibility and its mapping should derive from all of these assumptions but the application of the all principles is very often a difficult task (Carrara et al., 1995, 1999; Guzzetti et al., 1999).

3.2. METHODS FOR SUSCEPTIBILITY ASSESSMENT

Landslide susceptibility can be assessed either in qualitative or quantitative way. The qualitative approach is based on expert judgment. It expresses the susceptibility level in terms of descriptive categories and the stability map is derived without a clear indication of rules which have led to the assessment.

The quantitative methods use data treatment techniques which evaluate the relative significance of the parameters and then correlate them with the spatial distribution of landslide obtaining the best match (Varnes et al., 1984; Carrara et al., 1995; Hutchinson, 1995; Soeters and van Westen, 1996; van Westen et al., 1997; Guzzetti et al., 1999; Fell et al., 2008)

The direct methods consist in the creation of a susceptibility map in field or by using orthophoto or satellite images. Sometimes, those maps are aimed to the creation of a landslide inventory.

On the other hand, the evaluation of susceptibility using indirect methods consists of 4 phases:

1. Creation of the landslide inventory;

2. Identification and mapping of the variables which are directly or indirectly related with the slope instability;

3. Classification of the area in different susceptibility levels;

4. Validation of the model.

The most commonly used methods can be grouped in 5 classes: direct geomorphological mapping, analysis of landslide inventories, heuristic or index based methods, statistical methods, including neural networks and expert systems, and process based, conceptual models. Among the different classes there is not a clear distinction and the used method can be associable to different classes. (Carrara et al., 1995; van Westen, 1993; Hutchinson, 1995; Soeters and van Westen, 1996; van Westen et al., 1997; Guzzetti et al., 1999; Committee on the Review of the National Landslide Hazards Mitigation Strategy, 2004).

Geomorphological mapping or distribution analysis: It is a qualitative semi-direct which strongly depends on the ability of the investigator in identifying the slope failure.

It is the most straightforward way for distinguishing areas prone to slope failures from more stable areas. The result of geomorphological mapping is rather limited as they only represent one snapshot within a long history of slope evolution, and due to their purely descriptive nature, they have no power for predicting future events.

Analysis of inventories: Using this method the highest susceptible zones are determined studying the distribution of the past landslides. This is obtained preparing landslide density maps which are maps indicating the percentage of area covered by the landslide deposits without considering the

geoenvironmental variables. This is an indirect and quantitative method. The landslide density can be considered a good estimation of frequency. However, the errors of the method depend on the errors associated to the inventory.

Heuristic methods: this is a qualitative approach based on subjectively defined rules for relating landslide susceptibility to certain predictors. Two main type of heuristic analysis exist: geomorphic analysis and qualitative map combination.

In geomorphic analysis the susceptibility is determined by experts reasoning by analogies. The result is highly subjective. Qualitative map combination consists in assigning a weight to different input factor related to landslides. The susceptibility classes are determined on the bases of the sum of different weights (Fell et al., 2008).

Geostatistical methods: The statistical approaches are based on the relationships between each factors (predictors) and the past distribution of landslides (dependent variable). The use of a statistic method contemplates the creation of a landslide inventory and the mapping of a set of variables which are supposed to be related with the instability conditions. Therefore, interrelation among landslides and factors are evaluated in an objective way. There are various applicable statistical methods: bivariate analysis, multivariate statistical methods (logistic regression and discriminant analysis) and artificial intelligence methods (distribution free methods).

The results of statistical models should be performing, reliable and geomorphologically sound. In this case landslide susceptibility is evaluated trough a largely objective and reproducible procedure.

Experts choice must be taken regarding the selection of suitable statistical methods, potential predictors, diagnostic areas (Costanzo et al., 2012a; 2012b; Rotigliano et al., 2011; Süzen and Doyuran, 2004) and mapping units (Carrara et al., 1991; 1995; 1999; Guzzetti et al., 1999).

A geomorphological criteria must be adopted in order to select the independent variables (in this case a set spatial geoenvironmental attributes), which could directly or indirectly (as proxies) be related to debris flow activation. Those variables represent the potential landslide controlling factors. Consequently, a subset of performing variables must be chosen from the set of potential predictors through a statistically based selection procedure.

Process based models (deterministic or physically based models): these are based on the physical laws controlling the slope instability. Those models are divided in two classes: spatially distributed and physically based models. The spatially distributed models uses input variables which change in the space and are not concentrated in one point. On the other hand, the physically based models are based on theoretical laws and equations which describe the phenomenon on a physical point of view.

Deterministic (physically-based) models require the understanding of the physical process which regulates the slope failure. The parameterization of physically based models requests a wide dataset and therefore, they are usually only applicable to small areas (small catchment scale, few square kilometers).

An essential point for physically-based modelling of landslides is to know about the mechanics of the slope failure. In fact, different phenomena request the application of completely different model algorithms.

The basic concepts for physically-based slope stability modelling is the factor of safety, or factor of stability, FOS, in its most simple formulation:

$$FOS = \frac{Resisting\ force}{Driving\ force} = \frac{Shear\ strenght}{Shear\ stress} = \frac{S}{\tau} \qquad (1)$$

Values of $FOS < 1$ indicate unstable conditions.

Physically based models consist in a hydrological and a slope stability model. On the bases of different hydrological component it is possible to distinguish steady state and dynamic models. The steady state models assume a slope parallel flow either in its steady state as a function of slope and drainage area while dynamic models evaluate the entire process from rainfall to the transient response of the groundwater. Dynamic models are capable to run forward in time, using rules of cause and effect to simulate temporal changes in the landscape. A dynamic landslide hazard model addresses the spatial and temporal variation of landslide initiation or runout but the parameterization is often complicated because of the amount of requested data (Malet, 2005; van Beek and van Asch, 2004). In the Table 2.1 the most common physically based models are resumed.

Model	Main features	Distribution	Selected applications
CHASM	2-dimensional combined hydrological and slope stability model	commercial	WILKINSON et al. (2002)
LAPSUS-LS	extension to the landscape evolution model LAPSUS, based on critical rainfall and distribution maps, partly GIS-based		CLAESSENS et al. (2005)
GISLIP, SHESLIP	extensions to the SHETRAN sediment transport model: GISLIP computes hydrology and factor of safety (GIS-based), SHESLIP the failure patterns at coarser resolution		BURTON et al. (1998), BURTON & BATHURST (1998)
SHALSTAB	combined hydrological and slope stability model, assuming infinite slope and steady-state subsurface flow; extension to ArcView	free	GORSEVSKI et al. (2001)
TRIGRS	deterministic model for simulating rainfall infiltration and slope stability, developed by the USGS	free	CHEN-YUAN et al. (2005)
JUST-SLOPE	slope stability model for rotational failures, including ordinary method on slices and Bishop method		MALKAWI & TAQUIEDDIN (1996)
SINMAP	slope stability model based on infinite slope stability approach, allowing uncertainties; extension to ArcGIS/ArcView	free	THIEBES et al. (2007)

Tab. 2.4 - Selection of existing model framework dealing with deterministic modelling of slope stability (Mergili, 2008).

3.2.1. Logistic regression

Binary logistic regression (BLR) analysis is the multivariate statistical technique which was widely used in this research. It is based on a frequentist approach used to model the expected value of a response variable by a linear combination of continuous and discrete predictor variables (Hosmer and Lemeshow, 2000).

In logistic regression the response variable Y assumes binary values 0 or 1. In this case, Y= 0 is the absence of debris flows and Y=1 is the presence of debris flows.

The relationship between the predictors and the probability that the response variable assumes the value 1 is linearized by the logit function logit(Y) and corresponds to the following transformation:

$$logit(Y)= ln[P(Y=1)/(1-P(Y=1))]=\alpha+\beta_1 x_1+\beta_2 x_2+....+\beta_n x_n; \quad (2)$$

Where $P(Y=1)$ is the probability that the response variables assumes the value 1, α is the constant term or intercept, the $x_1,x_2,...x_n$ are the input predictor variables and the β_n their coefficients.

Therefore, ones the logit function is calculated, and the β_n values are known, the probability can be back estimated using the following formula:

$$P(Y=1)=e^{logit(Y)}/[1+e^{logit(Y)}]; \quad (3)$$

This equation ensures that, for any given case, the probability $P(Y=1)$ will not be less than 0 or greater than 1 with $logit\ (Y)=\pm\infty$.

The logistic regression uses the maximum likelihood technique to maximize the value of the log-likelihood function (LL), which indicates how likely is to obtain the observed value of Y, given the values on independent variables and coefficients (Menard, 2002). In other words, the maximum likelihood allows us to estimate the best intercept and βn coefficients.

To estimate the global fitting of the regressed model on the data domain, the -2LL (negative log-likelihood) is used. -2LL is an estimator of model fitting based on maximum likelihood technique. The differences in -2LL value between the model with only the intercept ($L_{INTERCEPT}$) and the full model (L_{MODEL}) have a $\chi 2$ distribution, so that we can use the chi-square test of significance of the regression

coefficients (Olmacher and Davis, 2003; Akgun, 2012). In other words, the -2LL tests the increase in model fitting produced by the introduction of the predictors: the larger its value, the better is the fitting. The model fitting can be also evaluated by exploiting two pseudo-R_2 statistics: the McFadden (1979) R_2 and the Nagelkerke (1991) R^2. The first is defined as $1-(L_{MODEL}/L_{INTERCEPT})$ being confined between 0 and 1. As a rule of thumb (Mc Fadden, 1979), values between 0.2 and 0.4 attest for excellent fit. Nagelkerke R^2 is a corrected pseudo-R^2 statistics, ranging from 0 to 1 (Nagelkerke, 1991).

The application of BLR has many advantages. One of them is given by the possibility of using all types of predictor variables (continuous, dichotomous or polychotomous), requiring linearization for the nominal ones. Another advantage is the easy interpretation of the results also in geomorphological terms. In particular, the sign of the β coefficients joined to the odd ratios (OR) values express the correlation between the response variable and the predictors. More in detail, the OR is calculated by exponentiation of b and indicates how likely (or unlikely) it is for the outcome to be positive (unstable cell) when a unit change of an independent variable occurs. Negatively correlated variables will produce negative β and OR limited between 0 and 1; positively correlated variables will result in positive β and OR greater than

One of the constraints that must be fit with BLR is to perform regression on balanced datasets of positive and negative cases (Atkinson and Massari, 1998; Süzen and Doyuran, 2004; Nefeslioglu et al., 2008; Van Den Eeckhaut et al., 2009; Bai et al., 2010; Frattini et al., 2010), so that a random extraction of negatives (whose number typically overhang that of positives) is required.

3.2.2. Mapping units

Evaluation of the likelihood of a landslide occurring in an area on the basis of local terrain conditions requires the preliminary selection of a suitable terrain mapping unit (TMU).

The term refers to a portion of the land surface which contains a set of ground conditions that differ from the adjacent units across definable boundaries. At the scale of the analysis, a mapping unit represents a domain that maximizes internal homogeneity and between-units heterogeneity.

Based on the concept of a distinct, clearly definable TMU, various methods have been proposed to partition the landscape for landslide susceptibility assessment and mapping. All methods fall into one of the following groups (Carrara et al., 1995; Soeters and van Westen, 1996; Guzzetti et al., 1999).

- **Grid cells:** in this case the territory is divided into regular areas ("cells") of pre-defined size, which become the mapping unit of reference.
- **Terrain units:** they are based on the interrelations between materials, forms and processes determined by the observation in natural environments. More precisely, they are units whose boundaries reflect geomorphological and geological differences.
- **Unique condition units:** They derive from the overlapping of layers classified on the basis of different criteria. Size and nature of this units depend on the criteria used in classifying the input factors.
- **Slope Units:** they derive from the partition of the territory in correspondence of drainage and divide-lines. This division results into homogenous hydrological regions. Slope Units can be identified manually or using specific tools for the automatic delineation.
- **Geo-hydrological units**: Geo-hydrological units are obtained by further partitioning the slope units based on the main lithological types cropping out in a region and considered important to separate dissimilar susceptibility conditions within the same slope.
- **Topographic units**: Topographic units are vector-based subdivisions obtained by partitioning a catchment, or a single slope, into stream tube elements of irregular size and shape. Thus, topographic units are a particular subdivision of slope units.
- **Political or administrative units:** When investigating very large areas, such an entire region or a nation, political, administrative or demographic units can be adopted (e.g., census zones, municipalities, districts, provinces).

Susceptibility methods and mapping units are conceptually and operationally interrelated (Carrara et al., 1995). Table 2.4 summarizes the main correlations.

	Direct Mapping	*Analysis of inventories*	*Index based*	*Statistical*	*Physically based*
Grid cell		✓		✓	✓
Terrain unit	✓				
Unique condition unit			✓	✓	
Slope unit		✓		✓	
Geo-hydrological unit				✓	
Topographic unit					✓
Geographical unit		✓		✓	

Tab. 2.5 - Relationship between mapping units and methods for landslide susceptibility assessment.

3.2.3. Diagnostic areas

The diagnostic areas are the core of the whole stochastic approach as they define where we expect the model will "learn" how to identify the geo-environmental conditions which lead to the presently recognized landslides. The diagnostic areas (Costanzo et al. 2012b, 2014; Rotigliano et al. 2011) are those portions of a landslide map where, on the basis of a failure model (which can be stated on the basis either of physical or geomorphological criteria), we hypothesized that the geo-environmental conditions that caused the past phenomena can be detected. In fact, under the assumption the past is the key to the future, a susceptibility map can be produced by any classification method that would result capable of predicting the spatial distribution of the diagnostic areas.

3.2.4. Validation

An important part of every statistical landslide susceptibility or hazard analysis is the validation. It has to be verified that the majority of the landslides of the inventory are in zones classified as highly susceptible.

In order validate the model a quantitative and rigorous validation procedures has to be applied. In particular, any evaluation of the skill and the reliability of a predictive model should consider both its accuracy and robustness. To accomplish this task, training and test data are needed, corresponding to known and unknown cases. The first set is the one we use to constrain the maximum likelihood estimator when regressing the model through BLR; the second dataset is the target we want to match (i.e. the future phenomena). According to Chung and Fabbri (2003), training and test datasets can be obtained by either exploiting multi-temporal landslide inventories (*time partition*), or partitioning single-epoch datasets (*random time partition*) or dividing the study area in two similar sub-sectors, one for training and one for testing (*spatial partition*). *Random time partition* procedures can be applied either on the landslide inventory (Conoscenti et al., 2008a) or on the mapping units database (Conoscenti et al., 2008b), whilst *spatial partition* can also be not adjacent such as in the study aimed at susceptibility model exportations (Costanzo et al. 2012a; von Ruette et al., 2011). Calculating a susceptibility means obtaining a prediction image Chung and Fabbri, 2003).

- **Accuracy**: It is calculated comparing the prediction image to the status (stable/unstable) of each mapping unit. It can be evaluated calculating both in terms of the *degree of fit* and the *prediction skill* when considering the accuracy of the model in predicting the known and unknown cases, respectively. In other words, the degree of fit is estimated if the model is able of classify known cases, whilst in the second case the model is asked to predict unknown cases. Two different outputs can be prepared to estimate both the *degree of fit* and the *prediction skill* accuracy indexes. A first method is based on classic contingency tables which compare classified/predicted to known/unknown stable and unstable cases, by considering a 0.5 cut-off value for $\pi(\boldsymbol{x})$. A partition in true positive (TP) and negatives (TN), and false positive (FP: Error Type I) and negatives (FN; Type II error) arises in this way and, together with the model error rate (TP+TN/FP+FN), single estimates of sensitivity or hit rate (TP/(TP+FN)) and 1

- specificity (FP/(TP+FN)), it is possible to compute a large number of other metrics which can attest for the goodness of the model (Carrara et al., 2003; Guzzetti et al., 2006; Frattini et al., 2010; Rossi et al., 2010). According to Frattini et al. (2010), we can define this accuracy assessment as a cut-off dependent accuracy estimation.

The second method is based on the ROC (Receiver Operating Curves) curves and is focused on testing the accuracy of the *prediction image*, when "tuning" the cut-off value for $\pi(\boldsymbol{x})$. In fact ROC curves plot the cumulated accuracy with which the classification/prediction matches the known/unknown status of all the mapping units. The method consists in plotting a ROC curve, which fits pairs of points in a TP-rate Vs. FP-rate graph, obtained for monotonically decreasing $\pi(x)$ cut-off values. The validation is based in this case on the quantitative evaluation of the tradeoff between sensitivity and 1-specificity, and can be synthetically expressed by measuring the area under the ROC-curve (AUC): the larger the AUC, the higher the accuracy. A similar but prevalence-affected version of the ROC curves method directly concentrates on the analysis of rate curves which plot the percentage of landslide area against the percentage of susceptible mapped area, for decreasing level of the susceptibility (Chung and Fabbri, 2003). This is typically performed after having reclassified the mapped area in equal interval or area susceptibility classes. ROC curves analysis gives a more complete estimate of the accuracy of the model, as it condenses an infinite number of contingency tables, enabling an estimation of the auto-consistency and linearity of the classification/prediction function in the domain of the two Types of Errors. Moreover AUC is a cut-off independent metric for accuracy (Frattini et al., 2010).

- **Robustness:** it establishes how much we can trust an apparently accurate model. To accomplish this task, we need to replicate n times the procedure which lead to the estimates of the model parameters (selected factors and coefficients) and the probability of each mapping unit, evaluating their mean values and dispersions. More clearly, it consists in repeating the susceptibility calculation many times and

evaluate how much different are the results of the experiment we carry out. The most uniform are the results the most robust is the model.

3.3. LANDSLIDE SUSCEPTIBILITY STUDIES IN EL SALVADOR

The landslide susceptibility has been the subject of several studies in El Salvador and the Central American region:

García-Rodríguez et al. (2008a) evaluated the probability of occurrence of earthquake-induced landslides throughout the country using a Multivariate Logistic Regression model and a inventory of landslide from the Ministry of Environment and Natural Resources related to the January 2001 earthquake, to produce a landslide earthquake-induced susceptibility map. The key factors in the model were the Roughness and the soil type, in this study did not include any validation process of the model.

Garcia Rodríguez et al. (2008b) used a methodology based on the Newmark and GIS model, which treats a potential landslide as a rigid sliding block on an inclined plane and requires information from Geology and earthquake as magnitude and source distance, soil moisture conditions and slope. These same authors (2010) evaluated using the Artificial Neural Networks (ANN) model to assess regional landslide susceptibility; The results of the susceptibility analysis to landslides with ANN are verified using the landslide location data and shows a high concordance between the inventory of landslides and the area estimated high susceptibility, nor does it detail a validation process of the model.

Kopačková and Šebesta (2007) used multivariate information to analyze the landslide susceptibility, a set of data derived from DEM, micro-alignment density obtained with LANDSAT images, land use, geology, geomorphology and an inventory of 363 landslides caused by Hurricane Mitch, applying Zonal Statistics (Zonal Statistics) to assign individual weights to each variable, this methodology did not detail the use of validation processes of the model.

Fernández-Lavado et al (2008), assessed the landslide susceptibility in the Metropolitan Area of San Salvador applying a Bivariate Analysis considering geological, slope, aspect, geomorphology, fracturing and land use as an conditioning variables, an inventory of landslides of the area taking into account Landslides caused by human actions (anthropic density).

The Ministry of Environment and Natural Resources (MARN, 2004), used a heuristic method known as Mora-Vahrson (Mora and Vahrson, 1991), uses 5 factors grouped into 2 categories: intrinsic factors are relative relief, lithology, soil moisture and external factors are intensity of earthquakes and rainfall intensity; for the analysis was not used inventory of landslides. The landslide susceptibility map of this work is officially used in El Salvador.

Ríos et al. (2016) created a landslide susceptibility evaluation model triggered by the earthquake of January 13, 2001 in the Metropolitan Area of San Salvador, where 4,792 landslides were identified, along with 7 conditioning factors: geomorphology, geology, precipitation maximums, seismic accelerations, slope of the terrain, distance to road and geological faults. For the evaluation of the susceptibility, a methodology based on Artificial Neural Networks (RNA) was used, compared with Logistic Regression to measure the performance of the model, incorporating the geostatistical method of kriging. No model validation process was detailed in this research.

B: STUDY AREA

4. REGIONAL SETTING

El Salvador, located in the central west portion of the Chortis Block on the Caribbean Plate (Martínez et al., 2009), a geographic region located approximately 150 kilometers from the Middle American Trench (Siebert et al., 2004). It is considered that 95% of the soil of the territory is of volcanic origin resulting from intense volcanism since the Tertiary period (Neogene), which gave rise to the formation of numerous stratovolcanoes, many of them with unstable slopes and fractured rocks.

The earliest materials appear at the Northwest of the country, mainly in Metapán, with a basic volcanism and a small stratigraphic sequence associated with the Jurassic and Cretaceous age (Babůrek, 2005), correlated with a similar development in Guatemala and Honduras and have been paleontologically Confirmed (Hradecky, 2011).

The territory is mainly linked to two genetically related tectonic systems (Canora et al., 2014): the first, has been contained in the western part of the Caribbean Plate, under which the Cocos plate is subducted in the southwestern region (Fig. 4.1) (Singh 1993), here the genetic quake zone called Middle American Trench in Central America (Benito et al., 2012), with convergent plate boundary at speeds of 73-84 mm/year (Tikoff and Demets, 2011).

The territory is also geologically influenced by the interaction of the tectonic plates of Pacific and North America, however the main seismic activity has been interpreted as the result of activity driven by the convergence between the Cocos and Caribe plate (White, 1991). The second tectonic system corresponds to the zone of deformation of the volcanic arc where there have been earthquakes of medium magnitude (Mw <= 7) (Canora et al., 2012), as occurred on February 13, 2001 (Mw 6.6), in the so-called El

Salvador Fault Zone (ZFES), which comprises a shear zone with a dextral-direction movement that runs through WNW-ESE El Salvador over more than 100 km and is divided into several segments (Martínez et al., 2009), the same structure where the largest historical earthquakes occurred along this volcanic arc in El Salvador (Canora et al., 2014) and have triggered large-scale landslides (Jibson et al., 2004).

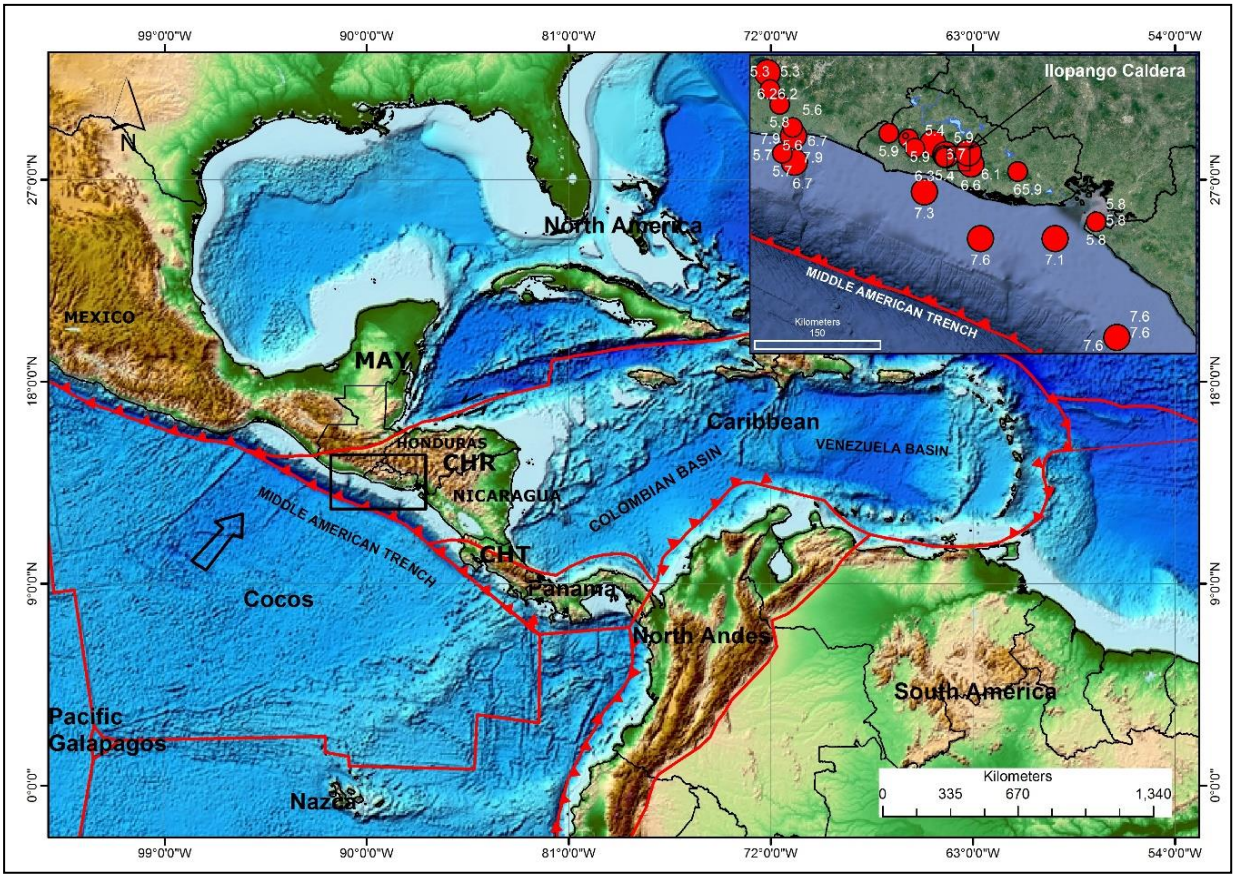

Fig. 4.1 - Tectonic plate influence in El Salvador (MAY: Mayan Block; CHR: Chorti Block, CHT: Chorotega Block) (mod. from USGS) and main earthquake in Central America.

The Central American Volcanic Arc (CAVA), or Coastal Volcanic Front (FVC), resulting from the subduction of the oceanic crust of the Cocos plate under the Caribbean plate mentioned by DeMets (2001) and Jibson et al (2004), extends From Guatemala to Panama, parallel to the Middle American Trench approximately 150-200 kilometers, presents an important alignment of active volcanoes is considered one of the most active volcanic regions of the world (De la Cruz sf), with numerous Plinian eruptions in hundreds of thousands of years, leaving thousands of square kilometers of layers of volcanic

materials like ashes, dust, pumice and lapillis. The steep slopes of these volcanoes and other mountainous terrain throughout El Salvador are susceptible to landslides, especially in areas where the underlying rocks are deeply fractured (Baum et al., 2001; Crone et al., 2001) and where the soils are formed by deposits Pyroclastics of the so-called Tierra Blanca originated from the eruptions of the Coatepeque and Ilopango calderas, which correspond to rhyolitic pyroclastic flows, producing the youngest and most susceptible soils to erosive processes and mass movements (García-Rodríguez et al., 2008a).

The regions most affected by landslide are the Cordillera El Bálsamo, south of San Salvador, the Ilopango caldera (Figure 2), the flanks of volcanoes mainly from San Vicente, Usulután, El Picacho San Salvador (Jibson et al., 2001) and the northern zone of Chalatenango characterized by geological formations of the lower Tertiary (Lleonart et al., 2000), where the highest elevations of the country are presented at 2,730 m and the largest landslides such as the La Zompopera (Crone et al., 2001).

At the end of the Neogene (lower Pliocene, 5-3 m.a.) a narrow but long area collapsed, crossing the Salvadoran territory from West to East (Meyer-Abich, 1953). It is an anticlinal structure (of convex form) orientated East-West, where they developed a series of faults with that same course, giving way to the formation to one of the most important structures of the country where the belt of youngest volcanoes such as Santa Ana, San Salvador, the volcano-tectonic depression of Ilopango, the San Vicente and the volcanoes of the Tecapa group to San Miguel volcano. This structure is the Central Graben or Central Depression (Fig. 4.2) mentioned by Meyer-Abich, (1953), Hernández (2005) and Rotolo et al. (2011).

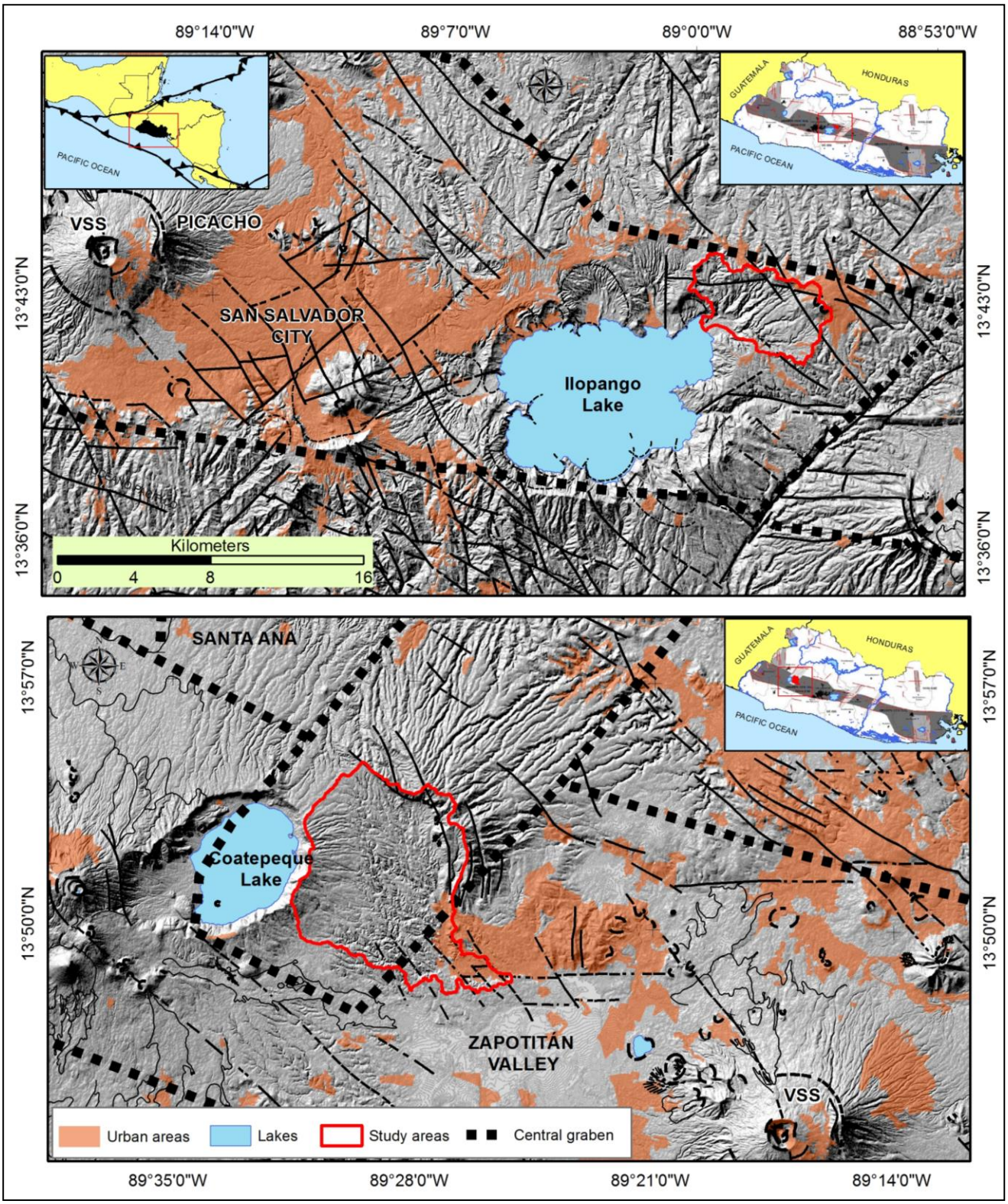

Fig. 4.2 – On the top: Basin of Ilopango caldera in relation to the Metropolitan area of San Salvador, Arenal de Cujuapa basin and the denominated Central Graben of El Salvador; on the bottom: the Agua Caliente river basin in relation to the Coatepeque caldera and the Central Graben of El Salvador.

4.1. CLIMATE

El Salvador and the entire Central American region is located in the intertropical zone between the Tropic of Cancer (23 degrees north of Ecuador) in the northern hemisphere and the Tropic of Capricorn (23 degrees south of the Equator) in the Southern Hemisphere (Serrano, 1995). The Pacific side of Central America has been identified as one of the largest landslides susceptible because it is located very close to the East Pacific Intertropical Convergence Zone (EP ITCZ) where the highest rainfall of this belt is produced (Karnauskas and Busalacchi, 2009, Lewis 2008). Climatic conditions are also affected by the state of the conditions of the waters of the Pacific Ocean and the Atlantic Ocean, redefined by irregular continental orography, where many meteorological events occur on the west coast of Africa and tropical cyclones originating in Caribbean Sea, associated with the temperatures of the Atlantic Ocean (López et al., 2012). The ITCZ, one of the most active cyclogenetic zones in the world (Alfaro 2011), presents in our region two important characteristics, the first to remain on the Central American Isthmus 60% of the year and the second because it is the most active with great implications in the climatology of Central America mainly due to the El Niño and La Niña phenomenon (CEPAL and CCAD, 2010). In El Salvador there are two seasons of the year: rainy season, concentrated between May and early November and the dry season from November to April, rainfall is concentrated in approximately six months of the year, during which an average 1,400 mm in the lower parts and 2800 mm in the high part, almost a quarter of the rain falls in September coinciding with the season of cyclonic events of the year (Serrano, 1995).

According to the Ministry of Environment and Natural Resources, the annual rainfall for the Ilopango caldera from 1981-2010 was 1,756 mm. The precipitation is manifested by intense storms in a short time or in the form of monsoon rainfall in more than three consecutive days, triggering serious problems of landslides and debris flows in the northern mountains, mountains and volcanoes flanks (Barrios et al., 2011).

4.2. GEOLOGY

4.2.1. Ilopango caldera

The Ilopango caldera is located in the central part of El Salvador, a few kilometers to the Southeast of the capital city, San Salvador, comprises a wide volcano tectonic depression, with an almost rectangular shape, measuring 16 km east-west and 13 km north-south and a morphology controlled by tectonic processes and mass movements (Mann, 2004). It is occupied by the lake of the same name, with an area of 75 km2 and reaching in its center a depth of 248 meters (ITALTEKNA-ITALCONSULT, 1988).

This caldera is located within the Central Graben, associated with the ZFES fault system and represents the most dangerous volcanic caldera in Central America due to its history of violent and explosive eruptions from dacitic to rhyolitic called Tierra Blanca, producing layers of ashes and ignimbrites in their last 75,000 years, of which they are known 4 pyroclastic sequences informally called TB4, TB3, TB2 and TBJ (Young White Earth) particularly susceptible to water erosion and landslides (Rolo et al., 2004). The latter dating to 430 + -20 after Christ are considered to be one of the most disastrous volcanic events of the Holocene in Central America (Fig. 4.3), directly affecting populations in El Salvador and bordering areas of Guatemala and Honduras where the ecological and cultural impact of this event was significant (Dull et al., 2001). The Ilopango caldera, which is dominantly differentiated, also shows a wide compositional variability that goes from rhyolitic to the most mafic terms (De La Cruz, 2015).

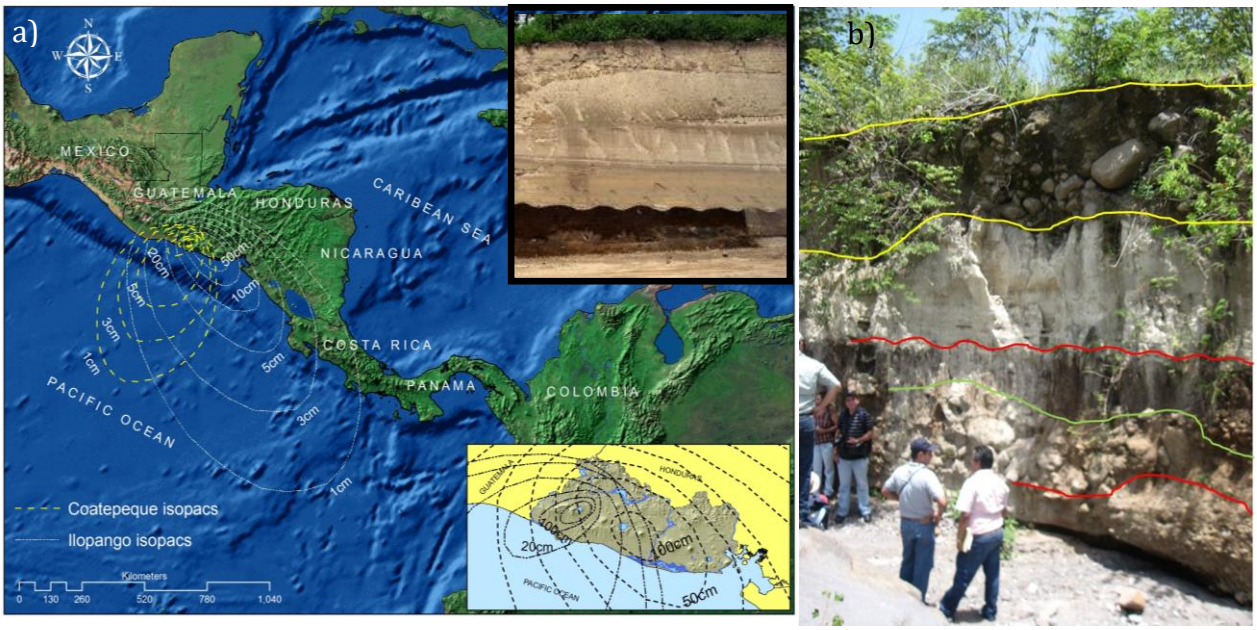

Fig. 4.3 – a)Map of Tefra Isopacs TBJ of the Freatoplinian Eruption of the Caldera of Ilopango and Coatepeque, thicknesses in cm. [Based on Kutterolf et al., 2008; mod. from Rolo et al. (2004) and Dull et al., (2010)). b) Profile soil near Verapaz city, showing the TBJ and debris flow deposit from San Vicente Volcano (photo Faculty Agriculture Science of Universidad de El Salvador, 2009)

In the caldera of the Ilopango three Geological Formations are present in their order: Bálsamo Formation, Cuscatlán Formation and San Salvador Formation, according to Baxter (1984) and Howel & Meyer-Abich, (1953), whose description details (Fig. 4.4):

Balsamo Formation

It consists of volcanic breccias, lavas and other consolidated volcanic rocks remnants of andesitic stratovolcanoes. In the San Salvador area the upper part of the Bálsamo Formation has soil strata containing clay and fine materials. In the center of El Salvador this Formation consists of a sequence of layers of ash coming from the late Pleistocene and Holocene rhyolithic and andesitic of the volcano of San Salvador and caldera of Ilopango. The majority consists of volcanic tertiary rocks (Pliocene),

essentially of andesitic and basaltic lavas, and 'volcanic muddy currents' with large wheeled blocks (Lahars).

Cuscatlán Formation

Lexa et al. (2011) characterized it as silicic domes, tuffs and ignimbrites and volcanic sediments of calderas, locally interstratified with andesitic basaltic lavas. Schmidt-Thomé (1975) describes it as a volcano-sedimentary sequence, predominantly covered by thin layers of younger materials, volcanic is composed of acidic tuffs at the base, followed by intermediate acid lavas and basaltic andesitic at the top, overlap to the Balsam Formation and do not present greater resistance to geomechanical processes, on the contrary the igninbritic tuff consisting of pyroclastic rocks of fine grain, presents greater mechanical resistance. On the slopes of the Ilopango caldera this formation has clearly been dynamized to epiclastic deposits of more than 30 m thick.

San Salvador Formation

Lexa et al. (2011) and (Baxter, 1984), related it with basalt-andesitic stratovolcano products associated with the evolution of the central graben, as well as ash and ignimbrites of the Ilopango and Coatepeque caldera. These materials are located in the main row of young volcanoes in El Salvador of the Quaternary Pliocene and consist of acid pyroclastic rocks and effusive basic-acid interspersed. The upper series called "s4" corresponds to a sequence of acid pyroclastic rocks informally named "Tierra Blanca", are products of the last eruption of the Ilopango caldera with thicknesses greater than 50 meters in the vicinity of the lake of Ilopango and particularly very susceptible to erosion and landslides, the pumice fragments reach sizes of 25 to 30 cm, the predominant thicknesses are towards the Northeast and East of Ilopango lake. The series s5b: composed by accumulation of slags, lapilli tuffs and cinder, example the located contiguous to the Cerro Las Pavas in Cojutepeque villige.

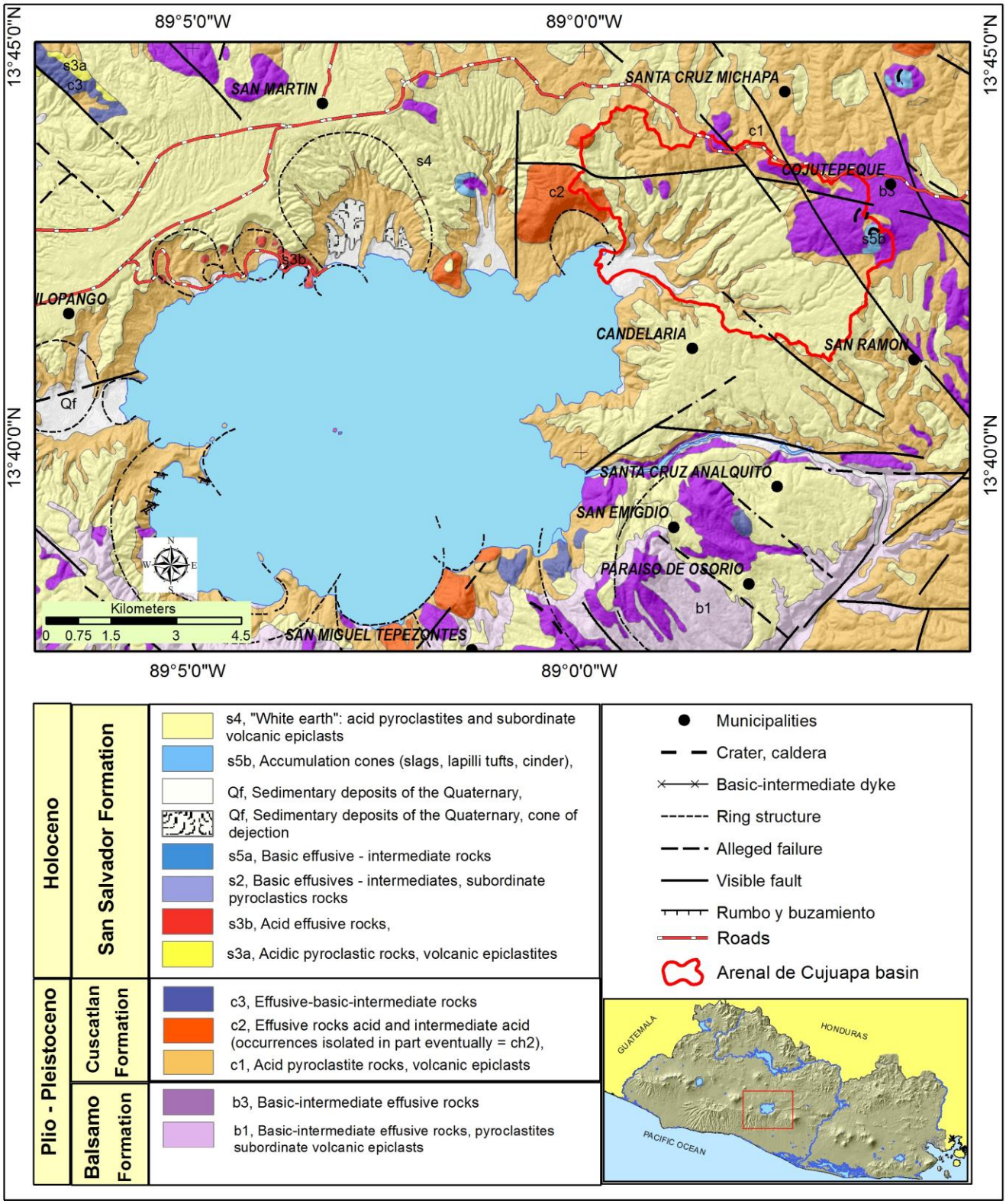

Fig. 4.4 - Ilopango caldera geology (mod. from Geological Map 1: 100,000 from El Salvador)

4.2.2. Coatepeque caldera

The Coatepeque caldera is one of the largest calderas located in the western part of Central America 40 kilometers from the city of San Salvador (Kitamura 2006). A succession of 4 tephras are associated to the evolution of this caldera, the so-called tephras of Bellavista, Arce, Congo and Conacaste, belonging to Plinian eruptive cycles produced between 50 and 80 thousand years. Arce tefra covers the western part of El Salvador and part of Guatemala, as well as to the west of the flank of the San Salvador volcano and the Cordillera El Balsamo range, 40 kilometers east of the Coatepeque caldera (Kutterolf, et al., 2008).

The largest and voluminous plinian eruptions of the Coatepeque caldera produced at first a layer of pumice and white dacitic ashes and later a layer of dacitic ashes intermixed with pieces of pumice and lytic fragments of andesites, basaltic and dacitic-andesites, with average thicknesses of 6-8 meters, often buried by ashes and younger lapillis product of the eruptions of the Santa Ana volcano and other adjacent cones. The accumulation of pumice and Coatepeque ashes was verified by a long series of explosions, and among several of them were intervals of calm sufficiently long to allow intense decomposition (Meyer-Abich & Williams, 1955). Predominate is this zone the geological formations Bálsamo, Cuscatlán and for the most part the San Salvador Formation (Fig. 4.5) (Wiesemann 1978).

Bálsamo formation

Formation referred to the Cerro Buena Vista (or Arce Volcano) to the northern part of Ciudad Arce villige (Fig. 4.5), predominantly constituted of the member B1, section constituted by epiclastics rocks, pyroclastics and ignimbrits locally effusive basic intermediate intercalated, and member B2, sequence of volcanic rocks of the type basic intermediate effusives, pyroclastics, subordinate volcanic epiclastics, locally with hydrothermal alteration.

Cuscatlán formation

Wiesemann (1978) and Baxter (1984) mentions in the Coatepeque caldera the Cuscatlán formation is predominantly formed by the geological member c2, described as a section of effusive volcanic rocks of acid type and intermediate acid of isolated occurrence.

San Salvador formation

Deposits of young tephra known as White Earth and tefra Arce/Congo, product of the evolution of the Coatepeque caldera and Ilopango products, are assigned to the San Salvador formation (Lexa 2011). Wiesemann (1978) and Baxter (1984) mention that in the Coatepeque caldera the San Salvador formation is predominantly formed by the geological member S3a: sequence of acid pyroclastite rocks and dacitic type materials, with thicknesses exceeding 15 meters, constituted by fragments of pumice up to 15 centimeters, which were deposited prior to the sinking of the caldera. Also present to a lesser extent are the geological members S1, consisting of individual castings, loose and laminar blocks, predominantly basalto-andesitic from eruptive centers currently sunk in the Coatepeque caldera; Member S2, sequence of intermediate basaltic and subordinate pyroclastic rocks; Member S3b: a unit composed of acidic effusive rocks, less voluminous than the previous members, consisting mainly of rhyodacitics materials of pumice and black obsidian, coming from the last phase of activity in the caldera; Member S5a, sequence of recent intermediate effusive rocks; Member S5b, slag accumulation, lapilli tufts and cinder, and member S5c; Made up of ashes and lapillis from the eruptions of Santa Ana and Izalco volcano and other adjacent cones, materials that overlap the layers of dacitic ashes from Plinian eruptions of Coatepeque caldera.

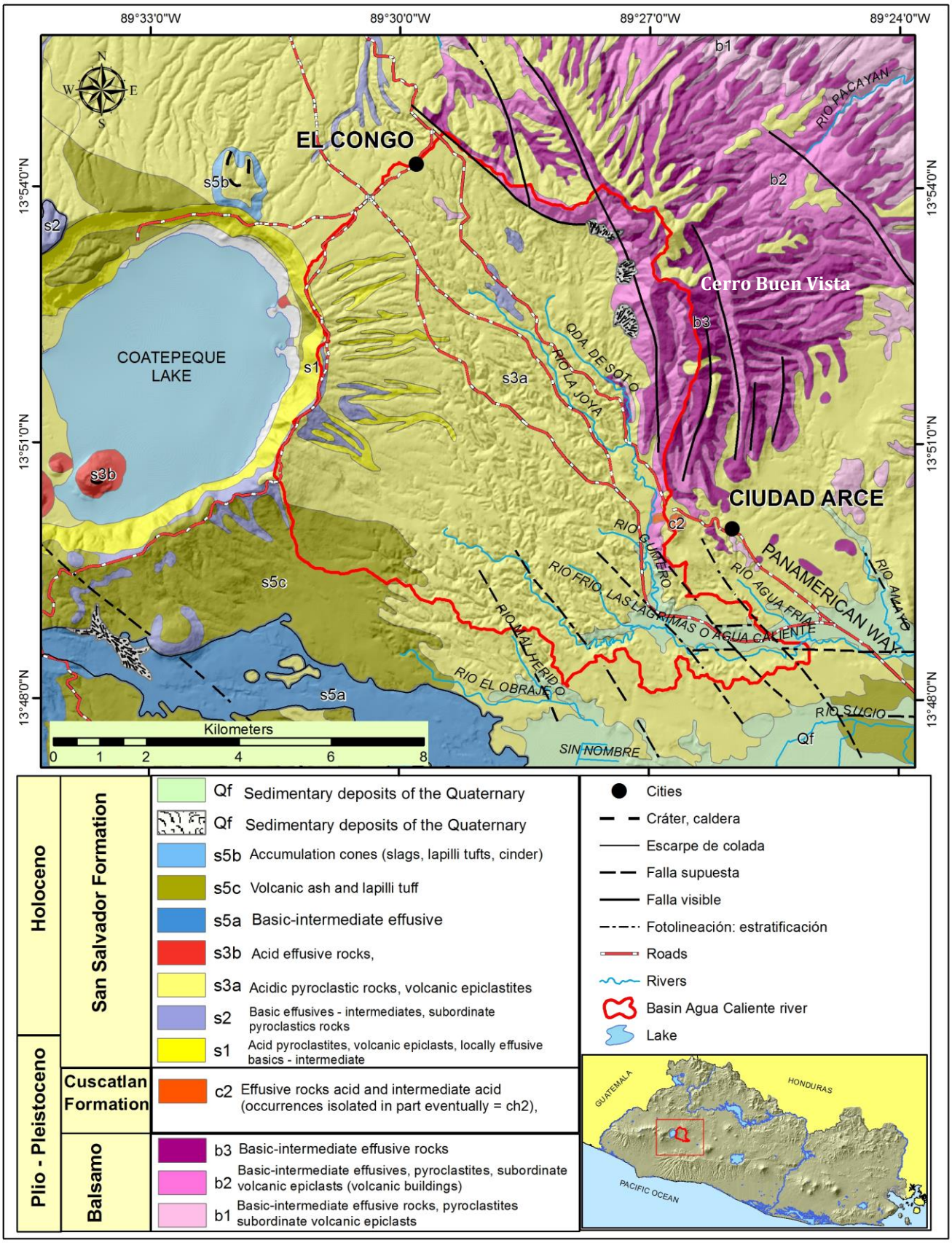

Fig. 4.5 – Geology associated with the Coatepeque Caldera (mod. from Wiesemann et al., 1978).

4.3. GEOMORPHOLOGY

4.3.1. Ilopango Caldera

The slopes of the Ilopango caldera are very irregular, because they are remodeled by some dacitic domes or separate collapses. Surrounded by highly inclined walls of 170-500 meters high, most of its strata are under a large layer of pumice product of its eruptions (Howel and Meyer-Abich, 1953).

The depression is occupied by the lake of the same name with an area of 75 square kilometers, the most important tributaries that feed it are to the east side by the El Chaguite river, the Guluchapa river to the North and the Arenal de Cujuapa to the Northeast, and a drainage that flows into the Jiboa River parallel to an East system of visible lines that are part of the ZFES. The relief of the caldera presents southern steep walls with a cover of recent pyroclastic flows and deposits of fall (Tierra Blanca) with thicknesses of up to 50 meters to the West of the caldera, that extend to the North East, of up to 2 meters in the valley of Jiboa and San Vicente volcano (Fig. 4.6) (ITALTEKNA-ITALCONSULT, 1988).

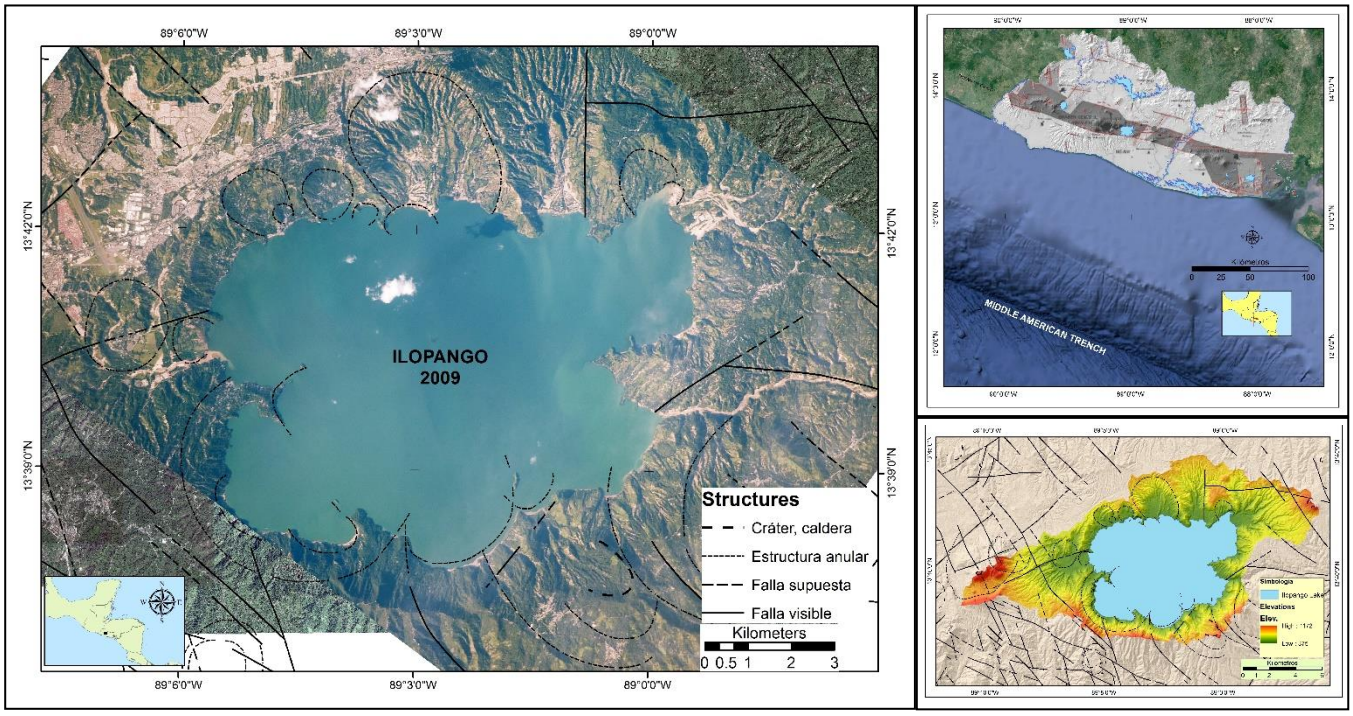

Fig. 4.6 - a. Satellite image Caldera de Ilopango, November 11, 2009. Source: NASA Earth Observatory. http://earthobservatory.nasa.gov/IOTD/view.php?id=41581, with a simplification of geological structures; B. Central Graben of El Salvador (Base image Google Earth c) Elevations of the Ilopango basin.

4.3.2. Coatepeque caldera

In the area between Ciudad Arce city and Lake Coatepeque, precisely in the La Joya river basin, erosion strongly affects deposits of dacitic ash, resulting in an intense dendritic network of narrow ravines, partially used for agriculture and secondary forest. The relief of the basin is irregular in the middle part, product of the water erosion in soils formed of volcanic ash and pumice. The predominant geological formation is the San Salvador geological member S3a with predominance of acid pyroclastic rocks.

The La Joya River Basin, with dimensions of 15 long by 10 wide and an area of 79.16 square kilometers, the highest part is 1180 meters and the lowest part is 460 meters above sea level. In the upper part of the basin, the cultivation of coffee predominates, while in the middle and lower part, the cultivation of corn predominates.

This area is characterized by a very rugged topography and soils originated from products of Plinian explosive eruptions predominantly of white lands from acidic volcanic ashes of dactic and rhyolitic type with abundant large grains pomicitic materials. These soils are characterized by very poor resistance to water erosion and a relatively young dendritic drainage system formed by progressive denudation originating deep ravines in the upper part of the basin and depositional reliefs where eroded materials accumulate.

4.4. LANDSLIDE DISASTER HISTORICAL RECORDS IN EL SALVADOR

4.4.1. Seismically induced landslides in El Salvador

The history of earthquakes associated with CO-CA subduction dynamics are of 40 kilometers east of the Coatepeque caldera, with records of up to 7.6 magnitude on January 13th, 2001 (USGS 2012) (*Figure 4.7*) earthquake that caused damages In thousands of houses and triggering hundreds of landslides (Bommer et al., 2002; Bent, 2004), mostly concentrated in the surroundings of the city of San Salvador, the Cordillera El Bálsamo region west and south of San Salvador, Los Chorros in the Panamerican Way and areas around Ilopango lake, most of them were relatively shallow falls and rock and debris detachment, especially in young volcanic pyroclastic deposits (Jibson et al., 2001, 2004), with the exception of the landslide of Colonia Las Colinas in Santa Tecla, in the so-called Cordillera El Bálsamo where 585 people died.

The landslide of Las Colinas was reported by Evans et al. (2004) as a relatively small but extremely fast and long trajectory, and classified as flow slide, with a slipped volume of 130000m^3, commonly occurring in Central America in pyroclastic deposits.

The February 13th, 2001, earthquake of Mw 6.5 triggered thousands of landslides from small volumes (lateral-spreading landslides) mainly to the North, South and East of the Ilopango caldera, whose hillsides characterized by weakly consolidated volcanic ash volcanic deposits from the so-called Terra Blanca Jóven (TBJ) to mobilized volumes of 1.5 million m3 and important landslides on the Northern slope of the San Vicente volcano (*Fig. 4.7*) (Baum et al., 2001).

The earthquake of 10th October 1986 (Ms 5.4), (USGS 2015, Evans et al. 2004), of tectonic origin and a maximum intensity of IX on the Mercalli Modified scale, with focal depth of 8 kilometers caused many landslides in the city of San Salvador, most of these landslides also confined to pyroclastic deposits (Tierra Blanca of the San Salvador Geological Formation).

Fig. 4.7 – Landslides triggered by earthquakes in El Salvador January 2001, a) Rockfall in Los Chorros Pan-American Highway (Civil Protection, 2001), b) Curva de La Leona Landslide Pan-American Highway, c) Las Colinas Santa Tecla landslide (Civil Protection, 2001).

4.4.2. Storm triggered landslides in El Salvador

According to records of the Ministry of Environment and Natural Resources (MARN 2011), El Salvador was impacted by 16 extreme weather events since the 1960s and 8 occurred between 2002 and 2011; Five of the eight events were formed in the Pacific Ocean, particularly destroyers such as Paul (September 1982) Hurricane Adrian (May 2005), low pressure 96E associated with Hurricane Ida (November 2009), Tropical Storm Agatha (May 2010), The recent tropical depression DT12E (October 2011), generating a high susceptibility to landslides (Table 4.1).

Event	24 hours	48 hours	72 hours	96 hours	Max. Acc.
Trifinio? (1934)			500		500
Fifí (1974)	252.8	379.1	394.1	404.0	404
Cesar (1996)	nd	nd	nd	nd	365
Mitch (1998)	314.5	387.6	415.6	419.2	861
Stan (2005)	207.2	411.5	580.5	705.4	805
DT96E+Ida (2009)	355.0	>400	>450	nd	483
Agatha (2010)	nd	nd	nd	nd	672
DT 12E (2011)	nd	nd	nd	nd	1,513

Table 4.1 - Maximum precipitation levels recorded in the area of San Vicente and Ilopango (1934-2011). Mod. from CEPAL (2011a, 2011b) and Ministry of Environment and Natural Resources MARN (2010, 2011).

The history of landslides trigger induce by extreme weather, shows an impact on the country's socioeconomic development and population, as mentioned in El Picacho in 1982, propagating 4 kilometers through the Quebrada El Níspero and affecting the Colonia Montebello in San Salvador (425,000m3) triggered by Paul Hurricane where 300 lives lost (Major et al., 2001; Daví and Fernández, 2008; MARN, 2011; CEPAL, 2011a;Medina-Cetina and Cepeda, 2012), the history of 1934 indicates a event five time more bigger in the same area, but at that time it was still depopulated (Daví and Fernández, 2008; Medina-Cetina and Cepeda, 2012).

On 6th and 7th June 1934 Hurricane Trifinio, generated in the Caribbean, penetrated Central America, which became a tropical storm, hit the Trifinio mountain range, where the borders of Guatemala, Honduras and El Salvador converge, the city of Antigua Ocotepeque in Honduras was affected by a debris flow (Ferradas and Medina, 2003), same day a landslide affects the city of Metapán near the point of convergence between Guatemala, Honduras and El Salvador (Babůrek et al., 2005) and a debris flow destroys a part of the city of Tepetitán in San Vicente, now retakes the name of Nuevo Tepetitán (Baum et al., 2001; Bowman and Henquinet, 2015).

The debris flows caused by the 96E/Ida system, traveled up to 6 kilometers and partially destroyed the city of Verapaz and Guadalupe in the department of San Vicente (*Table 4.2, Fig. 4.8*) (CEPAL, 2010; Bowman and Henquinet, 2015). Both cases preceded by seismic activity.

Event	Year	Place and volume	Trigger	Tipo	Reference
Las Colinas (Cordillera El Bálsamo)	January 2001	Cordillera El Bálsamo, 130000m^3, 585 Died	Earthquake 2001, M7.6	Flowslide en Formación Geológica San Salvador y Cuscatlán	Evans & Bent, 2004.
Curva de La Leona	January 2001	San Vicente, Panamerican Higway , 12 died, 750,000 m^3	Earthquake 13 enero 2001	Debris slide	Jibson, et al 2004
Landslides in Ilopango caldera	January 2001	Ilopango, caldera	Earthquakes 13th January and 13th febrero 2001	Lateral spreading landslides	Baum et al, 2001
Complex Landslide La Zompopera (Chalatenango)	June 1934	La Palma, Chalatenango	Rain	Traslational	Crone, et al, 2001
San Vicente Volcano	June 1934	Tepetitán, 500,00 m^3	Rain	Debris flow	Baum et al, 2001
Montecristo, Metapán	June 1934	Cerro Montecristo	Rain	Dbris flow	Babůrek, et al 2005
El Picacho-Montebello (San Salvador)	September 1982	El Picacho San Salvador volcano	Paul Hurricane from the Pacific Ocean	Debris flow	Fernández et al. 2008
Santa Ana volcano	October 2005	Santa Ana-Sonsonate	Santa Ana volcano eruption and Stan Hurricane , 0ctober 2005	Lahar	CEPAL, 2005
Verapaz-Guadalupe (San Vicente)	November 2009	San Vicente volcano	Sistema 96E/Ida	Debris Flow	Bowman and Henquinet 2009

Tab. 4.2 - Some landslides occurred and dates and classification in El Salvador (1934-2011). Mod. from CEPAL 2010 and Ministry of the Environment and Natural Resources; MARN (2010).

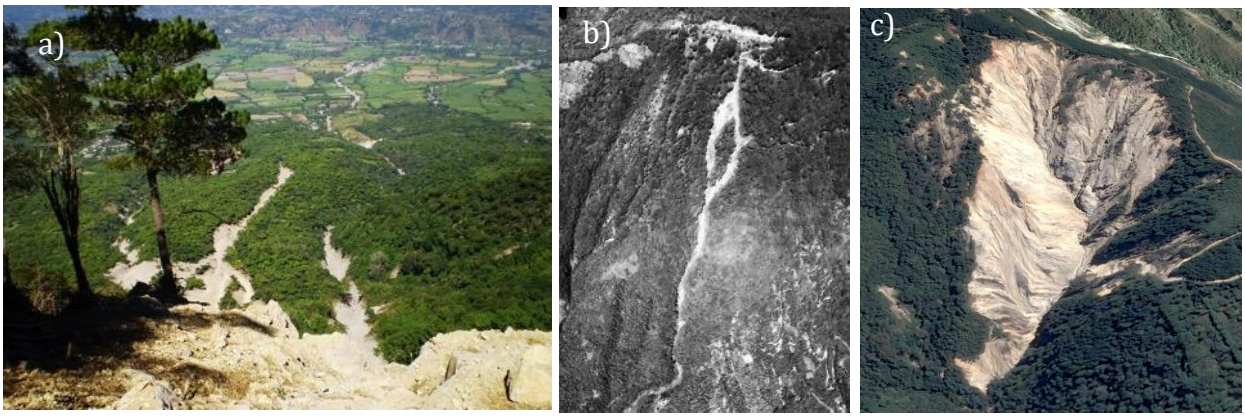

Fig. 4.8 - a) Debris flow volcano of San Vicente in 2009 (photo University of El Salvador 2009), b) Debris flow El Picacho 1982, c) Complex landslide La Zompopera (Taken from Google Earth 2016).

The most disastrous extreme weather events triggered landslides in El Salvador during 1998 to 2011 are: Hurricane Mitch (October 1998) (Baum et al., 2001), Category 5 at that date the most potent event in historical records, Flooding was the major problem, however it triggered many landslides throughout the territory (Crone et al., 2001); Hurricane Stan (October 2005), the low pressure 96E / Ida (Avila and Cangialosi, 2010) with impact mainly in the central and paracentral zone of El Salvador between

November 7th and 8th, 2009 that caused thousands of landslides in the Ilopango caldera and large debris flows in the volcano of San Vicente with volumes estimated between 250000 and 360000 m^3 impacting cities such as Guadalupe, Verapaz and San Vicente (CEPAL, 2010); Agatha, Alex and Mathew in 2010 and the tropical depression 12E in 2011 (CEPAL, 2011).

The meteorological system low pressure 96E/hurricane Ida 2009

Hurricane Ida developed in the Western Caribbean Sea as a tropical depression, was rapidly increased to form in a tropical storm on Saturday, November 7th, to land on the coast of Nicaragua and became a hurricane reaching the Category 2 at noon on Sunday 8th (Avila & Cangialosi, 2010). It was demoted to category 1 of the hurricane on Monday morning and was degraded by a tropical storm later Monday morning. According to CATHALAC (2009) and CEPAL (2010). The convergence of Tropical Storm Ida and low pressure of the 96E system in the Pacific Ocean from 5th-8th Nov 2009, reached 483 mm precipitations in a three day period 7th- 9th November 2009) (Table *4.1, figure 4.9*), with an intensity reaching its maximum limit of 355 mm over a period of five hours, five times the average rainfall for November. The highest concentration of rains was in an area of approximately 400 km2 between the lake of Ilopango and the volcano of San Vicente (Chichontepec), consequently the greatest impact is observed on the north side of the volcano and on the slopes to the South and Southeast of the Ilopango lake, causing great floods and landslides. According to El Salvador Civil Protection reports, Ida caused a total of 198 deaths, missing persons and economic losses of $239 million (MARN, 2010).

The Tropical Depression 12E

The tropical depression 12-E begins on October 9th, 2011, forming as a low pressure that took force becoming a tropical depression touching earth in the Southeast of Mexico until weakening. Its remnants kept the climate unstable in the following days affecting the coasts of the Central American Pacific, consolidating a belt of clouds derived from the Intertropical Convergence Zone that remained stationary

during October 10 and 11, releasing heavy rains causing landslides and floods, leaving 35 people dead and many economic losses. In El Salvador, DT12-E affected during the period from 10th to 20th October and was classified as the most severe meteorological event recorded with a cumulative maximum of 1513 mm, equivalent to 42% of the average annual rainfall of the period 1971- 2000 (figure 4.9) (CEPAL, 2010, 2011).

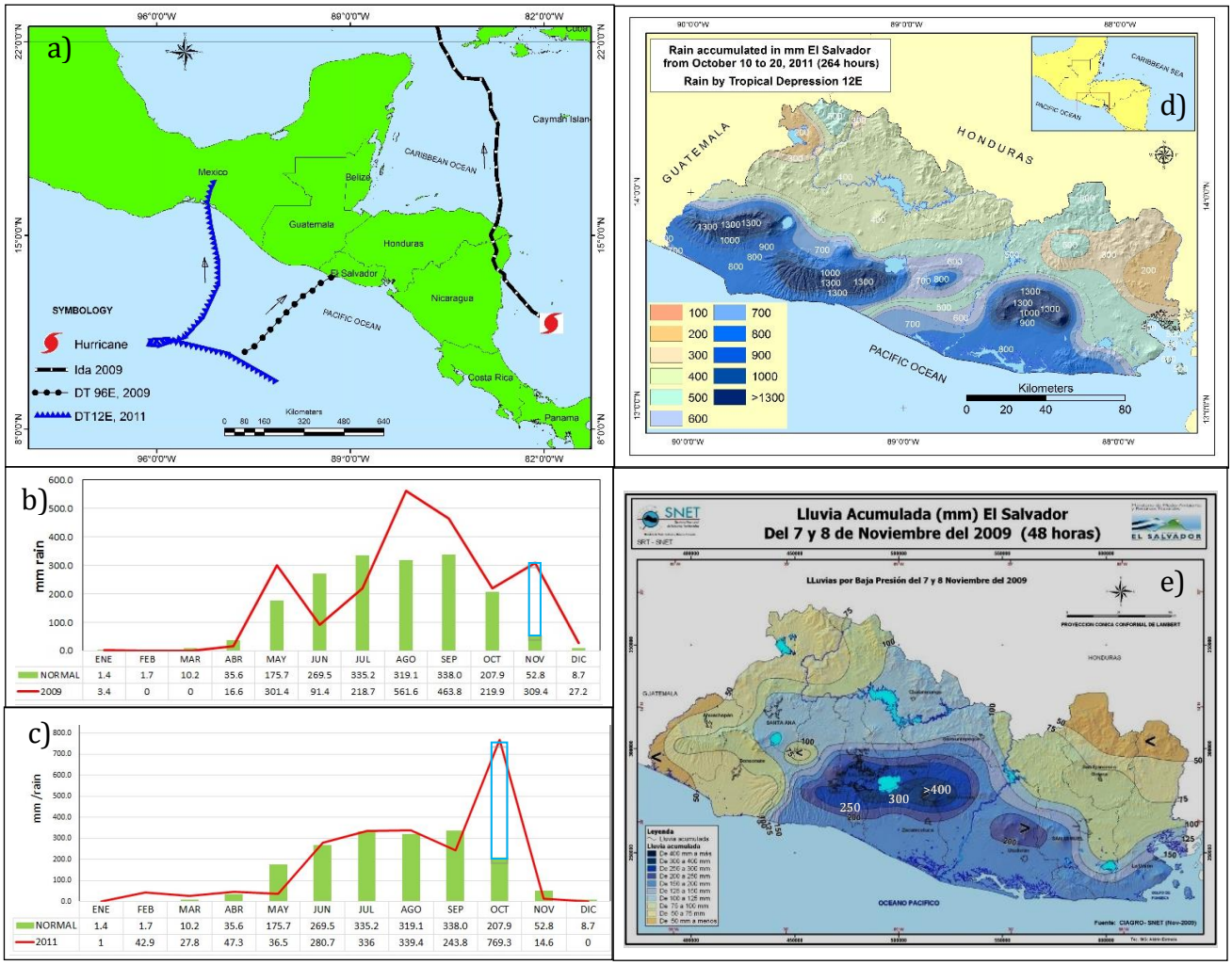

	ENE	FEB	MAR	ABR	MAY	JUN	JUL	AGO	SEP	OCT	NOV	DIC
NORMAL	1.4	1.7	10.2	35.6	175.7	269.5	335.2	319.1	338.0	207.9	52.8	8.7
2009	3.4	0	0	16.6	301.4	91.4	218.7	561.6	463.8	219.9	309.4	27.2

	ENE	FEB	MAR	ABR	MAY	JUN	JUL	AGO	SEP	OCT	NOV	DIC
NORMAL	1.4	1.7	10.2	35.6	175.7	269.5	335.2	319.1	338.0	207.9	52.8	8.7
2011	1	42.9	27.8	47.3	36.5	280.7	336	339.4	243.8	769.3	14.6	0

Fig. 4.9 - a) trajectory Hurricane Ida, modified from Avila and Cangialosi (2010) and low pressure 96E, modified from CATHALAC (2009). b) Monthly cumulative rainfall of the Ilopango Meteorological station year 2009 comparative with the average monthly rainfall of the Ilopango station years 1981-2010 (National Meteorological Service of the MARN Environmental Observatory 2016) c). monthly accumulated rainfall year 2011 of the San Andrés station (National Meteorological Service of the Observatory MARN 2016) comparing with the average monthly rainfall of the station of San Andres years 1981-2010., d) rainfall distribution of Tropical Depression 12E in El Salvador (Modified National Hydrological Service MARN, 2011). e) Rainfall distribution of Hurricane Ida/96E (MARN, 2009).

C: EXPERIMENTAL SECTION

The main scientific topic of this research was to investigate possible non-linear effects between predictive models (selected factors, regressed coefficients, accuracy and precision) and intensity of the trigger. To explore this topic, different calibration landslide inventories were to be prepared, each based on a landslide scenario produced by one of the storm events which recently stroke the study area with varying intensity. By exploiting the different calibration datasets, different susceptibility models can be obtained, which are to be compared in terms of inner structure (predictors importance and response curves) and predictive performance (skill, accuracy and precision). The analysis of the predictive results is based on multi-fold cross validation routine, based on random spatial partition and temporal partition schemes. ROC plots, error maps and plots are used to test the models and to compare their performances, whilst their inner structure is described by analyzing the distribution of the regressed b coefficients and the response curves.

The study area is composed of two sectors: Area 1, a catchment inside the Ilopango Caldera area (central El Salvador, East from San Salvador city), where different pyroclastic deposits largely outcrop on steep-very steep slopes where the Tierra Blanca Joven (TBJ) pyroclastites dominate; Area 2, a catchment located in the area called Coatepeque Caldera, West part from San Salvador, predominantly over very steep slopes and with deposits pyroclastites product of ancient plinian eruptions.

The selected events are: TD96E/Ida system 2009 and TD12E Storm 2011. Thanks to the availability of remote images, with respect to these events, three inventories can be prepared: at 2003 (as a normal year and before Ida), at 2009 (soon after Ida) for Ilopango caldera, and at 2011 (after 12E event) for Coatepeque Caldera.

5. LANDSLIDE EVENTS

Two triggering events were taken into accounts in the present thesis: the mixed TD96E/Ida hurricane, in 2009, and the TD12E in 2011.

The Hurricane Ida developed in the south-western Caribbean Sea on the 4th of November as a tropical depression, increasing its strength up to a tropical storm on the 7th of November, when it crossed the shoreline of Nicaragua, and to a second level hurricane at the midday of the 8th (Avila & Cangialosi 2010). The hurricane then moved northward crossing the Caribbean Sea and the Mexico Gulf, weakening back to tropical storm and depression on the 9th, completely dissipating on the 12th. During these same days, the low pressure system 96E moved from the eastern Pacific Ocean causing intense rainfall between November 7th and 8th (CEPAL 2010, 2011). In these two days, Ida and 96E simultaneously struck an area of around 400 km^2 centered between Ilopango Lake and San Vicente Volcano, recording more than 300mm/24hrs at the Ilopango and San Vicente villages. In this area, large damages were recorded caused by floods and landslides with around two-hundreds dead and a quarter of a billion dollars of economic losses (MARN 2010), the larger part of which in the north-western flank of San Vicente Volcano where huge debris flow phenomena severely struck the villages of Verapaz and Guadalupe. At the same time, in the Ilopango Caldera area, hundreds of landslides triggered from steep slopes causing damages to crops and rural houses and roads, as well as strongly affecting and modifying the connected fluvial system.

Tropical Depression 12E was developed from a low pressure system formed in the Tehuantepec Gulf Mexico, as a generalized rain phenomenon that is held stationary during the days 10 and 11 of October, which at day 12 is declared as DT12E. During October 13th, the end of the DT12E is announced, however it is warned of a low pressure that would affect Southeast Mexico, Guatemala, Belize, El Salvador, Honduras and Nicaragua that includes remains of Storm 12E on the Pacific side and Another

system depressed by the Atlantic, that it remain stationary on the Central American Region causing serious damages and losses of human lives (CEPAL 2011).

The greatest damage in El Salvador was the coastal plains and volcanic mountain range of western El Salvador between October 10 and 20, 2011, with the highest accumulated rainfall in the volcanic chain of the western zone with a total of 1513 mm in the Cordillera El Bálsamo range, in Coatepeque caldera an accumulated average of 600mm in the 10 days that lasted the storm. Cumulative rainfall in El Salvador was equivalent to 42% of the average annual rainfall from 1971-2000. The amount of accumulated rain saturated the soils causing high susceptibility to landslides and a flooded area that reached 10% of national territory (MARN 2011, CEPAL 2011).

5.1. TD96E/IDA IN THE ILOPANGO CALDERA

A landslide recognition was carried out in a selected catchment of the Ilopango caldera, where strong effects were produced by the TD96E/Ida system in 2009, with the activation of thousands of debris flows landslides (Fig. 5.1).

This area is in fact characterized by the large outcropping of pyroclastic rocks and derived soils, which under heavy rainfall can easily be saturated, with rapid water pressure increasing and shear strength lowering. Besides, depending on the high water content, once a landslide activated, it can move for long distance converging along the drainage lines toward the base of the slopes and, in same cases, along the streams assuming the form of debris flood phenomena (Fig. 5.2).

Fig. 5.1 – Slope response to the TD96E/Ida storm event in the Ilopango Caldera area.

Fig. 5.2 – Effects of debris flood phenomena along the main stream valley.

As regards the type of landslides which activated, a wide range of conditions, depending on the water content and the slope morphology was observed, including activation from the middle part of the slopes (Fig. 5.3) or, more frequently, from the head of the slopes (Fig. 5.4), activation as pure debris flow (lobate crown; Fig. 5.5) or, more frequently as debris slide (rectilinear crown; Fig. 5.6) or as, debris flows spreading into open slopes (Fig. 5.7) or channeling along the drainage network (Fig. 5.8), debris flows arresting into the slope or reaching the its foot (Fig. 5.9).

Fig. 5.3 – Examples of landslides activated from the middle part of the slopes in the Ilopango caldera.

Fig. 5.4 – Examples of landslides activated from the head of the slopes in the Ilopango caldera.

Fig. 5.5 – Examples of landslides activated as pure debris flows in the Ilopango caldera.

Fig. 5.6 – Examples of landslides activated as debris slides in the Ilopango caldera.

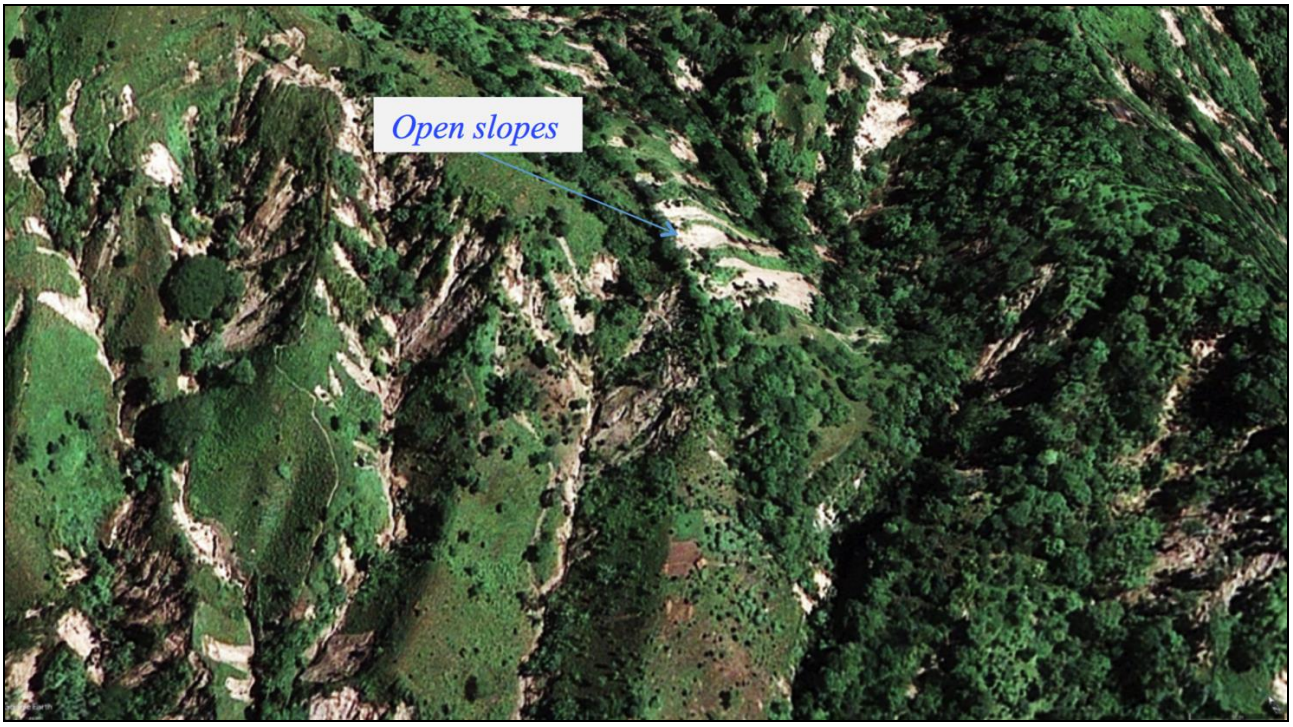

Fig. 5.7 –Examples of debris flows spreading into open slopes in the Ilopango caldera.

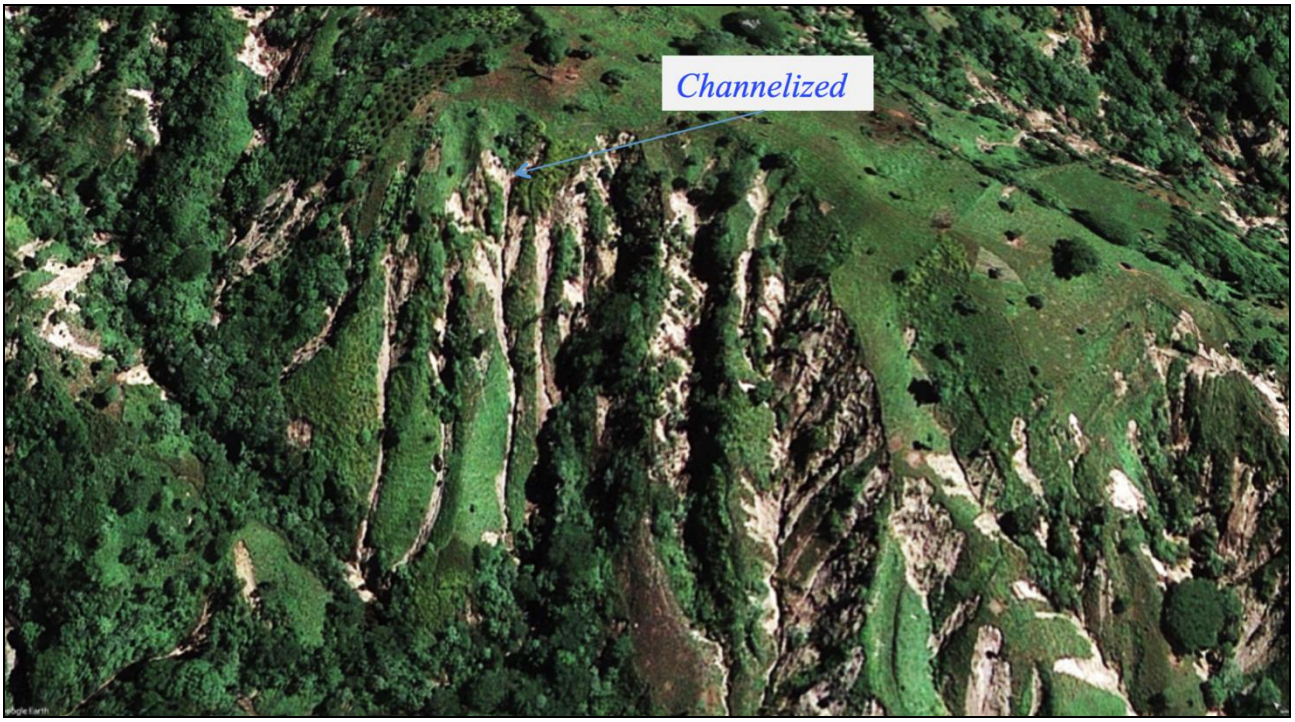

Fig. 5.8 –Examples of debris flows channelizing along the drainage network in the Ilopango caldera.

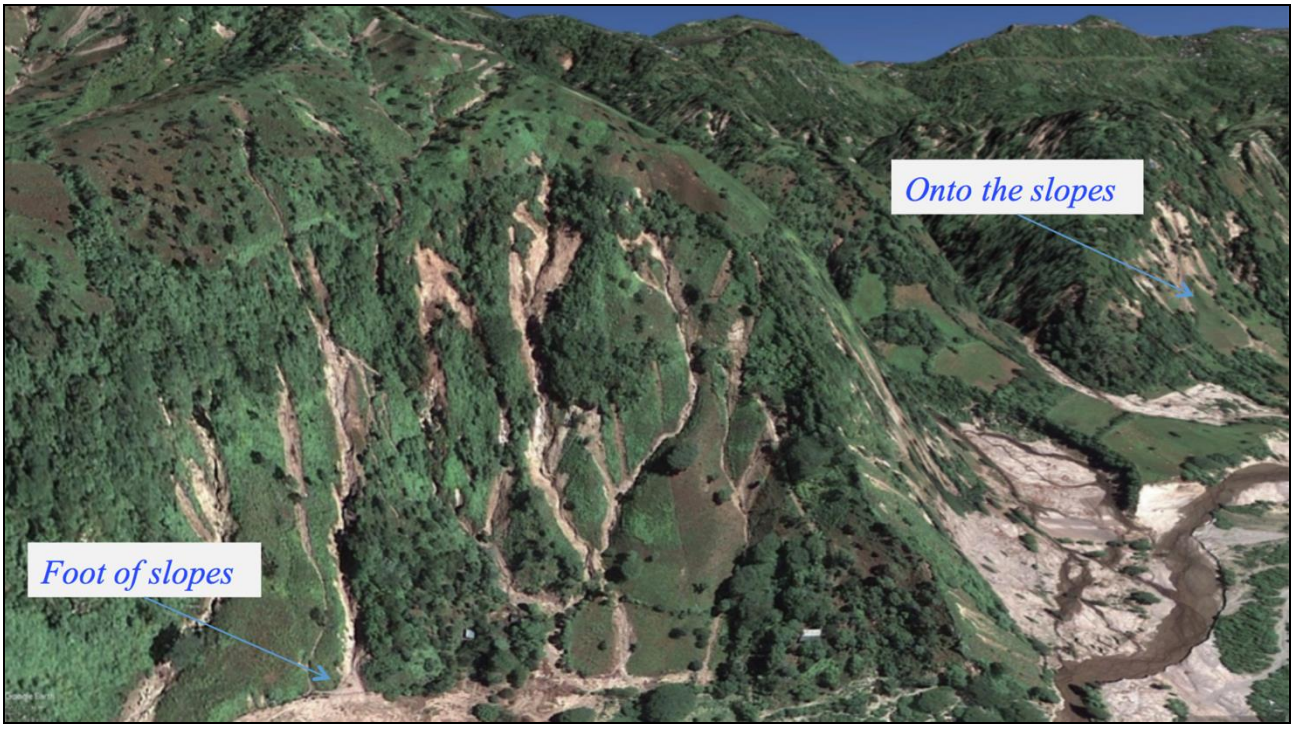

Fig. 5.9 – Different slope conditions for debris flow arresting in the Ilopango caldera.

5.2. TD12E IN THE COATEPEQUE CALDERA

A landslide recognition was carried out in a selected catchment of the Coatepeque caldera, where strong effects were produced by the TD12E system in 2011, with the activation of thousands landslides as debris flows (Figs. 5.10, 5.11). The TD12E was considered the meteorological event that surpassed the historical cumulative rain values in El Salvador, triggered many landslides in the area of the Coatepeque Caldera, however the behavior to present small and many landslides as debris flows less than Ilopango at 2009 Ida.

In the study area different types of landslides were observed, in a wide range of conditions similar to the Ilopango caldera, including the activation from the middle of the slopes, as well as others from the head of the slopes (Fig. 5.12), such as debris flows that are channeled along the drainage (Fig. 5.13), landslides extending to open slopes, or more frequently as debris sliding (rectilinear crown, Fig. 5.14).

Fig. 5.10 – Slope response to the TD12E storm event in the Coatepeque Caldera area.

Fig. 5.11 – Effects of debris flood phenomena along the main stream valley, La Joya basin.

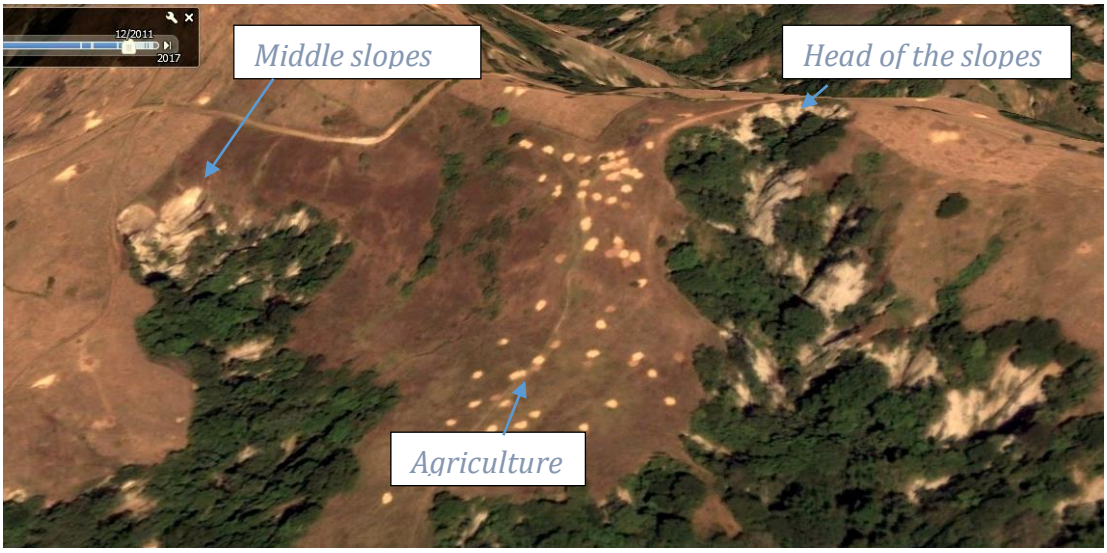

Fig. 5.12– Examples of landslides activated from the middle part of the slopes and from the head of the slopes in the Coatepeque caldera.

Fig. 5.13 – Examples of landslides activated as pure debris flows channelizing along the drainage network in the Coatepeque caldera.

Fig. 5.14 – Examples of landslides activated as debris slides in the Coatepeque caldera.

5.3. LANDSLIDE RECOGNITION AND MAPPING

In order to perform a first key study, in light of the geological and geomorphological characteristics of the two areas, representative catchments were taken into consideration.

For the Ilopango Caldera (Fig. 5.15), the study area corresponds to a very oblate catchment (about 5km long and 8km large) given by the convergence of several short highly steep streams into an alluvial plain named “Arenal de Cujuapa”, which progradates into the Ilopango lake with a marked delta-like head (“Punta El Pinar”). Actually, two main channels can be recognized in the alluvial plain, the southernmost of which corresponds to the ending branch of the El Borbollon river. Multi-temporal remote, cartographic and field surveys suggest the confluence of the two branches as recurrent.

The El Borbollón river catchment drains the inner slopes of the northeastern sector of the Ilopango Caldera, which are characterized by the outcropping of Holocenic acid pyroclastic sequences, locally named “Tierra Blanca” (TB), belonging to the San Salvador formation (Quaternary). The latter covers the underlying pyroclastic deposits of the Cuscatlán formation, which were unburied by erosion along the valley bottom of the streams. Finally, in the upper sectors of the catchment, near the town of Cojutepeque, pyroclastites of the Bálsamo formation outcrop.

At the time of our field survey (May, 2015), the study area resulted as generally affected by dormant and active landslides which were mainly classifiable as debris slides and debris flows. In fact, the warm-humid climate is responsible for the fast growing of the vegetation, so that, with the exception of few cases of very recent landslides, the large part of the study area showed only smoothed forms of the previous gravitational phenomena on the slopes (Fig. 5.16). Only the lower parts of the river banks resulted as frequently affected by small but very fresh debris slide phenomena.

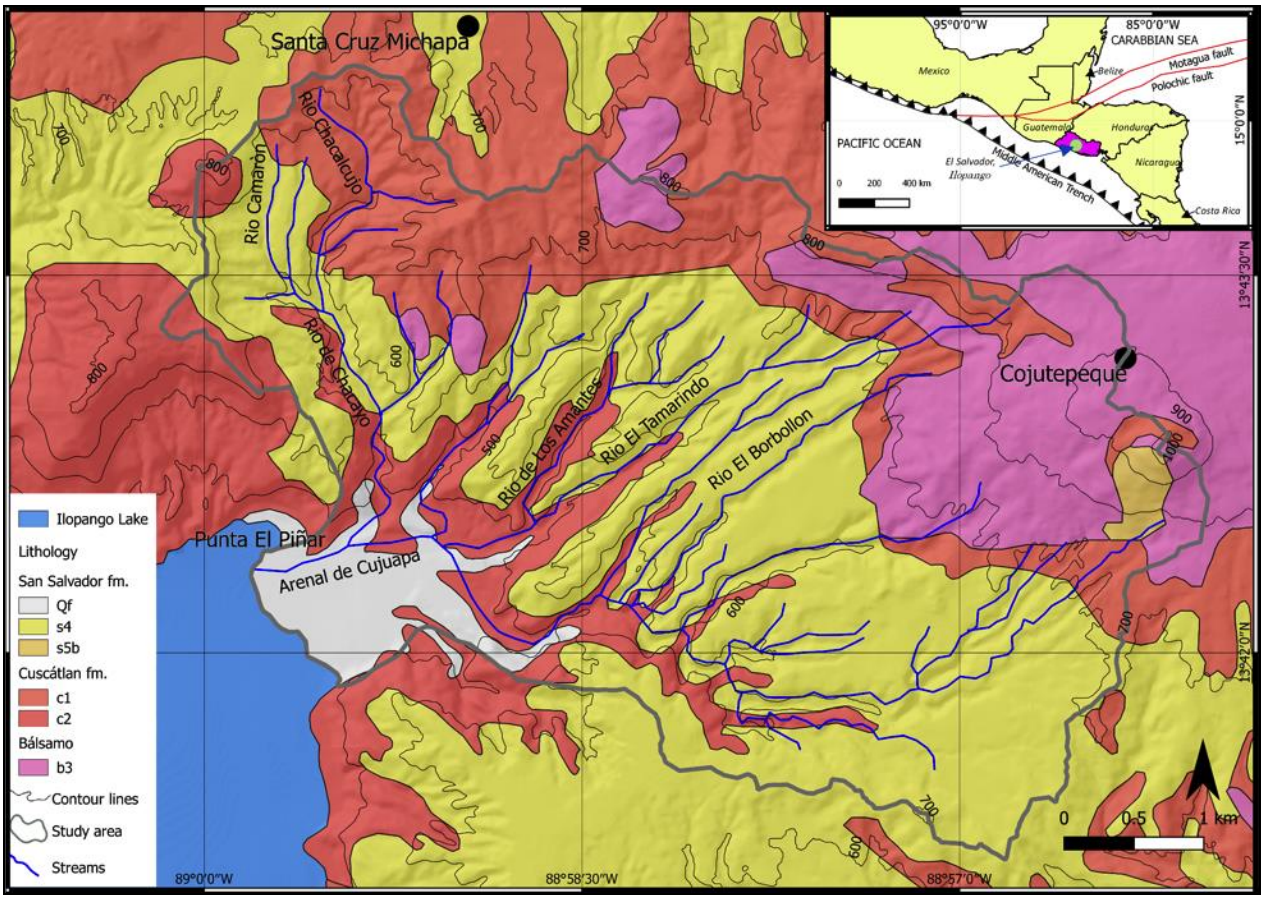

Fig. 5.15 – Selected study area, representative of the Ilopango caldera.

Then, to prepare the two (ante- and post-event DT96E/Ida 2009) required inventories, a landslide recognition was carried out through a systematic remote Google Earth-based analysis, which was performed on two different epochs: one dated at 9/9/2003 (Digital Globe Catalog ID: 1010010002459C02) and one dated at 21/11/2009 (Digital Globe Catalog ID: 1050410001EC3300) (Fig. 5.17-5.18), the latter being taken two weeks the E96/Ida event. Unfortunately, the 2003 GE images were affected by a partial cloud coverage (Fig. 5.18), so that the study area was subdivided into a 2003 cloud-free ("CF") and a cloudy blind ("CB") sector.

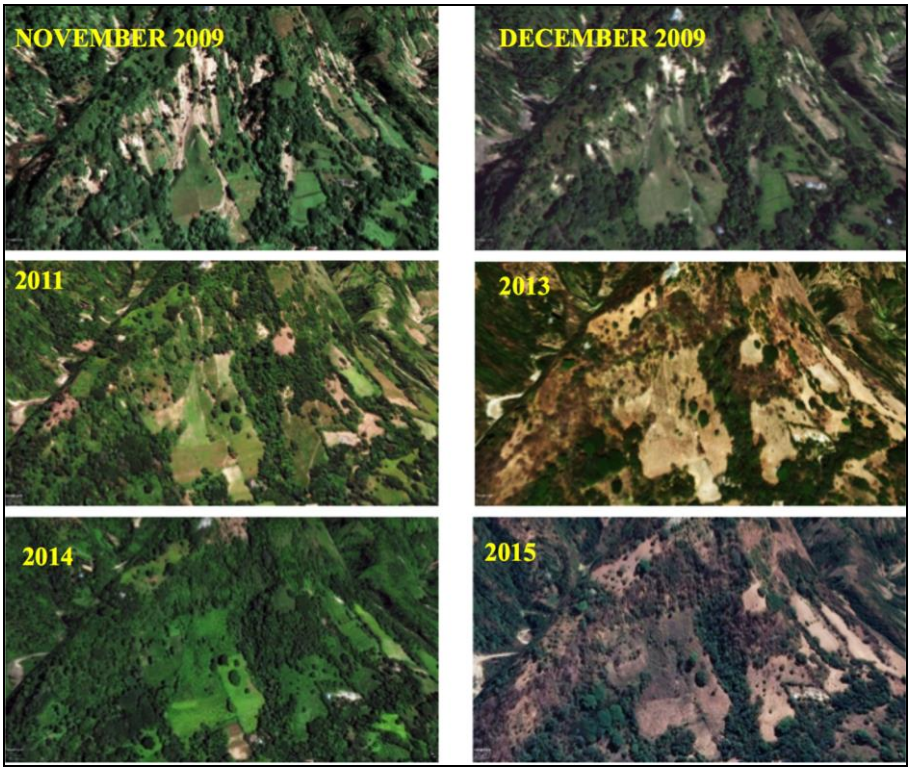

Fig. 5.16 – Fast shape smoothing after 2009, due to vegetation growing in the Ilopango caldera.

Fig. 5.17 –Google Earth view at 09/09/2003 of the Ilopango caldera.

Fig. 5.18 –Google Earth view at 21/11/2009 of the Ilopango caldera.

Landslides were mapped by means of a Landslide Identification Point (LIP) positioned on the highest point along the crown line (Fig. 5.19), finally obtaining the two landslides inventories (Fig. 5.20-5.21) which included 1503 (2003) and 2237 (2009) landslides, respectively.

In light of the type of slope movements, the adoption of a point representation for the landslides was assumed as effective in order to detect those site conditions responsible for past failures and, as such, the LIPs were then used as diagnostic landforms in the model building procedures. Using a LIP inventory for calibrating the susceptibility model results obviously leads to estimating the probability for a pixel to be an initiating area, without any connection with propagation and/or runout stage.

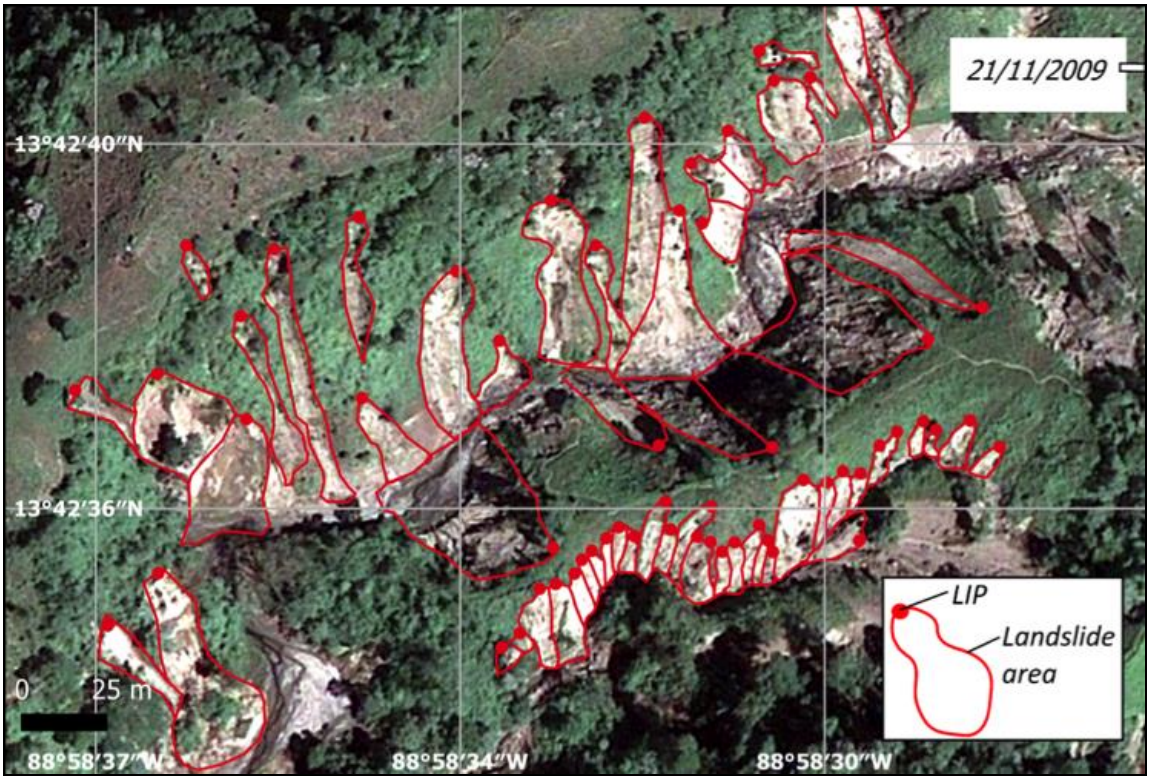

Fig. 5.19 – Example of the adopted landslide mapping scheme: LIPs and landslide areas.

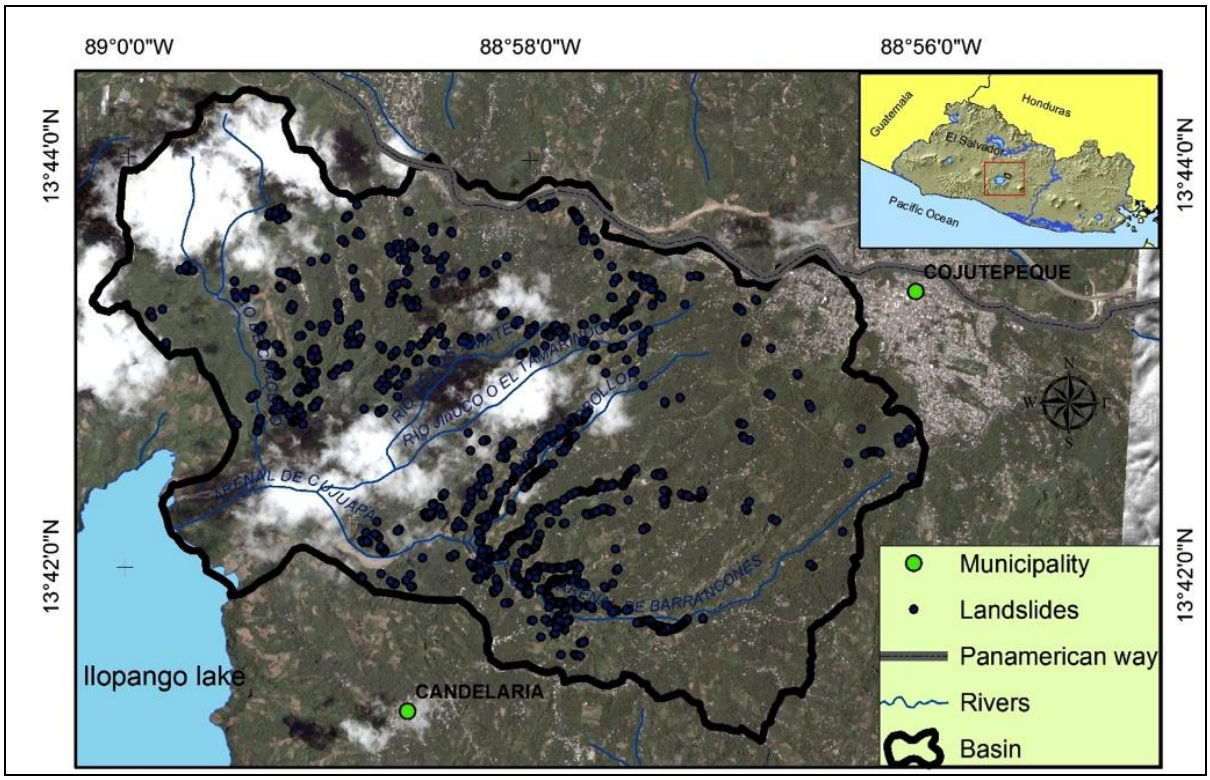

Fig. 5.20 - LIP inventory at 2003, before the TD96E/Ida event.

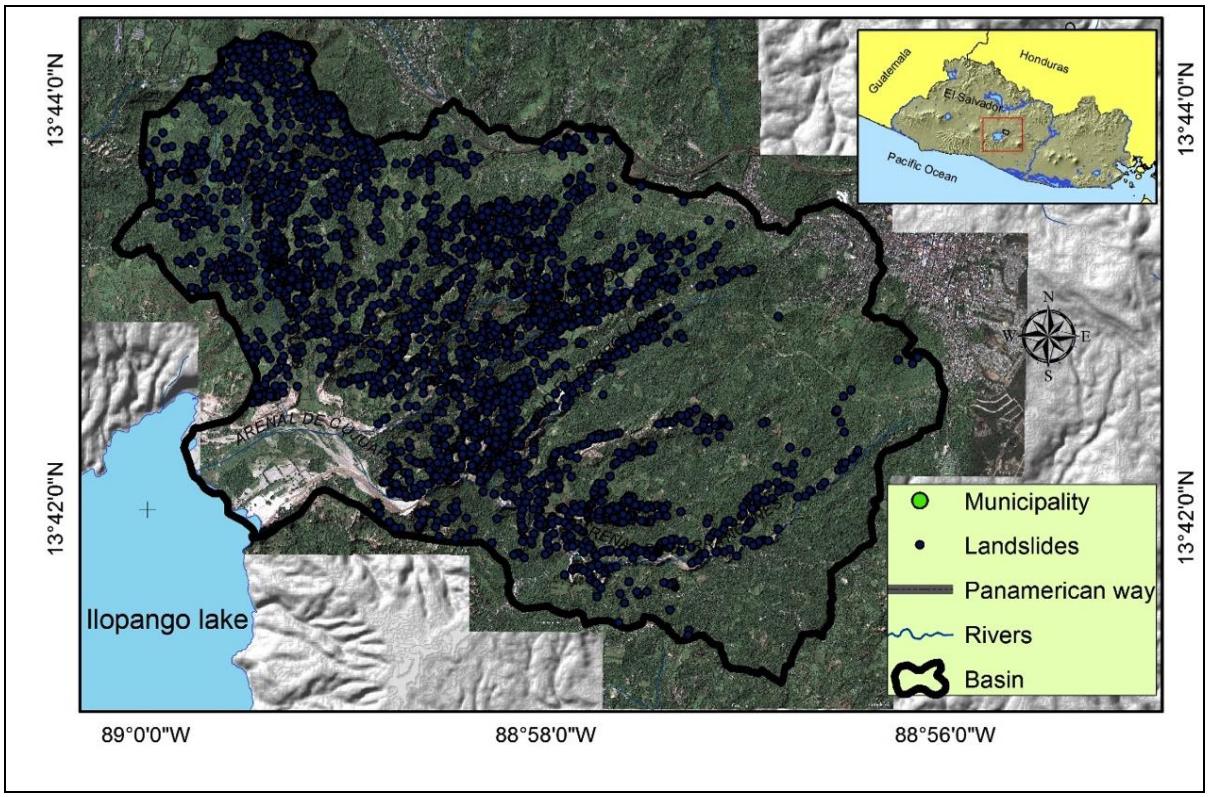

Fig. 5.21 - LIP inventory at 2009, after the TD96E/Ida event.

By comparing the two landslide inventories and applying a geometrical criterion base on a distance of 10m, near 250 2009 landslides resulted as re-activation of the 2003 (Fig. 5.22).

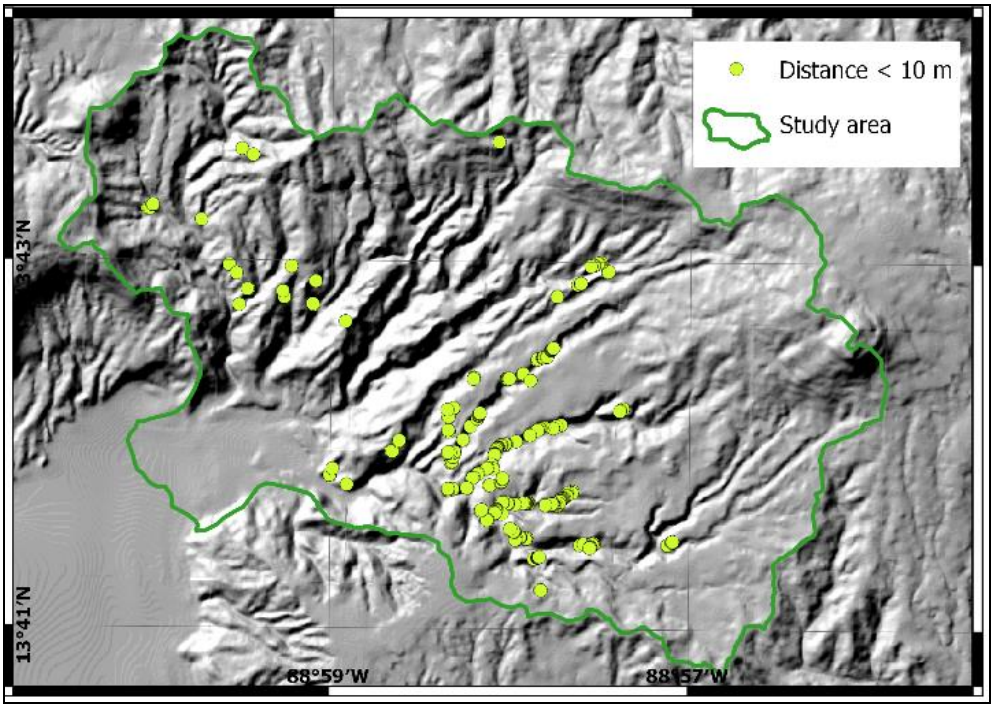

Fig. 5.22 – 2009 landslides, classified as re-activations of 2003.

Similarly, for the Coatepeque Caldera, a representative catchment was selected (Río La Joya basin) where 1904 landslide were founded (Fig. 5.23). The 12E-2011 inventory was recognized on the remote image ID: 101001000E684300 of the Digital Globe Catalog dated, at 03/11/2011 (Fig. 5.23).

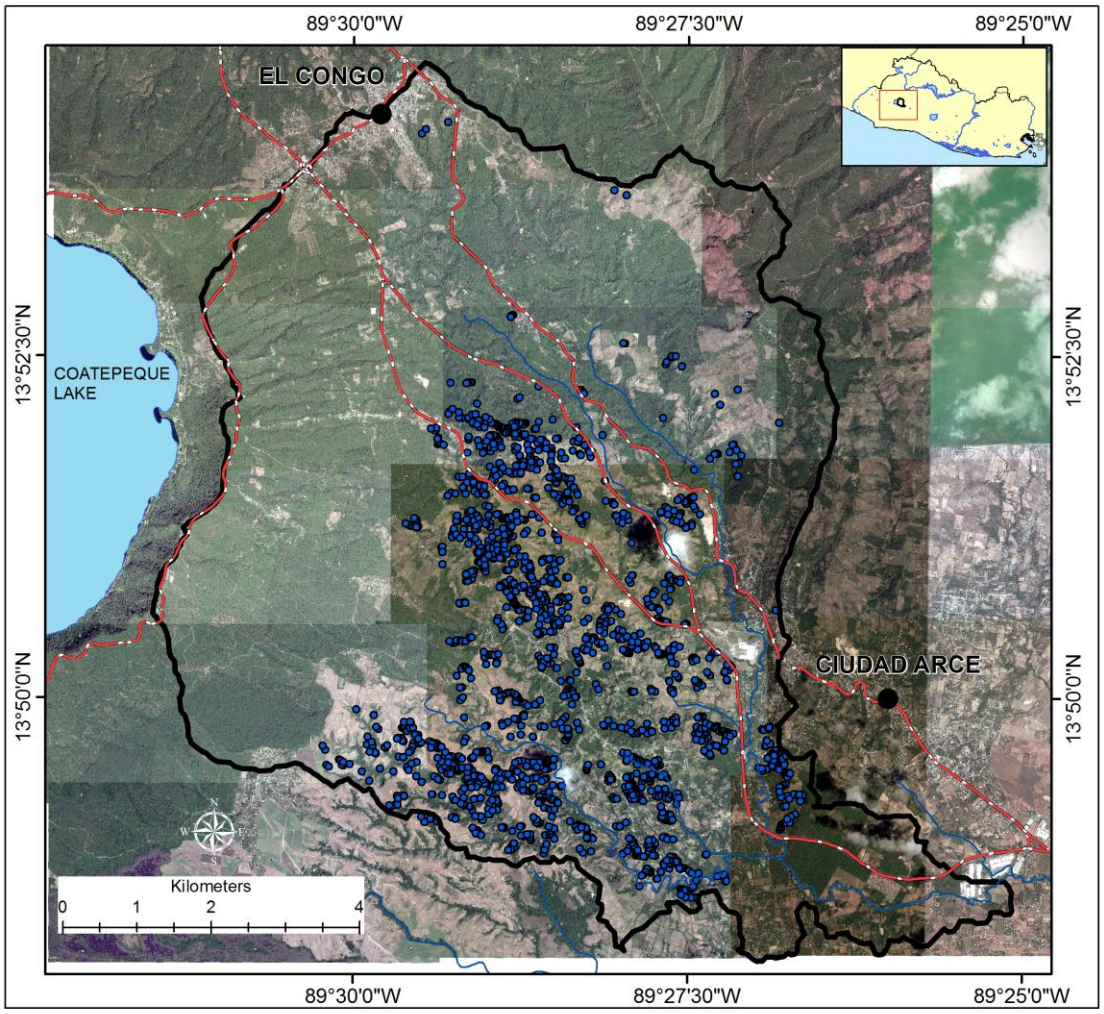

Fig. 5.23 - LIP inventory at 2011, after the TD12E event in Coatepeque caldera.

5.4. APPROACH AND METHODS

Landslide susceptibility modeling through stochastic approaches requires the definition of a set of independent variables or covariates, which are expected to play the role of predictors, and of a dependent variable, representing the outcome to be predicted. Therefore, a values for all of the variables considered is assigned to each of the mapping units in which the study area is spatially partitioned. In particular, the predictors are selected among those geo-environmental variables which are supposed to have controlled the slope failure mechanisms responsible for the observed past landslide scenario; the latter directly expresses the spatial distribution of the outcome, in terms of stable/unstable status of each mapping unit and constitutes the calibration dataset. The application of statistical methods allows then optimizing and testing for significance quantitative relationships which link the probability of the observed outcome status (stable/unstable) and the site multivariate conditions of each mapped pixel. Once the susceptibility model is calibrated, its predictive capability is then submitted to quantitative validation tests, which must be based on the evaluation of the accuracy, precision and general reliability of the derived predictive images (i.e., the susceptibility maps) in matching the spatial distribution of one or more unknown validation landslide inventories

Three different validation schemes were adopted: self-validation, based on random partition; chrono-validation, based on time partition; model transferring, based on spatial partition. In fact, due to the presence of the cloudy area in the 2003 Google Earth coverage, an evaluation of the effect in terms of potential decreasing of prediction skill produced by the blind zone in the calibration landslide inventory was to be estimated.

5.4.1. Integrating Logistic regression and MARS

A large fan of statistical techniques has been proposed in literature in the last decades, among which binary logistic regression (BLR) has gained in the last years more and more importance (Conoscenti et

al., 2015; Lombardo et al., 2015; Cama et al., 2015, 2016). Among the generalized linear modeling techniques, BLR exploits the logit transformation to linearize and constrain between 0 and 1 the relationship between the outcome and the predictors, according to the well-known relation (Hosmer and Lemeshow, 2000):

$$ln\left[\frac{p_{unst}}{1-p_{unst}}\right] = logit(p_{unst}) = \alpha + \sum_{i=1}^{n} \beta_i \, x_i$$

Where p_{unst} is the probability for a mapping unit to be classified/predicted as unstable, α is the model intercept and the βs the coefficients of the *n x* covariates. Once the intercept and the coefficients are regressed, by rearranging the logit expression, the probability (i.e., the susceptibility) of each pixel will be obtained as a function of the *x* values assumed by the predictors as

$$p_{unst} = \frac{e^{\alpha+\sum_{i=1}^{n}\beta_i x_i}}{1 + \ e^{\alpha+\sum_{i=1}^{n}\beta_i x_i}}.$$

The α coefficients are the core of the inner structure of the model expressing the extent and the positive/negative impact that each of the predictors plays in the logit value, being regressed under the assumption that the logit is linear in the continuous variables. The larger the depart from this assumption, the larger the ambiguity of the regressed model.

Recently, the adoption of MARS (Friedman, 1991) has proved to strengthen the predictive skill of generalized linear modeling techniques such as logistic regression. MARS is a non-parametric regression techniques which aims at fitting un-linear relationships between predictors and outcome, by fragmenting their range into an optimized number of linear branches. Each branch defines into the covariate axis a basis function (BF) which is structured as hinge functions delimited by knots. More complex BFs are

defined as the product of one or more hinge functions associated to different covariates. A particular case is the BF which correspond to the model intercept which is set to a constant value of 1.

The application of MARS algorithm is based on a two stages procedure. In a first stage (forward pass) MARS generates a model by stepwise adding (starting from a constant only model) pairs of terms corresponding to the mirrored hinge functions generated by a knot. At each step, the added pair of terms which results in the linear regression giving the maximum reduction of the residual sum-of-squares error (RSS) is added. In light of the simple structure and fast computing, the searching of the best pair is run systematically (in a "brute force" fashion). This stage can be run up either a minimum RSS gain is obtained or the whole set of possible BFs are added. In the second stage (backward pass) MARS stepwise prunes the best fitting but typically overfitted model, by dropping out of the model at each step the single term whose removal results in the lowest Generalized Cross-Validation parameter (GCV; Craven and Wahba, 1979). The criterion expressed by the GCV parameter is in fact the best compromise between fitting (low RSS) and model complexity, the latter depending on the number of terms. At each pruning step, a best model subset is then obtained.

expression is so given by:

$$logit(p_{unst}) = \alpha + \sum_{i=1}^{N} \beta_i \, h_i(x),$$

where N is the number of h_i basis functions obtained by knots-splitting the range of the x variables.

In this research, MARS (MultiAdaptive Regression Splines) modeling was performed using the "earth" package (Milborrow et al., 2011) of R software. In order to reduce the complexity of the models, the maximum degree of interaction was set equal to 1, thus avoiding terms given by combinations of two or more BFs. The software semi-automatically determined the maximum number of terms entering the MARS models. The "evimp" function of "earth" was employed to estimate the variable importance, as a

function of the number of entered model subsets. Only subsets equal to or smaller than the final model are considered to evaluate predictor importance (Milborrow, 2015).

In light of its flexibility and fast/easy to apply software/hardware structure the MARS algorithm has been recently adopted in stochastic modeling of geomorphological phenomena, including soil erosion and landslides. In this paper a first application to debris flow phenomena prediction in the framework of a time-partition based validation scheme is presented.

5.4.2. Predictors

The following covariates were assumed at the initial stage as potential predictors for slope failures in the study area: outcropping lithology (LIT), land use (USE), elevation (ELE), steepness (STP), aspect (ASP), plan (PLN) and profile (PRF) curvatures, topographic wetness index (TWI) and terrain ruggedness index.

The selection of the predictors was based on largely adopted geomorphological criteria and was here supported by a multi-collinearity analysis based on classic VIF (Variance Inflation Factor) estimation which exploited the "usdm" package (Naimi, 2015), setting a VIF value of 10 to exclude collinear variables from the models (Heckmann et al., 2014; Jebur et al., 2014; Bui et al., 2015).

Figures 5.24-5.25 (Fig. 28-29 for Coatepeque Caldera), show the maps of the variables which were selected as predictors, while Figures 5.26-5.27 summarize the frequency distributions of the eight variables in Ilopango Caldera.

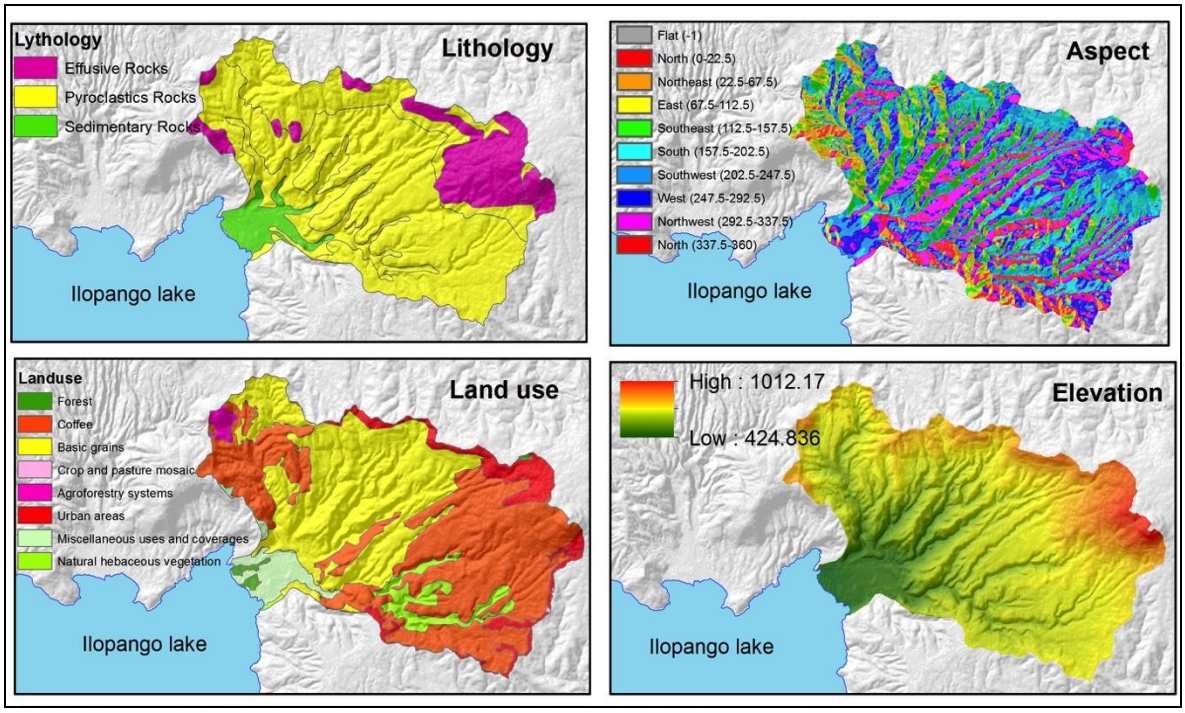

Fig. 5.24 – Maps of the geo-environmental variables which were selected as predictors.

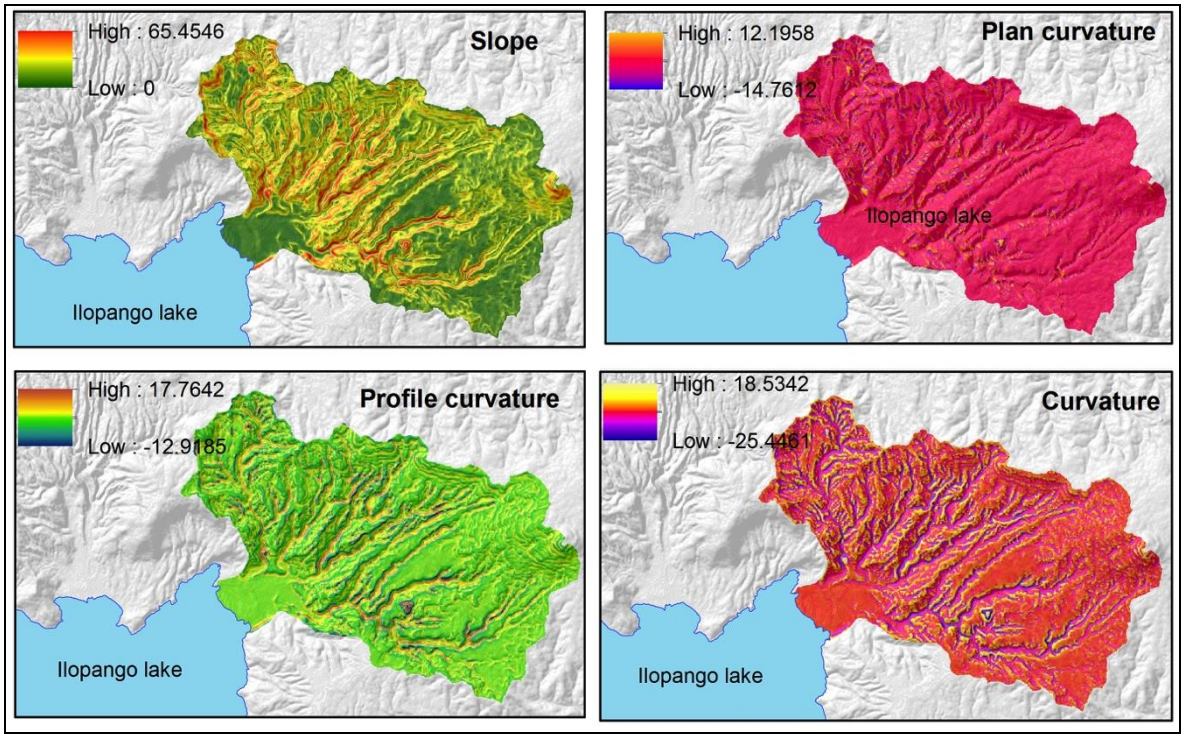

Fig. 5.25 – Maps of the geo-environmental variables which were selected as predictors.

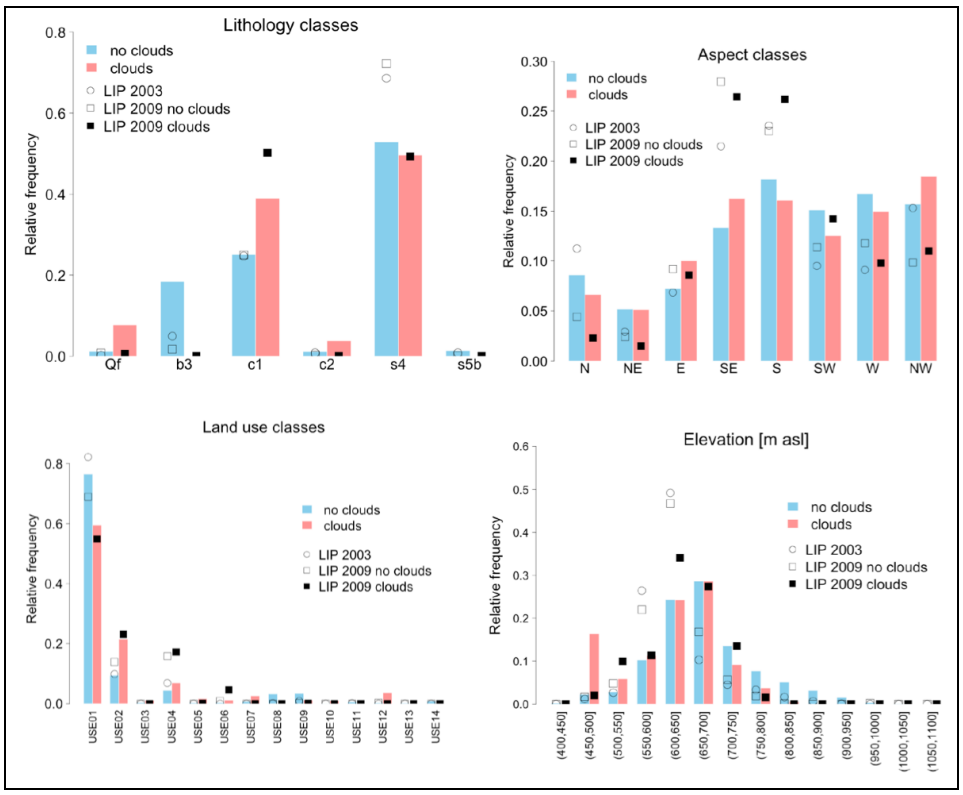

Fig. 5.26 – Frequency distributions of the predictors in the three sectors.

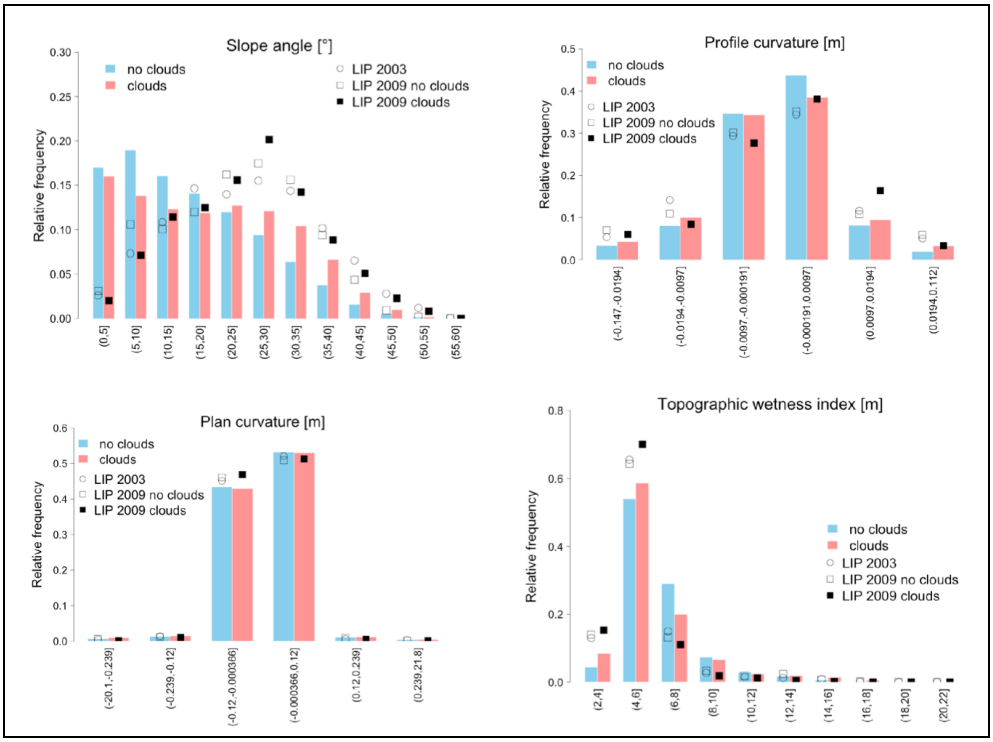

Fig. 5.27 – Frequency distributions of the predictors in the three sectors.

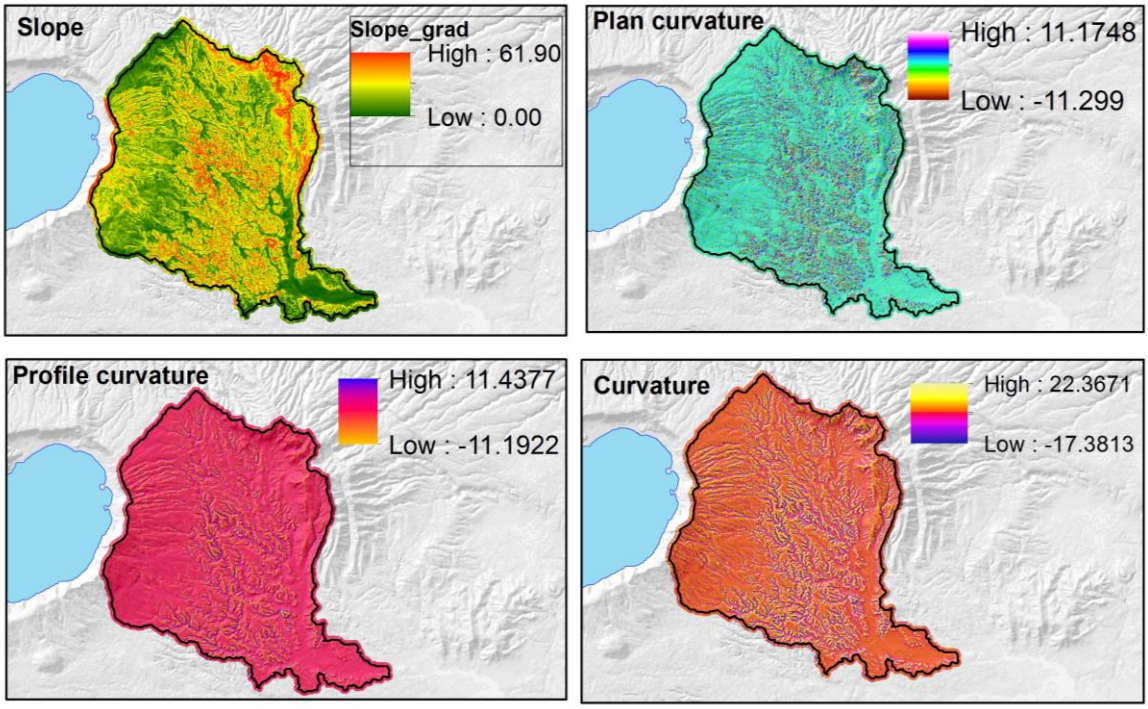

Fig. 5.28 – Maps of the geo-environmental variables which were selected as predictors in Coatepeque Caldera

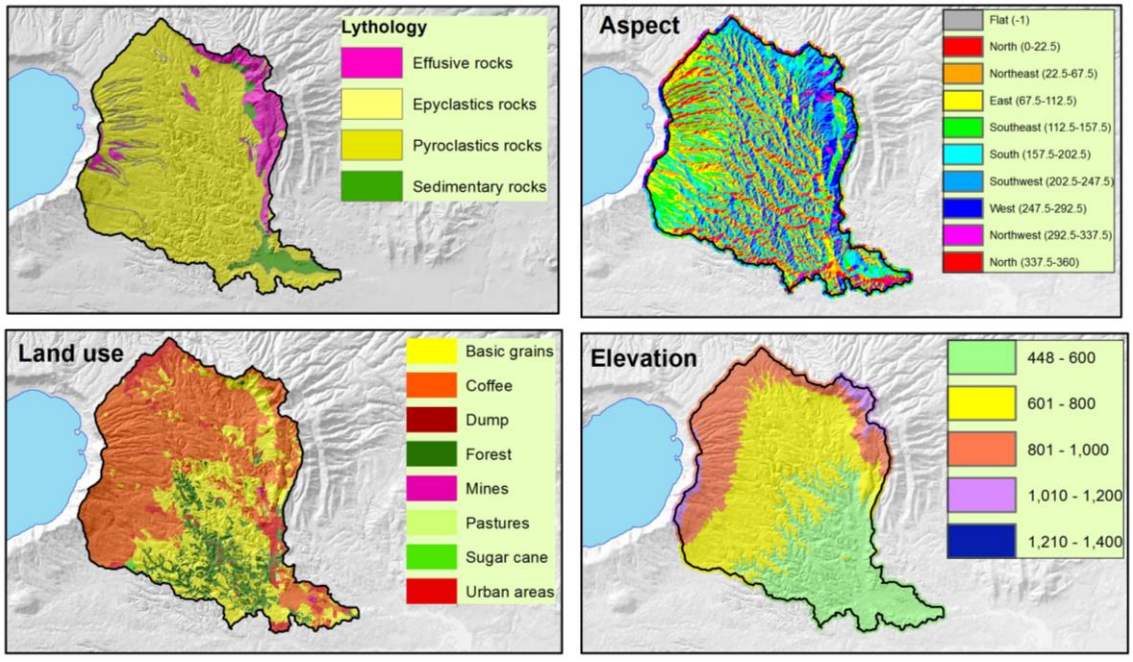

Fig. 5.29 – Maps of the geo-environmental variables which were selected as predictors in Coatepeque Caldera

5.4.3. Model building and validation strategy

Ilopango Caldera

According to the adopted research design, three different validation schemes were applied: self-validation, based on random partition; chrono-validation, based on time partition; model transferring, based on spatial partition (Chung and Fabbri, 2003; Lombardo et al., 2014; Cama et al., 2015). In fact, due to the presence of the cloudy area in the 2003 GE coverage, an evaluation of the effect in terms of potential decreasing of prediction skill produced by the blind zone in the 2003 calibration landslide inventory was to be also estimated. For this reason the 2003_{CF} model, which was calibrated in the CF sector, was tested through forward chrono-validation procedures in predicting the whole 2009 landslide inventory (2009_{ALL}), as well as its two CF (2009_{CF}) and CB (2009_{CB}) subsets. At the same time, a backward chrono-validation procedure was also performed in the CF sector, by calibrating with 2009 landslides and validating in predicting the 2003 phenomena, so to investigate, by comparison to the forward chrono-validated model, the effects in the predictive performance of the models produced by differences in the trigger intensity responsible for calibration and validation inventory. At the same time, a 2009_{CF} model (calibrated in the CF) sector was calibrated and transferred to predict the coeval landslides in the CB sector, through a spatial partition scheme. In this case, the calibration of the transferred model was blind to the CB sector, but based on a calibration landslide inventory which was produced by the same 2009 triggering event.

In order to have a reference for evaluating the performance of random partition based homogenous predictions the 2003_{CF}, 2009_{ALL}, 2009_{CF} and 2009_{CB} were before submitted to self-validation.

Each regressed dataset was balanced by adding to the positives (i.e. 10x10m pixels hosting a LIP) an equal number of randomly selected negatives (LIP free pixels). For chrono- and spatial partition based validations, one-hundred replicates were also obtained each including a different subset of negatives both

in the calibration and validation datasets. Self-validations were based on 10-folds with 10 repetitions cross-validation schemes, obtaining one hundred estimates of the model parameters and performance metrics.

The performances of the models were evaluated by adopting both cut-off dependent and independent approaches. In particular, the accuracy of the model was evaluated both by computing the AUC (Area Under Curve) in the ROC (Receiver Operating Characteristics) sensitivity Vs. fall out plots, as well as from confusion matrixes distinguishing the true/false positive/negative cases (TP, TN, FP and FN, respectively), obtained from Youden index optimized cut-off (Youden, 1950). The one hundred replicates which were produced for each of the validation procedures allowed to obtain mean and variance of the metrics which were selected to express the model performances in terms of accuracy and reliability.

Table 5.1 gives a summary of the adopted model building and validation strategy.

MOD.	VALIDATION SCHEME	CALIBRATION	VALIDATION	DATASET	REPLICATES
A	$SELF_{2003CF}$	$2003_{CF\_RND(90\%)}$	$2003_{CF\_RND(10\%)}$	10-folds cross-validation	100
B	$^{FRW}CHRONO_{CF\text{-}CF}$	$2003_{CF\_(100\%)}$	$2009_{CF\_(100\%)}$	100 (CAL X VAL)	100
C	$^{FRW}CHRONO_{CF\text{-}ALL}$	$2003_{CF\_(100\%)}$	2009_{ALL}	100 (CAL X VAL)	100
D	$^{FRW}CHRONO_{CF\text{-}CB}$	$2003_{CF\_(100\%)}$	$2009_{CB\_(100\%)}$	100 (CAL X VAL)	100
E	$^{BCK}CHRONO_{CF\text{-}CF}$	$2009_{CF\_(100\%)}$	$2003_{CF\_(100\%)}$	100 (CAL X VAL)	100
F	$SELF_{2009ALL}$	$2009_{ALL\_RND(90\%)}$	$2009_{ALL\_RND(10\%)}$	10-folds cross-validation	100
G	$SELF_{2009CF}$	$2009_{CF\_RND(90\%)}$	$2009_{CF\_RND(10\%)}$	10-folds cross-validation	100
H	$SELF_{2009CB}$	$2009_{CB\_RND(90\%)}$	$2009_{CB\_RND(10\%)}$	10-folds cross-validation	100
I	$TRANSF_{2009CF\text{-}CB}$	$2009_{CF\_(100\%)}$	$2009_{CB\_(100\%)}$	100 (CAL X VAL)	100

Tab. 5.1 – Model building and validation scheme.

Coatepeque Caldera

For the Coatepeque Caldera, a total transferring scheme was tested, by verifying if the model calibrated with the 2009 Ilopango dataset would be effective in predicting the Coatepeque 2011 event. To have a

reference value for evaluating the performance of the transferred model, a self-validation scheme was also applied by randomly partitioning the 2011 landslide inventory of Coatepeque.

5.4.4. Results

Ilopango Caldera

Figure 5.30 shows a boxplot of the nine one-hundred AUCs sets was prepared.

The 2003CF and 2009CF self validated models obtained (Fig. 5.30) the same highest excellent performances, with AUC above 0.8 (Hosmer and Lemeshow, 2000). As regards the forward chrono-validations (Fig. 5.32, tab. 5.2), starting from a fully good performance in the CF sector (AUC>0.76), a marked AUC decreasing was observed for the ALL (AUC=0.74) and, more dramatically, the CB datasets (AUC=0.65), with the latter validation well below the acceptance threshold. At the same time, if focusing on 2009 self-calibrated models, a slightly performance decreasing was observed from 2009CF, to 2009ALL, down to 2009CB. In the CF sector, forward and backward chrono-validations produced (Fig. 5.31, tab. 5.2) almost the same results in terms of AUCs. Finally, the transferred 2009 model, from CF to CB performed just above the acceptance 0.7 AUC thresholds.

If cutoff dependent performance metrics are taken into consideration (Tab. 5.2), it is evident how the loss in prediction skill in the CF sector from 2003 self-validation (model A) to forward chrono-validation (model B) depends on a sensitivity decreasing. Besides, if the blind sector is included in (model C) or totally defines (model D) the prediction areas, a coupled lowering of specificity (false negative occurrences) is responsible for more marked AUC decreasing. On the contrary, if comparing the backward (model E) to the forward (model B) chrono-validated models in the same CF sector, the slightly higher AUC of the first is correlated to a higher sensitivity but a lower specificity.

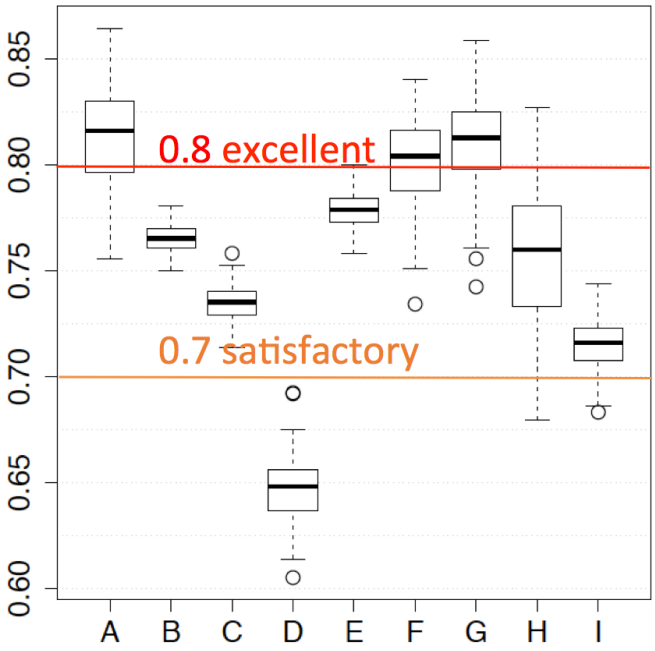

Fig. 5.30 – Box plot of the model performances (see tab. 5.1 for captions).

As regards the self-validated 2009 models, the results highlighted the better sensitivity performance for the ALL model and the lower for the CB; however, the changings in specificity and sensitivity are not coupled in these cases, as the higher value was for the CB model and the lower for the CF.

Finally, the transferred model (model I) produced high sensitivity but a fall of specificity (TN-rate < 0.5), so that, if compared to the correspondent forward chrono-validated model (model D), a marked higher sensitivity but lower specificity arises.

Figure 5.33 shows the nine susceptibility maps obtained by averaging for each of the mapped pixels the one-hundred values of probability for unstable conditions.

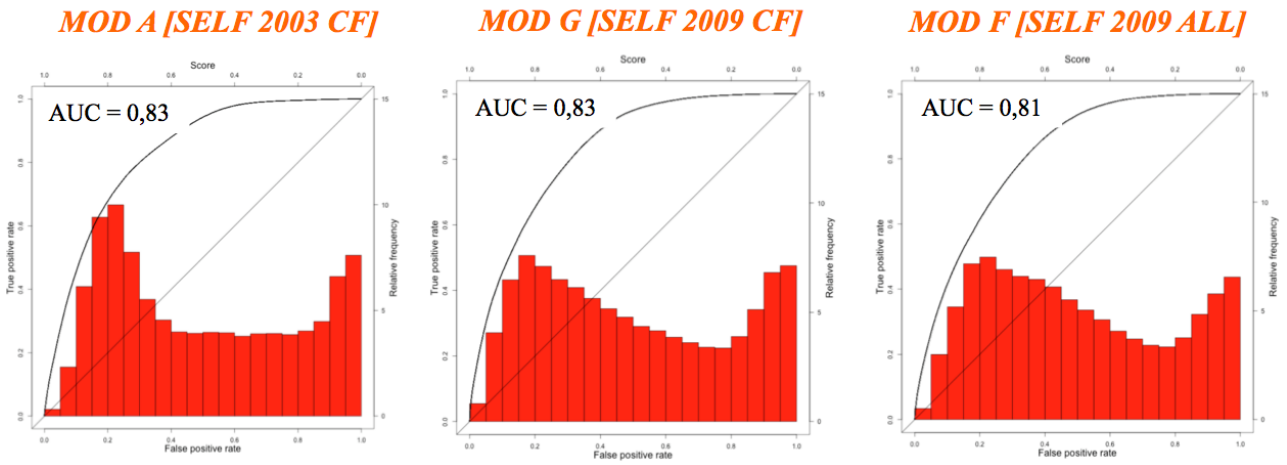

Fig. 5.31 – Averaged ROC-plots for the self-validated models (see tab. 5.1 for captions).

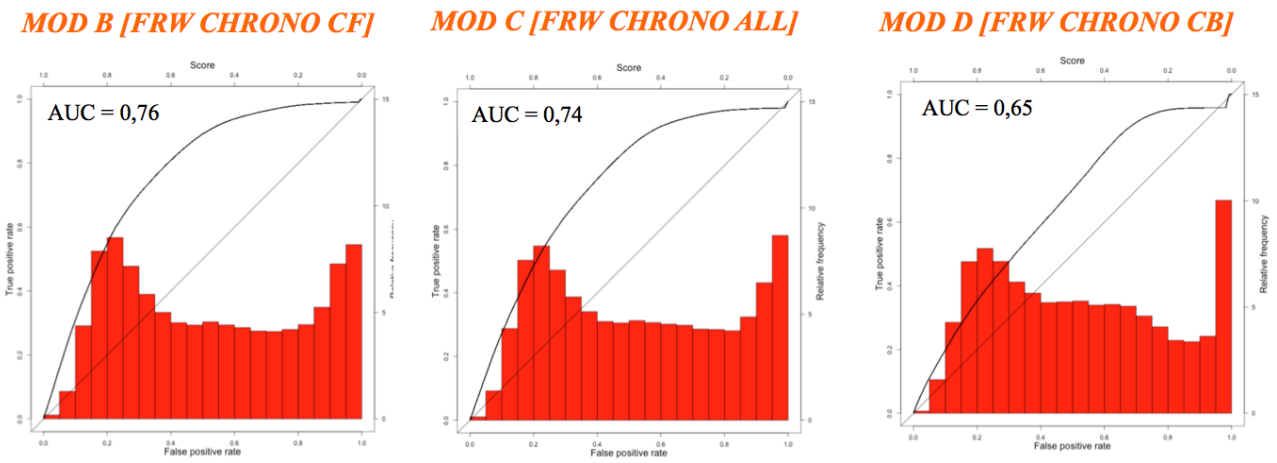

Fig. 5.32 – Averaged ROC-plots for the forward chrono-validated models (see tab. 5.1 for captions).

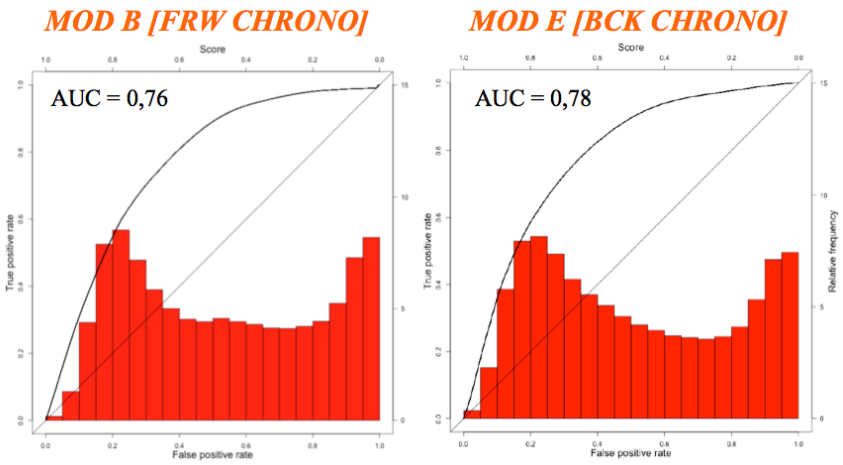

Fig. 5.33 – Averaged ROC-plots for the forward and backward chrono-validated models in the CF sector (see tab. 5.1 for captions).

		ROC AUC	RECALL				PRECISION		ACCURACY
MOD.	VALIDATION SCHEME	MEAN	SENSIT.	SPECIF.	FALL OUT	FNR	PPV	NPV	
A	$SELF_{2003CF}$	0.83	0.78	0.72	0.28	0.22	0.74	0.76	0.75
B	$^{FRW}CHRONO_{CF\text{-}CF}$	0.76	0.68	0.72	0.28	0.32	0.71	0.69	0.70
C	$^{FRW}CHRONO_{CF\text{-}ALL}$	0.74	0.64	0.70	0.30	0.36	0.68	0.66	0.67
D	$^{FRW}CHRONO_{CF\text{-}CB}$	0.65	0.58	0.61	0.39	0.42	0.60	0.59	0.59
E	$^{BCK}CHRONO_{CF\text{-}CF}$	0.78	0.79	0.63	0.37	0.21	0.68	0.76	0.71
F	$SELF_{2009ALL}$	0.81	0.84	0.66	0.34	0.16	0.71	0.80	0.75
G	$SELF_{2009CF}$	0.83	0.83	0.63	0.37	0.17	0.69	0.79	0.73
H	$SELF_{2009CB}$	0.80	0.75	0.70	0.30	0.25	0.71	0.73	0.72
I	$TRANSF_{2009CF\text{-}CB}$	0.72	0.83	0.46	0.54	0.17	0.61	0.73	0.65

Tab. 5.2 – Summarized results of all the models, both for AUC and contingency tables analysis (see tab. 5.1 for captions).

Coatepeque Caldera

In order to verify the ability of the model calibrated in the Ilopango caldera, under the 2009 event, to predict other events in other catchments, a test was carried out to fit the landslides activated in the Coatepeque Caldera south-western slopes in 2011.

In particular, the model obtained by exploiting the whole set of landslides activated in 2009 for calibration was tested in predicting the landslide distribution at Coatepeque Caldera in 2011, triggered by the 12E Tropical Depression.

However, in light of the difference in terms of outcropping lithologies, a new model was run, based only on land use and DEM-derived predictors. First, this no-lithology model (self-ilop) was calibrated and self-validated in the Ilopango Caldera, observing a slight lowering of the ROC AUC (Fig. 5.34) with respect to the AUC obtained with the full-model (including lithology; self-ilop_full).

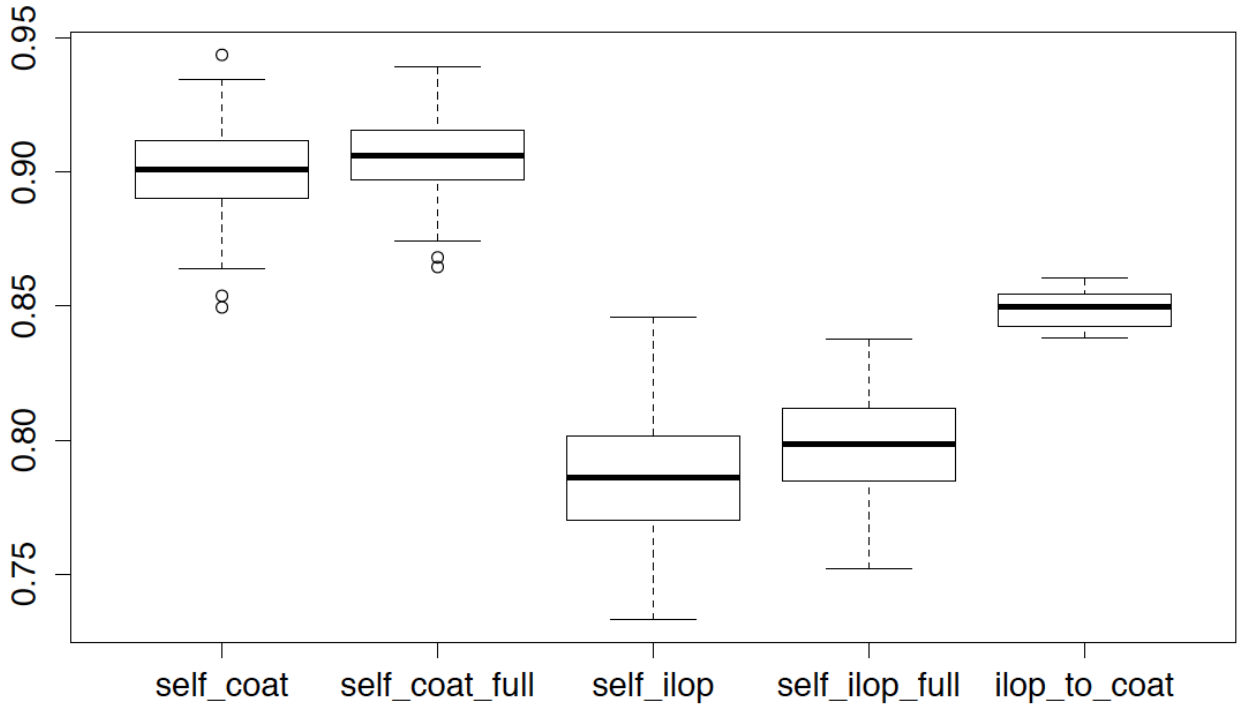

Fig. 5.34 – Results (ROC-AUCs) of the exportation from Ilopango – 2009 to Coatepeque 2011. self_coat: Coatepeque self-validated no-lithology model; self_coat_full: Coatepeque self-validated full model; self_ilop: Ilopango self-validated no-lithology model; self_ilop_full: Ilopango self-validated full model; ilop_to_coat: Ilopango to Coatepeque transferred no lithology model.

Surprisingly, the transferred model (calibrated in the Ilopango and validated in the Coatepeque calderas: ilop_to_coat) performed markedly better than the "self_ilop", suggesting the model calibrated in the Ilopango Caldera at 2009 more skilled in predicting the landslides triggered into the other catchment by another event. At the same time, it is worth to note how the self-validated model into the Coatepeque Caldera generally performed excellently, with AUC above 0.9 and very low increasing when including the lithology among the predictors. Fig. 5.35 shows the marked difference between the ROC curves of the self-validated and the transferred models, in blue and red, respectively.

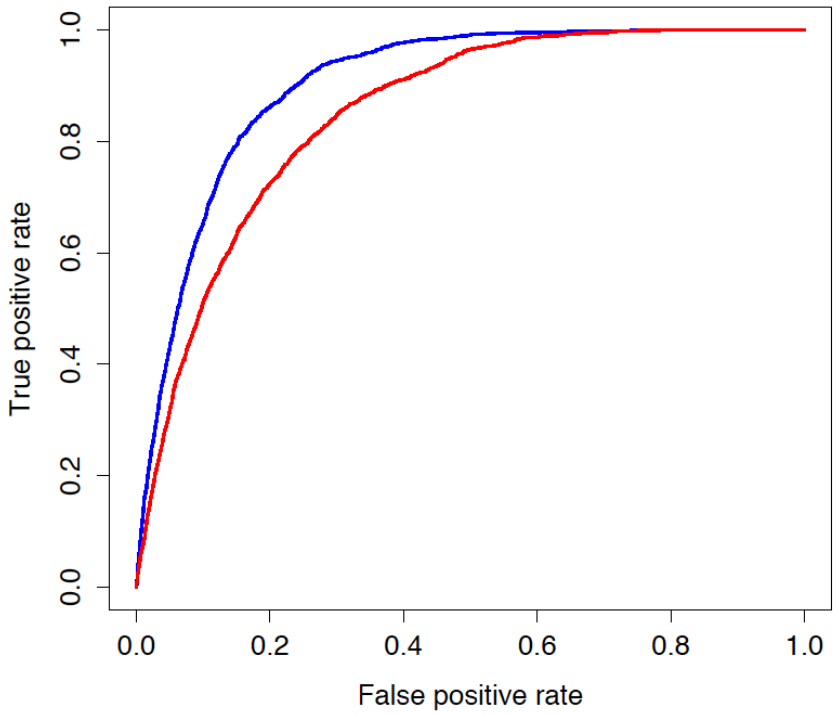

Fig. 5.35 – Comparison between the two ROC curves of the self-validated and the transferred models, in blue (AUC = 0.902) and red (AUC = 0.850), respectively.

It is worth to observe how the two models (transferred and self-validated) work in the Coatepeque catchment. In fact, although the performance of the transferred model seems to be also fully satisfying (even if lower than the excellent level of the self validated), very low values of score (probability or susceptibility) characterize the curve (Fig. 5.36). That doesn't affect the good value of the AUC, as this index just expresses the goodness of the shape of the ROC-curve, but it obviously poses limits in trying to assign the score values a meaning in terms of probability. In fact, very few pixels have a score higher than 0.5, in spite of the good avoiding (Fig. 5.37).

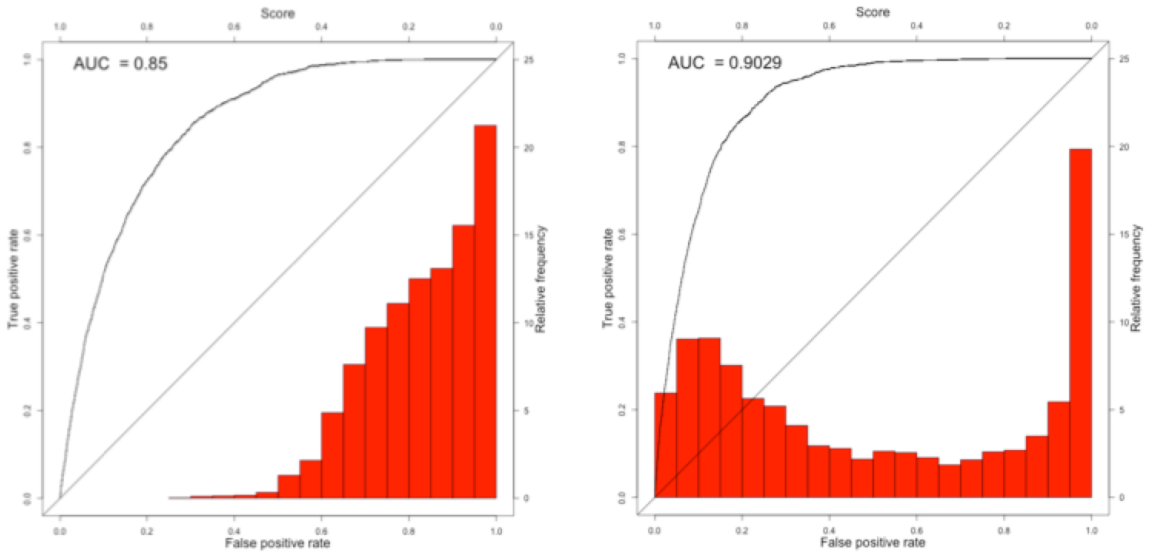

Fig. 5.36 – ROC-curves and frequency distribution of the scores for the transferred (on the left) and self-validated (on the right) models.

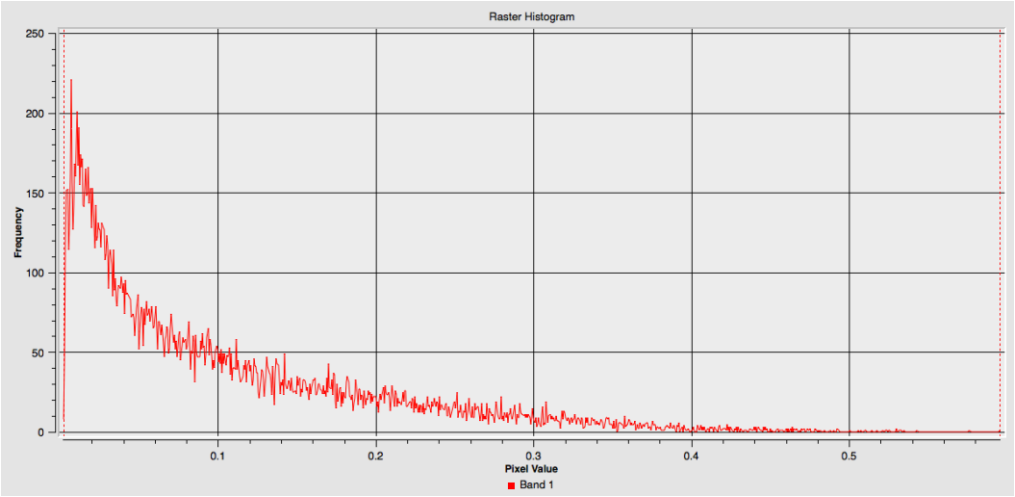

Fig. 5.37 – Frequency distribution of the pixel score for the ilo_to_coat model.

The above consideration has direct consequences when estimating the quality of the model by using a cut-off dependent measure such us the accuracy or the error rate. In fact, if taking a 0.5 score as cut-off between positive/negative cases, a very low performance arises (Tab. 5.3). It is then necessary to adopt an optimal cut-off selection, such as the Youden index criterion, to recover the good performance of the model. However, the difference in the Youden index cut-off score values can be taken into account for further considerations regarding the two events and the two catchments.

	Transferred	Transferred	Self-validated
	cut-off=0.5	Youden cut-off 0.12	Youden cut-off 0.56
Accuracy	0.506	0.775	0.832
Sensitivity	0.014	0.855	0.852
Specificity	0.998	0.695	0.812
PosPredValue	0.903	0.737	0.82
NegPredValue	0.503	0.827	0.846

Tab. 5.3 – Comparison between the transferred (with optimized and 0.5 cut-off) and the self- validated model in the Coatepeque Caldera.

Fig. 5.38 shows the susceptibility maps obtained for the Coatepeque Caldera by self-calibrating the model, using the landslides which activated there in 2011, and by calibrating the model in the Ilopango Caldera, using the landslides which activated there in 2009. The tow maps were reclassified into quantiles and it is evident how the two models generally agree in indicating the lower-central sector of the Rio Agua Caliente catchment as the more susceptible, in spite of the low susceptibility values of the upper water divide sector. However, it is also clear that the two maps differently depict the susceptibility pattern in both the two sectors. Moreover, if comparing the two legends, the large differences in the absolute values of score arise.

The map of the residuals (Fig. 5.39) generally highlights large differences of scores only in the susceptible sector, where the self-calibrated model systematically produces probabilities higher for a more than 0.1.

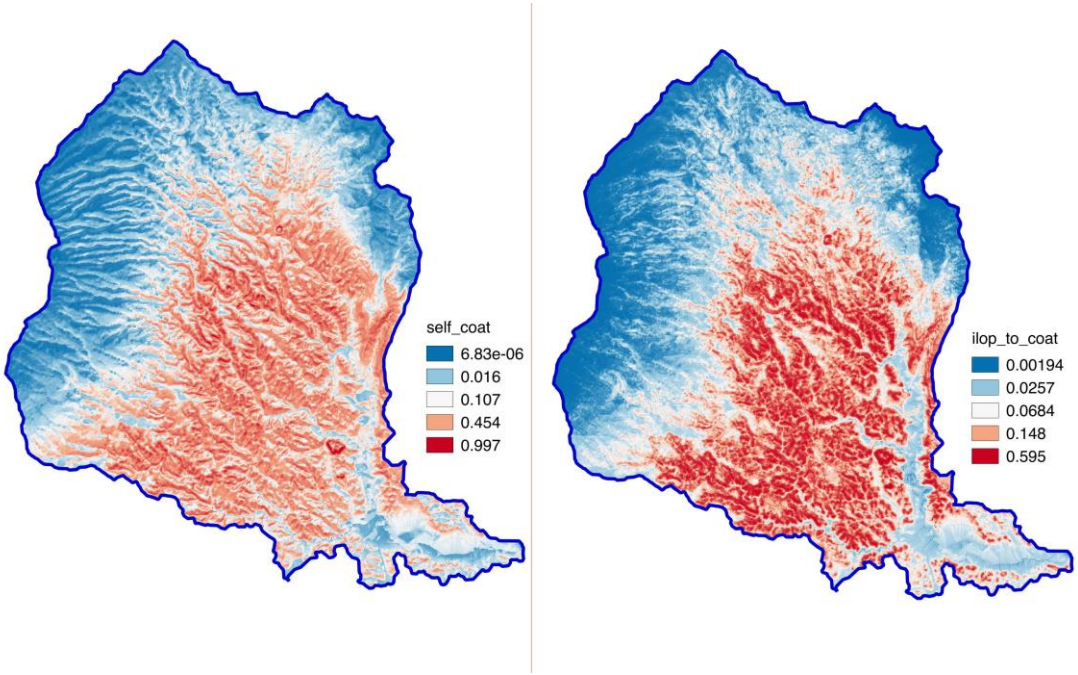

Fig 5.38 – Susceptibility map for the Coatepeque Caldera: self-calibrated model (on the left); transferred model, calibrated in the Ilopango Caldera (on the right).

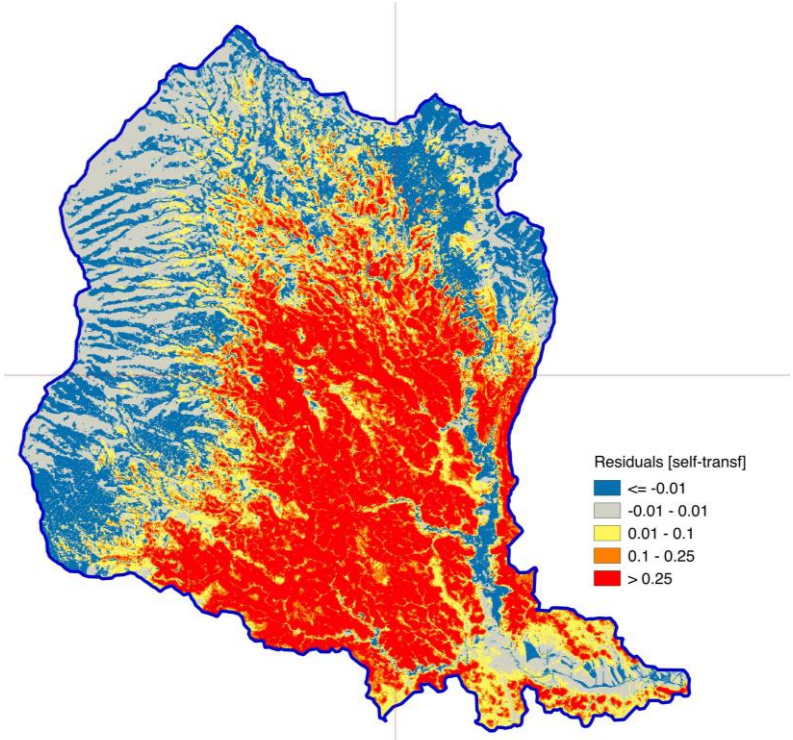

Fig 5.39 – Map of the residuals for the Coatepeque Caldera: [self-calibrated model] – [transferred model].

A different perspective to the residuals can be obtained by looking at their frequency distribution (Fig. 5.40). In very few cases the score of the transferred model is higher (>0.1) than the one assigned to the

pixels by the self-calibrated model, whilst a great number of pixels are characterized by higher self-calibrated scores.

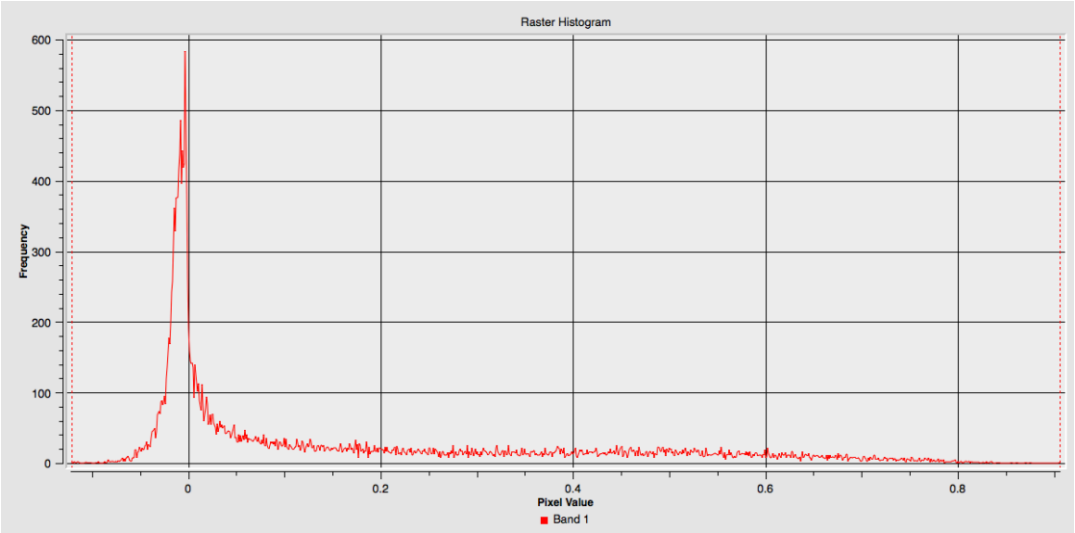

Fig 5.40 – Frequency distribution of the residuals for the Coatepeque Caldera: [self-calibrated model] – [transferred model].

5.4.5. Discussion

Ilopango Caldera

In order to face the two main topics of this research, different perspectives are here adopted for discussion. In the time domain, the results of forward and backward chrono-validations are compared so to analyze if the different triggering conditions did affect the predictive performance of susceptibility modeling. Second, by comparing the predictive performances of the models calibrated in the different sectors (CF, CB and ALL), the incidence of the blind zone is weighted both in the chrono-validation and spatial domain results.

The results attested that the 2003 landslide inventory allowed to calibrate a predictive model, whose performance was estimated as very high when a self-validation procedure was applied. However, if trying to predict the sites were the IDA/96E event has then (in 2009) activated debris flow phenomena, a relevant number of false negative occurrences was recorded (lower of sensitivity and higher fallout), causing a clear AUC decreasing (from above to below the 0.8 threshold). Due to a coupled marked

decreasing of specificity (limits in predicting stable conditions), this effect is greater, if extending the chrono-validation to the whole catchment (model C), up to dramatic if restricting only to the CB sector (model D). An analogous AUC decreasing arose in the CF sector for the backward chrono-validation (model E) with respect to the 2009CF self-validated model (model G), caused by a high number of false positives but a stable low specificity. However, the same model E showed a higher accuracy with respect to the forward chrono-validated model B with a higher sensitivity albeit with a lowering of specificity. It is worth to note that the skill in predicting the 2009 negatives in the CF sector is higher for the forward chrono-validated than for the 2009 self-validated.

The compared analysis of the forward and backward chrono-validations in the same CF sector suggests that the model calibrated with the landslide inventory associated to the normal triggering (i.e. the 2003 LIPs) is less capable to predict the sites of landslide activation under tropical storms, resulting in very critical type-II errors (false negative occurrences). On the contrary, the 2009LIPs-calibrated model is capable to detect nearly the 80% of the 2003 landslides but expecting a high number of positives, actually corresponding to 2003 stable sites (type-I errors), with low specificity and high number of false positives. This seems to confirm non-linear stochastic relationships between predictors and outcome under different driving conditions, as the validation onto a more severe landslide scenario corresponds to a false-to-true conversion of the predicted positives (high PPV for the forward chrono-validated CF model), which does not compensate for the sensitivity decreasing.

In terms of geomorphological model, a more intense triggering of the slopes is responsible for the activation of large part of the site conditions which typically activate under normal triggering but together with other regions of the multivariate parameter hyperspace, having stable status under normal triggering. This means that, if we focus on the applicative relevance of the prediction, exploiting landslide scenarios caused by more intense triggering events, allows to fit large part of the low-trigger caused landslides as well as the same high-trigger landslides. This same effect arises if we compare the

performances of the models in predicting the 2009CB landslides. In fact, a much more marked lowering of the performance was observed for the chrono-validated model D (AUC = 0.647) with respect to the transferred model I (AUC=0.715); both the two models are calibrated only in the CF sector, but the landslide calibration dataset of the transferred model was produced by the same triggering event which caused the landslides in the blind zone. At the same time, it is worth to note that the specificity decreasing is greater for the transferred model than the forward chrono-validated model.

An analysis of the susceptibility maps obtained for cloud-free sector (Fig. 5.41) and the whole catchment (Fig. 5.42), highlights how, depending on the landslide inventory which is adopted for calibrating the model, the susceptibility map changes. In particular, the analysis of the residuals demonstrates that the 2003 model tends to overestimate the susceptibility in the inner head sector and along the ridges whilst the models calibrated at 2009 overestimate the susceptibility along the valley bottom.

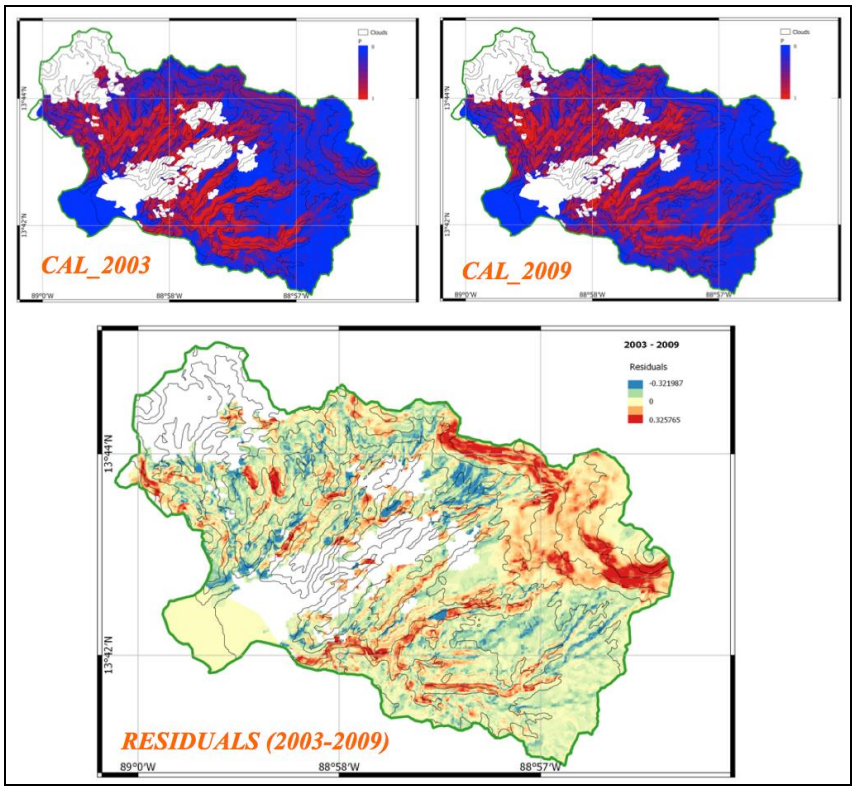

Fig. 5.41 – Susceptibility map for the cloud-free (CF) sector, obtained by calibrating the model at 2003 (top-left and 2009 (top right). In the bottom the map of the residuals.

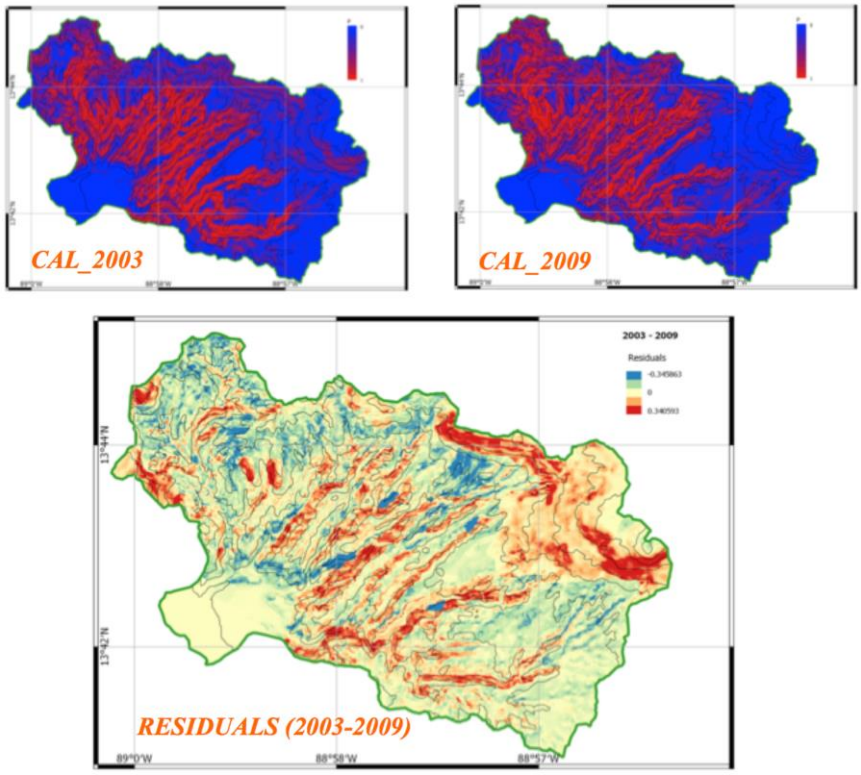

Fig. 5.42 – Susceptibility map for the whole catchment (ALL), obtained by calibrating the model at 2003 (top-left and 2009 (top right). In the bottom the map of the residuals.

Coatepeque Caldera

The test of model transferring in the Coatepeque Caldera furnished several important elements to the main topic of this research. Before to go into details, it is worth to note that all the tested models gave AUC values well above the satisfactory threshold, attesting that the adopted approach and method is suitable for landslide prediction in El Salvador. However, as regards the methodological aspects which were the topics of the doctorate research, some important results have been obtained. In fact, it is very interesting how the model calibrated in the Ilopango Caldera performed in reproducing the 2011 landslide scenario. The performance was higher than the one of the self-calibrated model in the Ilopango Caldera, confirming that the dataset under the 96E/Ida event is characterized by strong un-linearity resulting in clear limit both in chrono- and spatial validation. That could be ascribed to a critical coupling between the geo-environmental features and the spatial distribution of the trigger intensity.

The above mentioned effect is confirmed when comparing the large difference between the performance of the two self-calibrated models, with the Coatepeque 2011 model reaching the excellence level. In this sense, the geologic setting of the Agua Caliente catchment are more uniform and homogenous; at the same time the 2011 event was less concentrated and more homogeneously distributed, producing large landslide activations in the susceptible sectors. This is confirmed by the large shift between the scores estimated for the Coatepeque Caldera area by calibrating the model with the Ilopango dataset.

The underestimation of the score (or susceptibility levels) for the transferred model poses in a dramatic way the key role of the proper selection of the cut-off values for susceptibility mapping. A default values at 0.5 would result in a very misleading prediction image (Fig. 5.43). The application of proper methods for the optimal selection of the cut-off values, as the one based on the Youden index (Fig. 5.44), allows to prevent enormous failing in landslide prediction, obtaining a ma very similar to best one optimized through self-calibration (Fig. 5.45).

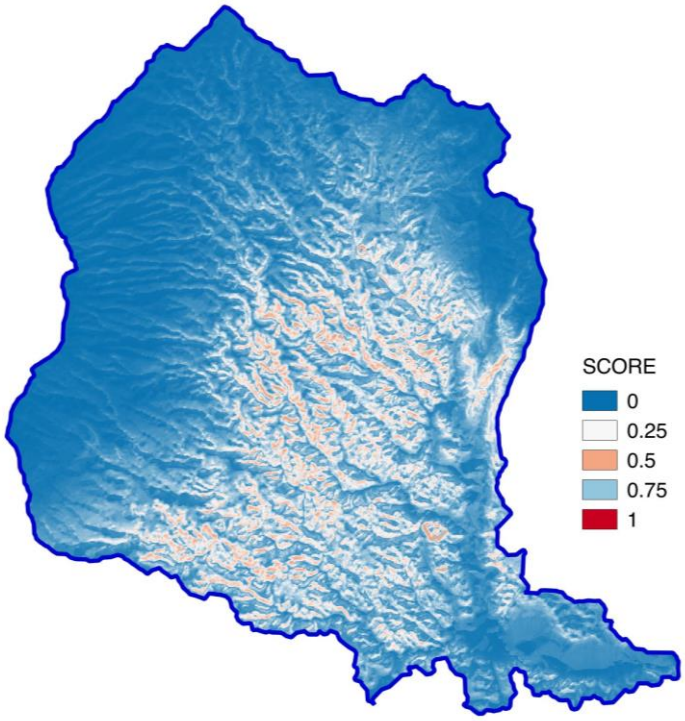

Fig. 5.43 – Susceptibility map for the Agua Caliente catchment, based on a 0.5 cut-off five classes, through model transferring from Ilopango Caldera.

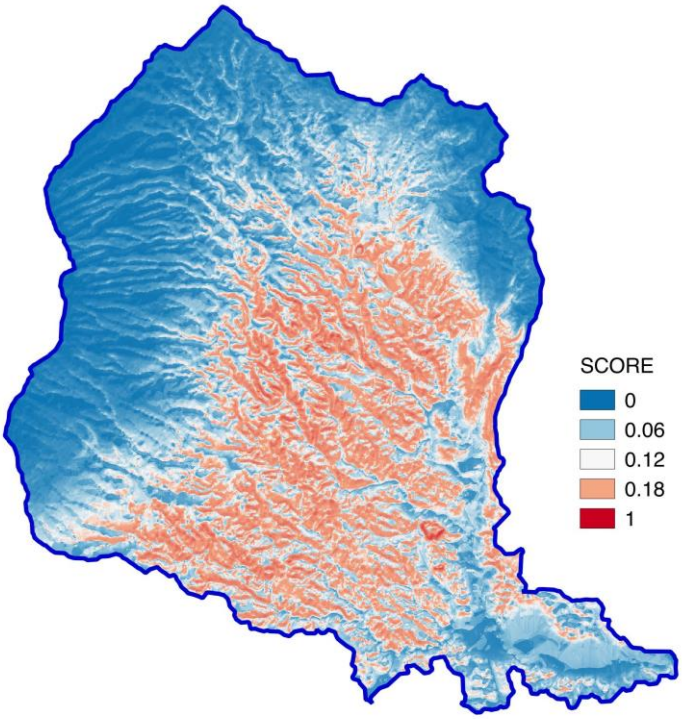

Fig. 5.44 – Susceptibility map for the Agua Caliente catchment, based on a optimized 0.12 cut-off five classes, through model transferring from Ilopango Caldera.

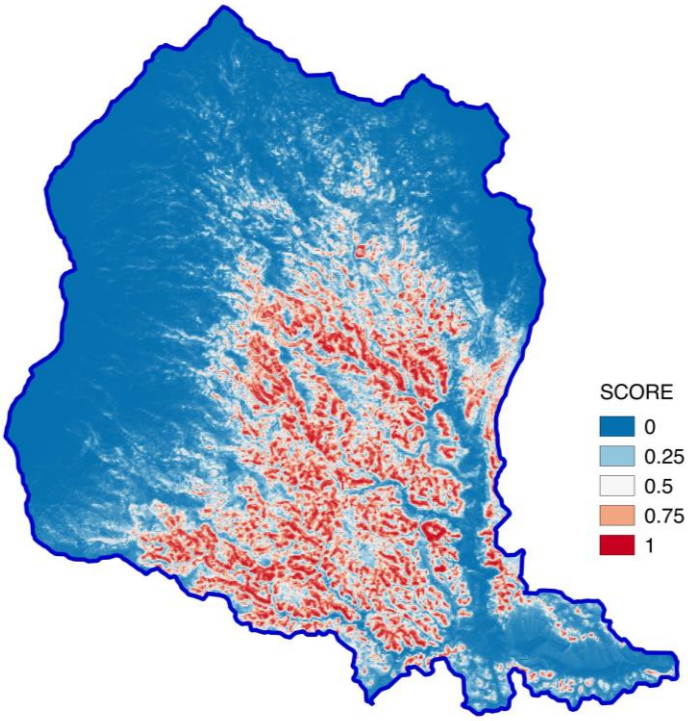

Fig. 5.45 – Susceptibility map for the Agua Caliente catchment, based on a 0.5 cut-off five classes, through self-calibration.

5.4.6. Conclusions

Predicting storm triggered landslides always poses the problem of the morphodynamic coherence between calibration and validation datasets. In fact, the regressed relationships which link predictors and outcome can show non-linear behavior in the trigger intensity dimension, which could result in limiting the performance of the models with either false negative or false positive predictions.

In the present research a test was carried out in a very representative area of center America, based on two different landslide inventories: one produced by normal rainfall, the other being the result of a very intense triggering storm (the Ida/96E 2009 event). The results confirmed the influence in the predictive performance of the susceptibility models caused by the difference in the triggering conditions which produced the calibration and the validation inventories. In particular, the model calibrated with the tropical storm landslide inventory, resulted in higher false positives, whilst the one calibrated with the normal inventory faced a lot of false negatives in predicting the Ida/96E landslides. Focusing only in a AUC estimation for assessing the quality of the prediction could be misleading in terms of the applicative using of the susceptibility maps, which has to look at the correctness of positive/negative discrimination. This research demonstrated that crossing an extreme event triggered landslide inventory with a susceptibility map which was calibrated with a normal landslide inventory does not result into a simple conversion from false to true positives, but that new susceptible conditions arises under intense triggering, which cannot be predicted if a normal event inventory is used for calibration. Conversely, extreme landslide inventories allow to calibrate susceptibility maps which are very effective in predicting the landslides produced by normal events but with limits in discriminating stable conditions.

What above summarized is obviously of great importance in terms of applicative consequences. In fact, it means that landslide susceptibility stochastic modeling requires multi-temporal calibration inventories so to detect and estimate the effects of differences in the intensity of the trigger, optimizing positive and negative predictions. Strategies for integrating low and high trigger landslide inventories are to be issued

and constitute the logical conclusive perspective of this research. It does not escape from authors consideration that the performance of the 2003 forward chrono-validation was acceptable for CF and ALL sector, which means that in 2003 it was possible to predict with a good accuracy the position of the 2009 source areas.

The test performed by transferring the model calibrated in the Ilopango Caldera with respect to the 2009 event to predict the 2011 event in the Coatepeque Caldera gave several elements to confirm how the trigger intensity and spatial distribution can control the quality and the effectiveness of the susceptibility models. In particular, less intense and more homogeneous rainfall in a more uniform area resulted in a very high performing self-validated predictive model. This same conclusion was supported by comparing the probabilities estimated for the same pixel from the two models, which resulted systematically lower in the susceptible sector for the transferred model from the Ilopango Caldera.

The 2009 event at Ilopango Caldera was in fact more intense and concentrated both in time and space.

The present research allowed to verify the importance of the coupling between trigger and geologic features in a landslide event, which, in the case of fast surficial landslides and very intense triggering events, such is the case of the tephra slopes in caldera area in El Salvador, can affect very heavily the meaning of the obtained maps. To this, the research whose results are here described give an experimental and methodological contribution.

6. REFERENCES

Akgün, A., 2012. A comparison of landslide susceptibility maps produced by logistic regression, multi-criteria decision, and likelihood ratio methods: a case study at İ zmir, Turkey. Landslides 9, 93–106. DOI: 10.1007/s10346-011-0283-7.

Atkinson, P.M., Massari, R., 1998. Generalised linear modelling of susceptibility to landsliding in the central Apennines, Italy. Computers & Geosciences 24 (4), 373-385. DOI: 10.1016/S0098-3004(97)00117-9.

Alfaro, E.J., 2011. Algunos aspectos relacionados con la variabilidad climática de los ciclones tropicales en el Pacífico tropical del este.

Álvarez Guerrero, S.J., 1987. Informe técnico sismológico del terremoto de San Salvador del 10 de octubre de 1986. Ministerio de Obras Públicas. Centro de Investigaciones Geotécnicas. El Salvador.

Aleoti P., Chowdhury, R., 1999. Landslide hazard assessment: summary review and new perspectives. Bull Eng Geol Env (1999) 58: 21–44. 7 Q Springer-Verlag.

Avila, L.A., Cangialosi, J., 2010. Tropical Cyclone Report Hurricane Ida. National Hurricane Center.

Babůrek, J., Baratoux, L., Baroň, I., Čech, S., Hernandez, W., Hradecký, P., Kopačková, V., Novák, Z., Rapprich, V., Šebesta, J., Ševčík, J., Vorel, T., Zemková, M., 2005. Estudio geológico de los peligros naturales, área de Metapán, El Salvador. Unpublished Final Report, Czech Geological Survey, Prague, Servicio Nacional de Estudios Territoriales, San Salvador, 1-107.

Bai, S.-B., Wang, J., Lü, G.-N., Zhou, P.-G., Hou, S.-S., Xu, S.-N., 2010. GIS-based logistic regression for landslide susceptibility mapping of the Zhongxian segment in the Three Gorges area, China. Geomorphology 115 (1-2), 23-31. DOI: 10.1016/j.geomorph.2009.09.025.

Barrios, L., Hernández, B., Quezada, A. Pullinger, C., 2011. Geological hazards and geotechnical aspects in geothermal areas, the El Salvador experience. Short Course on Geothermal Drilling, Resource Development and Power Plants, UNU-GTP and LaGeo, Santa Tecla, El Salvador.

Baum, R.L., Lidke, D.J., Sather, D.N., Bradley, L., Tarr, A.C., 2001a. Landslides induced by hurricane Mitch in El Salvador: An inventory and descriptions of selected features. US Department of the Interior, US Geological Survey.

Baum, R.L., Crone, A.J., Escobar, D., Harp, E.L., Major, J.J., Martinez, M. Smith, M.E., 2001b. Assessment of landslide hazards resulting from the February 13, 2001, El Salvador earthquake. US Geological Survey Open-File Report, 01-119.

Baxter, S., 1984. Léxico estratigráfico de El Salvador, Comisión Ejecutiva Hidroeléctrica del Rio Lempa, San Salvador.

Benito, B., A. Rivas, J.M., Gaspar-Escribano, Murphy, P., 2012. El terremoto de Lorca (2011) en el contexto de la peligrosidad y el riesgo sísmico en Murcia. Física de la Tierra 24, 255-287.

Bent, A.L., Evans, S.G., 2004. The Mw 7.6 El Salvador earthquake of 13 January 2001 and implications for seismic hazard in El Salvador. Geological Society of America Special Papers, 375, 397-404.

Bommer, J.J., Rodríguez, C.E., 2002. Earthquake-induced landslides in Central America. Engineering Geology, 63(3), 189-220.

Bommer, J.J., Benito, M.B., Ciudad-Real, M., Lemoine, A., López-Menjívar, M.A., Madariaga, R., Rosa, H., 2002. The El Salvador earthquakes of January and February 2001: context, characteristics and implications for seismic risk. Soil Dynamics and Earthquake Engineering, 22(5), 389-418.

Bommer, J.J., Rolo, R., Mitroulia, A. Berdousis, P., 2002. Geotechnical properties and seismic slope stability of volcanic soils. In Proceedings of the 12th European Conference on Earthquake Engineering, London.

Bowman, L.J., Henquinet, K.B., 2015. Disaster risk reduction and resettlement efforts at San Vicente (Chichontepec) Volcano, El Salvador: toward understanding social and geophysical vulnerability. Journal of Applied Volcanology, 4(1), 1-18.

Brabb, E.E., 1984. Innovative approaches to landslide hazard and risk mapping, Proceedings of the 4th International Symposium on Landslides, 16–21 September, Toronto, Ontario, Canada (Canadian Geotechnical Society, Toronto, Ontario, Canada), 1, 307-324.

Bui, D.T., Tuan, T.A., Klempe, H., Pradhan, B., Revhaug, I., 2015. Spatial prediction models for shallow landslide hazards : a comparative assessment of the efficacy of support vector machines, artificial neural networks, kernel logistic regression, and logistic model tree. Landslides http://dx.doi.org/10.1007/s10346-015-0557-6.

Cama, M., Lombardo, L., Conoscenti, C., Agnesi, V., Rotigliano, E., 2015. Predicting storm-triggered debris flow events: Application to the 2009 Ionian Peloritan disaster (Sicily, Italy). Natural Hazards and Earth System Sciences: 15 (8), 1785-1806

Cama, M., Conoscenti, C., Lombardo, L., Rotigliano, E., 2016. Exploring relationships between grid cell size and accuracy for debris-flow susceptibility models: a test in the Giampilieri catchment (Sicily, Italy). Environmental Earth Sciences, 75 (3): 238, 1-21

Canora, C., Villamor, P., Díaz, J.M., Berryman, K.R., Gómez, J.Á., Capote, R., Hernández, W., 2012. Paleoseismic analysis of the San Vicente segment of the El Salvador Fault Zone, El Salvador, Central America.Geologica acta, 10(2), 103-123.

Canora, C., Martínez-Díaz, J.J., Villamor, P., Staller, A., Berryman, K., Álvarez-Gómez, J.A., Diaz, M., 2014. Structural evolution of the El Salvador Fault Zone: an evolving fault system within a volcanic arc. Journal of Iberian Geology, 40(3), 471-488.

Carrara, A., Cardinali, M., Detti, R., Guzzetti, F., Pasqui, V., Reichenbach, P., 1991. GIS techniques and statistical models in evaluating landslide hazard. Earth Surface Processes & Landforms 16 (5), 427-445.

Carrara, A., Cardinali, M., Guzzetti, F. Reichenbach, P., 1995. GIS technology in mapping landslide hazard. In Geographical information systems in assessing natural hazards (pp. 135-175). Springer Netherlands.

Carrara, A., Crosta, G., Frattini, P., 2003. Geomorphological and historical data in assessing landslide hazard. Earth Surface Processes and Landforms 28 (10), 1125-1142. DOI: 10.1002/esp.545.

CATHALAC, 2009. Mapa de rutas de sistemas meteorológicos IDA y Baja 96E noviembre 2009. En línea. Disponible en http://www.servir.net/images/desastres/2009-11-02_TT_Ida/ida_baja96_20091111.jpg .

Chávez, J.A., Valenta, J., Schröfel, J., Hernandez, W., Sebesta, J., 2010. Engineering geology mapping in the southern part of the Metropolitan Area of San Salvador. Revista Geológica de América Central, (46), 161-178.

CEPAL, 2005. Efectos en el salvador de las lluvias torrenciales, tormenta tropical Stan y erupción del volcán Ilamatepec (Santa Ana), octubre del 2005. CEPAL. Ciudad de México.

CEPAL, 2010. El Salvador: Impacto Socioeconómico, Ambiental y de Riesgo por la Baja Presión Asociada a la Tormenta Tropical Ida en Noviembre de 2009. CEPAL. Ciudad de México, CEPAL: 21.

CEPAL, 2010. La economía del cambio climático en Centroamérica. Síntesis.

CEPAL, 2011. El Salvador: Evaluación de daños y pérdidas en El Salvador ocasionados por la depresión tropical 12E. CEPAL. San Salvador. En línea. Disponible en http://www.marn.gob.sv/phocadownload/informe_depresion_tropical_12E.pdf.

Chung, C.J., Fabbri, A.G., 2003. Validation of spatial prediction models for landslide hazard mapping. Natural Hazards 30 (3), 451-472. DOI: 10.1023/B:NHAZ.0000007172.62651.2b.

Chung, C.J.F., Fabbri, A.G., Van Westen, C.J., 1995. Multivariate regression analysis for landslide hazard zonation. In Geographical information systems in assessing natural hazards (pp. 107-133). Springer Netherlands.

Committee on the Review of the National Landslide Hazards Mitigation Strategy, 2004. Partnerships for Reducing Landslide Risk. Assessment of the National Landslide Hazards Mitigation Strategy. Board on

Conoscenti, C., Di Maggio, C., Rotigliano, E., 2008a. GIS analysis to assess landslide susceptibility in a fluvial basin of NW Sicily (Italy). Geomorphology 94, 325–339. DOI: 10.1016/j.geomorph.2006.10.039.

Conoscenti, C., Di Maggio, C., Rotigliano, E., 2008b. Soil erosion susceptibility assessment and validation using a geostatistical multivariate approach: a test in southern Sicily. Natural Hazard 46, 287–305. DOI: 10.1007/s11069-007-9188-0.

Conoscenti, C., Ciaccio, M., Caraballo-Arias, N.A., Gómez-Gutiérrez, Á., Rotigliano, E., Agnesi, V., 2015. Assessment of susceptibility to earth-flowlandslide using logistic regression and multivariate adaptive regression splines: a case of the Belice River basin (western Sicily, Italy). Geomorphology 242, 49–64. http://dx.doi.org/10.1016/j.geomorph.2014.09.020.

Craven, P., Wahba, G., 1979. Smoothing noisy data with spline functions. Numer. Math. 31, 377–403.

Costanzo, D., Rotigliano, E., Irigaray, C., Jiménez-Perálvarez, J.D., Chacón, J., 2012a. Factors selection in landslide susceptibility modelling on large scale following the gis matrix method: Application to the river Beiro basin (Spain). Natural Hazards and Earth System Science 2(2), 327-340. DOI:10.5194/nhess-12-327-2012.

Costanzo, D., Cappadonia, C., Conoscenti, C., Rotigliano, E., 2012b. Exporting a Google Earth™ aided earth-flow susceptibility model: A test in central Sicily. Natural Hazards 61 (1), 103-114. DOI 10.1007/s11069-011-9870-0.

Coussot, P., Meunier, M., 1996. Recognition, classification and mechanical description of debris flows. Earth-Science Reviews, 40(3), 209-227.

Crozier, M.J., Glade, T., 2006. Landslide hazard and risk: issues, concepts and approach. Landslide hazard and risk. Wiley, West Sussex, 1-40.

Crone, A.J., Baum, R.L., Lidke, D.J., Sather, D.N., Bradley, L.A., Tarr, A.C., 2001. Landslides induced by hurricane Mitch in El Salvador—An inventory and descriptions of selected features. US Geological Survey Open-File Report, 01-0444.

Daví, J.M., Fernández, C., 2008. Movimiento de ladera en la vertiente este del Picacho, finca Santa María (Mejicanos). Programa IPGARAMSS Integración Participativa de la Gestión Ambiental y de Riesgos en los Planes de Ordenamiento Territorial del AMSS. Geólogos del Mundo.

Davies, T.R.H., McSaveney, M.J., 2012. Mobility of long-runout rock avalanches. Landslides: types, mechanisms and modeling. Cambridge University Press, Cambridge, 50-58.

De la Cruz, A.H., Gimeno, D., Gisbert, G., 2015. Caracterización geoquímica básica de lavas de El Salvador (Centroamérica): principales tendencias registradas en el Frente Volcánico Costero.

DeMets, C., 2001. A new estimate for present-day Cocos-Caribbean plate motion: Implications for slip along the Central American volcanic arc. Geophysical Research Letters, 28(21), 4043-4046.

Dull, R.A., Southon, J.R., Sheets, P., 2001. Volcanism, ecology and culture: a reassessment of the Volca´n Ilopango TBJ eruption in the southern Maya realm. Latin American Antiquity 12, 25–44.

Dull, R. A., R. J. Nevle, W. I. Woods, D. K. Bird, S. Avnery, and W. M. Denevan, 2010. The Columbian Encounter and the Little Ice Age: Abrupt land use change, fire, and greenhouse forcing, Ann. Assoc. Am. Geogr., 100(4), 1–17.

DYGESTYC, 2007. Censo de población y vivienda 2007. Dirección General de Estadísticas y Censos. San Salvador. Disponible en http://www.digestyc.gob.sv/index.php/temas/des/poblacion-y-estadisticas-demograficas/censo-de-poblacion-y-vivienda/poblacion-censos.html

Evans, S.G., Bent, A.L., 2004. The Las Colinas landslide Santa Tecla: A highly destructive flowslide triggered by the January 13, 2001, El Salvador Earthquake.

Fell R., Corominas J., Bonnard C., Cascini L., Leroi E., Savage W., 2008. Guidelines for landslide susceptibility, hazard and risk zoning for land use planning. Engineering Geology, 102, 83-84.

Fernandez-Lavado, C., Malo, A.S., 2008. Susceptibility Map of Landslides Triggered by Rain in the Metropolitan Area of San Salvador (AMSS). In 2008 Joint Meeting of The Geological Society of America, Soil Science Society of America, American Society of Agronomy, Crop Science Society of America, Gulf Coast Association of Geological Societies with the Gulf Coast Section of SEPM.

Ferradas, P., Medina, N. 2003. Riesgos de desastres y derechos de la niñez. Pág. 25. Disponible en http://www.unicef.org/paraguay/spanish/MR_3_Ninez_y_Desastres_ITDG.pdf.

Frattini, P., Crosta, G., Carrara, A., 2010. Techniques for evaluating the performance of landslide susceptibility models. Engineering Geology, 111 (1–4), 62-72. DOI: 10.1016/j.enggeo.2009.12.004.

Friedman, J.H., 1991. Multivariate adaptive regression splines. Ann. Stat. 19, 1–141.

Fookes, P.G., Lee, E.M., Griffiths, J.S., 2007. Engineering geomorphology: theory and practice. 307, 113-120.

García-Rodríguez, M.J., Malpica, J.A., Benito, B., Díaz, M., 2008a. Susceptibility assessment of earthquake-triggered landslides in El Salvador using logistic regression. Geomorphology, 95(3), 172-191.

García Rodríguez, M.J., Havenith, H., Benito Oterino, B., 2008b. Evaluation of earthquake-triggered landslides in El Salvador using a Gis based newmark model.

García-Rodríguez, M.J., Malpica, J.A., 2010. Assessment of earthquake-triggered landslide susceptibility in El Salvador based on an Artificial Neural Network model. Natural Hazards and Earth System Science, 10(6), 1307-1315.

Gorsevski, P.V., Foltz, R.B., Gessler, P.E., Cundy, T.W., 2001. Statistical modeling of landslide hazard using GIS. Seventh Federal Interagency Sedimentation Conference, Silver Legacy, Reno, Nevada, City, pp. 103-109.

Guzzetti, F., Carrara, A., Cardinali, M., Reichenbach, P., 1999. Landslide hazard evaluation: a review of current techniques and their application in a multi - scale study, Central Italy. Geomorphology 31 (1-4), 181 - 216. DOI: 10.1016/S0169-555X(99)00078-1.

Guzzetti, F., Reichenbach, P., Cardinali, M., Galli, M., Ardizzone, F., 2005. Probabilistic landslide hazard assessment at the basin scale. Geomorphology 72 (1-4), 272-299.

Guzzetti, F., Reichenbach, P., Ardizzone, F., Cardinali, M., Galli, M., 2006. Estimating the quality of landslide susceptibility models. Geomorphology 81, 166–184.

Heckmann, T., Gegg, K., Gegg, A., Becht, M., 2014. Sample size matters: investigating the effect of sample size on a logistic regression susceptibility model for debris flows. Nat. Hazards Earth Syst. Sci. 14, 259–278. http://dx.doi.org/10.5194/nhess-14-259-2014.

Hernández, W., 2005. Nacimiento y Desarrollo del río Lempa. MARN/SNET.

Hradecky, P., 2011. Introduction to the special volume. Journal of GEOsciences, 56(1), 1-7.

Highland, L.M., Bobrowsky, P., 2008. The landslide handbook—A guide to understanding landslides: Reston, Virginia, U.S. Geological Survey Circular 1325, 129 p.

Hosmer, D.W., Lemeshow, S., 2000. Applied logistic regression, Wiley Series in Probability and Statistics. Wiley.

Hungr, O., Leroueil, S., Picarelli, L. 2014. The Varnes classification of landslide types, an update. *Landslides*, *11*(2), 167-194.

Howel, W., Meyer-Abich, H., 1953. El origen del Lago de Ilopango con un mapa de profundidades del lago, un mapa geológico preliminar y secciones diagramáticas. Comunicaciones, 2(1), 1-8.

Hutchinson, J.N., 1995. Keynote paper: Landslide hazard assessment. In: Bell (ed.) Landslides, A.A. Balkema, Rotterdam, 1805-1841.

Iverson, R.M., Denlinger, R.P., 1987. The physics of debris flows—a conceptual assessment. IAHS-AISH publication, (165), 155-165.

Jakob, M., Hungr, O., Jakob, D.M., 2005. Debris-flow hazards and related phenomena Berlin: Springer. (Vol. 739) p9,10, 81.

Jebur, M.N., Pradhan, B., Tehrany, M.S., 2014. Optimization of landslide conditioning factors using very high-resolution airborne laser scanning (LiDAR) data at catchment scale. Remote Sens. Environ. 152, 150–165. http://dx.doi.org/10.1016/j.rse.2014.05.013.

Jibson, R.W., Crone, A.J., 2001. Observations and recommendations regarding landslide hazards related to the January 13, 2001 M-7.6 El Salvador earthquake. US Department of the Interior, US Geological Survey.

Jibson, R.W., Crone, A.J., Harp, E.L., Baum, R.L., Major, J.J., Pullinger, C.R., Escobar, C.D., Martínez, M., Smith, M.E., 2004. Landslides triggered by the 13 January and 13 February 2001 earthquakes in El Salvador. Geological Society of America Special Papers, 375, 69-88.

Karnauskas, K.B., Busalacchi, A.J., 2009. The Role of SST in the East Pacific Warm Pool in the Interannual Variability of Central American Rainfall. J. Climate, 22, 2605–2623, doi: 10.1175/2008JCLI2468.1.

Kitamura, S. 2006. A preliminary report of the tephrochronological study of the eruptive history of Coatepeque Caldera, El Salvador, Central America.

Kopačková, V., Šebesta, J., 2007. An approach for GIS-based statistical landslide susceptibility zonation: With a case study in the northern part of El Salvador. In Remote Sensing (pp. 67492R-67492R). International Society for Optics and Photonics.

Kutterolf, S., Freundt, A., Peréz, W., 2008. Pacific offshore record of plinian arc volcanism in Central America: 2. Tephra volumes and erupted masses. Geochemistry, Geophysics, Geosystems, 9(2).

Lewis, Y.W., 2008. Geologic Controls for Landslides in the Central American Highlands of Northern El Salvador (Master dissertation, Michigan Technological University).

Lexa, O., Schulmann, K., Janoušek, V., Štípská, P., Guy, A. & Racek, M., 2011. Heat sources and trigger mechanisms of exhumation of HP granulites in Variscan orogenic root. Journal of Metamorphic Geology, **29**, 79–102.

Lexa, J., Sebesta, J., Chávez, J. A., Hernández, W., & Pecskay, Z. 2011. Geology and volcanic evolution in the southern part of the San Salvador Metropolitan Area. Journal of Geosciences, 56(1), 106-140.

Lleonart, R.M., Espuny, J., Ferrés, D., Font, J., Mata-Perelló, J.M., Puiguriguer, M., Rubio, J., 2000. Las grandes cárcavas: deslizamientos en El Salvador, el ejemplo de la cuenca del río La Palma.

Lombardo, L., Cama, M., Maerker, M., Rotigliano, E., 2014.- A test of transferability for landslides susceptibility models under extreme climatic events: Application to the Messina 2009 disaster. Natural Hazards: 74 (3), 1951-1989.

Lombardo, L., Cama, M., Conoscenti, C., Märker, M., Rotigliano, E., 2015. Binary logistic regression versus stochastic gradient boosted decision trees in assessing landslide susceptibility for multiple-occurring landslide events: application to the 2009 storm event in Messina (Sicily, southern Italy). Natural Hazards: 79 (3), 1621-1648.

López, B.F., Alfaro, E.J., 2012. Uso de herramientas estadísticas para la predicción estacional del campo de precipitación en América Central como apoyo a los Foros Climáticos Regionales. 2: Análisis de Correlación Canónica. Revista de Climatología, 12.

Major, J.J., Schilling, S.P., Pullinger, C.R., Escobar, C.D., Howell, M.M., 2001. Volcano-Hazard Zonation for San Vicente Volcano, El Salvador: U.S. Geological Survey Open-File Report 01-367, 22 pp., 1 plate, http://pubs.usgs.gov/of/2001/0367/.

Major, J.J., Schilling, S.P., Pullinger, C.R., Escobar, C.D., 2004. Debris-flow hazards at San Salvador, San Vicente, and San Miguel volcanoes, El Salvador. Geological Society of America Special Papers, 375, 89-108.

Malet, J.P., van Asch, T.W.J., van Beek, R., Maquaire, O., 2005. Forecasting the behaviour of complex landslides with a spatially distributed hydrological model. Nat. Hazards Earth Syst. Sci. 5, 71–85. doi:10.5194/nhess-5-71-2005.

Mann, C.P., Stix, J., Vallance, J.W., Richer, M., 2004. Subaqueous intracaldera volcanism, Ilopango Caldera, El Salvador, Central America. Geological Society of America Special Papers, 375, 159-174.

MARN (Ministerio de Medio Ambiente y Recursos Naturales, SV), 2004. Memoria técnica para el mapa de susceptibilidad de deslizamientos de tierra en el salvador.

MARN (Ministerio de Medio Ambiente y Recursos Naturales, SV), 2010. Síntesis de los informes de evaluación técnica de las lluvias del 7 y 8 de noviembre 2009 en El Salvador: Análisis del impacto físico natural y vulnerabilidad socio ambiental.

MARN (Ministerio de Medio Ambiente y Recursos Naturales, SV), 2011. Depresión Tropical 12E/Sistema Depresionario sobre El Salvador y otros eventos extremos del pacífico. http://www.marn.gob.sv/phocadownload/DT12_SD_Pacifico_Media.pdf

Martínez, J., Canora, C., Álvarez, J., Béjar, M., Benito, B., Berryman, K., Capote, R., Staller, S., Tsige, M., Villamor, P., 2009. Análisis del ciclo sísmico de la Zona de Falla de El Salvador,(Arco Volcánico Centroamericano) mediante la utilización de datos geológicos y sismológicos: aplicación a la peligrosidad sísmica y de deslizamientos. Santiago, 22, S3_010.

McFadden, D., 1979. Quantitative methods for analysing travel behavior of individuals: Some recent developments. In D. A. Hensher & P. R. Stopher (Eds.), Behavioural travel modelling , London: Croom Helm, p.p. 279–318.

Medina-Cetina, Z., Cepeda, J., 2012. Clasificación probabilista de umbrales de lluvia para predecir deslizamientos de tierra. Revista Internacional de Desastres Naturales, Accidentes e Infraestructura Civil, 12(1).

Menard, S., 2002. Applied Logistic Regression Analysis, Second Editino, SAGE University Paper, 111 p.

Mergili, M., 2008. r.debrisflow, version 1.3. User's manual and model outline. A model framework for simulating mobilization and movement of debris flow, Institute of Geography, University of Innsbruck, Austria.

Meyer-Abich, H., 1953. Los ausoles de El Salvador con un sumario geológico-tectónico de la zona volcánica occidental. Comunicaciones, 2(3-4), 55-102.

Meyer-Abich, H., Williams, H. s.f. Historia volcánica del lago de Coatepeque (El Salvador) y sus alrededores.

Milborrow, S., Hastie, T., Tibshirani, R., 2011. Earth: Multivariate Adaptive Regression Spline Models. R Software Package.

Milborrow, S., 2015. Notes on the earth package [WWW Document]. URL http://www.milbo.org/doc/earth-notes.pdf.

Mora S., Vahrson, W., 1991. Determinación a Prior de la Amenaza de Deslizamientos in Grandes Áreas y Utilizando Indicadores Morfodinámicos. Universidad de Costa Rica y Universidad Nacional de Costa Rica. Julio, Instituto Costarricense de Electricidad, Costa Rica

Nagelkerke, N.J.D., 1991. A note on a general definition of the coefficient of determination. Biometrika 78(3), 691–692.

Naimi, B., 2015. Uncertainty Analysis for Species Distribution Models. R Software Package.

Nefeslioglu, H.A., Gokceoglu, C., Sonmez, H., 2008. An assessment on the use of logistic regression and artificial neural networks with different sampling strategies for the preparation of landslide susceptibility maps. Engineering Geology 97 (3–4), 171-191. DOI: 10.1016/j.enggeo.2008.01.004.

Pardeshi, S.D., Autade, S.E., Pardeshi, S.S., 2013. Landslide hazard assessment: recent trends and techniques. SpringerPlus, 2(1), 1.

Pierson, T.C., 2005. Distinguishing between debris flows and floods from field evidence in small watersheds (No. 2004-3142). US Geological Survey.

Ríos, R., Ribó, A., Mejía, R., Molina, G., 2016. Combining neural networks and geostatistics for landslide hazard assessment of San Salvador metropolitan area, El Salvador. Revista de Matemática: Teoría y Aplicaciones, 23(1), 155-172.

Rocchi, G., Vaciago, G., 2013. Geomechanical basis of landslide classification and modelling of triggering. In Landslide Science and Practice (pp. 3-9). Springer Berlin Heidelberg.

Rolo, R., Bommer, J.J., Houghton, B.F., Vallance, J.W., Berdousis, P., Mavrommati, C., Murphy, W., 2004. Geologic and engineering characterization of Tierra Blanca pyroclastic ash deposits. Geological Society of America Special Papers, 375, 55-68.

Rossi, M., Guzzetti, F., Reichenbach, P., Mondini, A.C., Peruccacci, S., 2010. Optimal landslide susceptibility zonation based on multiple forecasts. Geomorphology, 114 (3), 129-142. DOI: 10.1016/j.geomorph.2009.06.020.

Rotigliano, E., Agnesi, V., Cappadonia, C., Conoscenti, C., 2011. The role of the diagnostic areas in the assessment of landslide susceptibility models: a test in the Sicilian chain. Natural hazards, 58(3), 981-999.

Rotolo, S.G., Aiuppa, A., Pullinger, C.R., Parello, F., Tenorio-Mejia, J., 2011. An introduction to San Vicente (Chichontepec) Volcano, El Salvador. Revista Geológica de América Central, (21).

Schmidt-Thomé, m., 1975. The geology in the San Salvador area (El Salvador, central America), a basis for city development and planning. in: Geologisches Jahrbuch, Vol. 13, p. 207–228, Hannover.

Siebert, L., Kimberly, P., Pullinger, C.R., 2004. The voluminous Acajutla debris avalanche from Santa Ana volcano, western El Salvador, and comparison with other Central American edifice-failure events. Geological Society of America Special Papers, 375, 5-24.

Sebesta, J., 2006. Elaboración de cartografía geomorfológica para incorporar el análisis de riesgo en el plan de desarrollo urbano del Área Metropolitana de San Salvador. Proyecto Fortalecimiento de la Gestión Ambiental en El Salvador SLV/B7-3100/98/O232 UE – GOES.

Serrano, F., 1995. Historia natural y ecológica de El Salvador. Tomo I 1a Ministerio de Educación de El Salvado ry Offset, SA de CV México, 397.

Singh, S.K., Gitiérrez, C., Arboleda, J., 1993. Peligro sísmico en El Salvador. Centro de Investigaciones Geotécnicas de El Salvador.

Soeters, R. and van Westen, C.J., 1996. Slope instability recognition, analysis and zonation. In: Turner, A.K. and Schuster, R.L. (eds.) Landslide investigation and mitigation, National Research Council, Transportation Research Board Special Report 247, 129-177.

Süzen, M.L., Doyuran, V., 2004. A comparison of the GIS based landslide susceptibility assessment methods: multivariate versus bivariate. Environmental Geology. 45 (5), 665 - 679. DOI: 10.1007/s00254-003-0917-8.

Takahashi, T., 2014. Debris flow: mechanics, prediction and countermeasures. CRC press. 541, P9.

Tikoff, B., Demets, C., Garibaldi, N., Hernández, W., Hernández, D., 2011. Interaction of deformation and magmatism along the El Salvador volcanic arc.

Tsige, M., García, I., Capote, R., Martínez, J., Benito, B., 2009. Factores litológico-geotécnicos en el peligro de movimientos co-sismicos de ladera en El Salvador. Santiago, 22, S3_011.

UNISDR (Estrategia Internacional para la Reducción de Desastres, ZU), 2009. Terminología sobre reducción del riesgo de desastres. 43, 10.

USGS, 2004. Landslides Types and Processes. https://pubs.usgs.gov/fs/2004/3072/

USGS, 2012. Historic World Earthquakes.

Available at http://earthquake.usgs.gov/earthquakes/world/historical_country.php.

USGS, 2015. Earthquake hazard program.

http://earthquake.usgs.gov/earthquakes/eventpage/usp000jqvm#general_summary.

Van Beek, L.P.H., Van Asch, Th.W.J., 2004. Regional assessment of the effects of land-use change on landslide hazard bymeans of physically basedmodelling. Natural Hazards 31, 289–304.

Van Den Eeckhaut, M., Reichenbach, P., Guzzetti, F., Rossi, M., Poesen, J., 2009. Combined landslide inventory and susceptibility assessment based on different mapping units: an example from the Flemish Ardennes, Belgium. Nat. Hazards Earth Syst. Sci. 9, 507–521.

van Westen, van Duren, I., Kruse, H.M.G. and Terlien, M.T.J., 1993. GISSIZ: training package for geographic information systems in slope instability zonation. ITC Publication number 15, 2 volumes, ITC, Enschede, The Netherlands.

van Westen, C.J., Rengers, N., Terlien, M.T.J. and Soeters, R., 1997. Prediction of the occurrence of slope instability phenomenal through GIS-based hazard zonation. Geologische Rundschau, 86: 404-414.

Varnes, D.J., 1978. Slope movement 43. types and processes, in Schuster, R.L., and Krizek, R.J., eds., Landslides—Analysis and control: Transportation Research Board Special Report 176, National Research Council, Washington, D.C., p. 11–23.

Varnes, D.J., 1984. IAEG Commission on Landslides and other Mass-Movements, Landslide hazard zonation: a review of principles and practice. UNESCO Press, Paris.

Von Ruette, J., Papritz, A., Lehmann, P., Rickli, C., Or, D., 2011. Spatial statistical modeling of shallow landslides — Validating predictions for different landslide inventories and rainfall events. Geomorphology 133 (1–2), 11-22. DOI:10.1016/j.geomorph.2011.06.010.

White, 1991. Tectonic implications of upper-crustal seismicity in Central America, in: Slemmons (Ed.), et al., Neotectonics of North America, Geological Society of America, Decade Map, vol. 1 (1991), pp. 323–338

Wiesemann, G., 1978. Mapa geológico de la República de El Salvador, escala 1:100 000. Bundesanstalt für Geowissenschaften und Rohstoffe, Hannover.

Wilkinson, P.L., Anderson, M.G., Lloyd, D.M., Renaud, J-P., 2002. Landslide hazard and bioengineering: towards providing improved decision support through integrated numerical model development. Environmental Modelling and Software 17(4): 333–344.

Youden, W.J., 1950. Index for rating diagnostic tests. Cancer 3 (1), 32–35 doi:10.1002/1097-0142(1950)3:1b32::AID-CNCR2820030106N3.0.CO;2-3.